

SAI-74-502-AQ
May 23, 1974

ELECTROMAGNETIC PULSE
ENVIRONMENT STUDIES

FINAL REPORT

by

R. E. Knight
E. R. Parkinson
V. W. Pire

Prepared under

Contract No. DAAC39-73-C-0131

Sponsored by

DEPARTMENT OF THE ARMY
Harry Diamond Laboratories
Washington, D. C. 20315

This work was partly supported by the
Air Force Weapons Laboratory,
Randall Air Force Base, New Mexico.

1974-05-23
1974-05-23
1974-05-23

1974-05-23

ABSTRACT

A number of investigations related to the development of a near-surface EMP code were carried out. Important considerations in the development of a near-surface burst EMP code include the choice of coordinate system, the form of the electromagnetic field equations that is chosen for solution, the differencing scheme used to represent the field equations, and the choice of boundary conditions applied to the problem to be solved. Such considerations are also affected by requirements that the conductivity and dielectric constant have spatial structure, and that far-field predictions also be provided, either directly or by extrapolation techniques.

In the investigations carried out, primary emphasis was put on development of a differencing scheme. Several approaches were investigated in detail, with the algorithms considered programmed for actual machine computation. The theoretical basis of each of the algorithms, the differencing approach implemented in detail, and general descriptions of the computational procedure, together with some programming details and computational results, are presented.

TABLE OF CONTENTS

<u>Section</u>		<u>Page</u>
1	INTRODUCTION	1
	1.1 Basic Considerations	1
	1.2 Major Problem Areas	4
2	FIELD ALGORITHMS INVESTIGATED	10
	2.1 Algorithm "A"	10
	2.2 Algorithm "B"	14
	2.3 Real-time Fields Algorithm in Cylindrical Coordinates for an Infinitely Conducting Ground: Algorithm "C"	31
	2.4 Algorithm "D"	53
3	SUMMARY	57
	APPENDIX A	58
	APPENDIX B	74
	APPENDIX C	86
	APPENDIX D	102
	REFERENCES	109

ILLUSTRATIONS

<u>Figure</u>		<u>Page</u>
1.1	Sketch of Near-Ground EMP Problem	2
1.2	Coordinate Grid for Zero-Burst Height Computations	5
1.3	Prolate Spheroidal Coordinate Grid	6
2.1	Algorithm "B" Differencing Conventions	17
2.2	Specific Fields Involved in Typical Differencing for Equations 2.2.5 and 2.2.7	20
2.3	(I, J) Computation Grid for Sample Problem	25
2.4	Fields Near 530 Meters Ground Range and 33 Meters Above the Ground	26
2.5	Fields Near 530 Meters Ground Range and 20 Meters Above the Ground	27
2.6	Fields Near 550 Meters Ground Range and 7 Meters Above the Ground	28
2.7	Fields Near 730 Meters Ground Range and 45 Meters Above the Ground	29
2.8	Fields Near 730 Meters Ground Range and 27 Meters Above the Ground	30
2.9	Coordinate Grid for Algorithm "C"	31
2.10	Differencing for Equation 2.3.17	36
2.11	Differencing for Equation 2.3.18	38
2.12	Differencing for Equation 2.3.19	40
2.13	Radial Current at 500 Meters	45
2.14	Conductivity at 500 Meters	46
2.15	Vertical Electric Field at 500 Meters	47
2.16	Magnetic Field at 500 Meters	48
2.17	Radial Current at 1000 Meters	49
2.18	Conductivity at 1000 Meters	50
2.19	Vertical Electric Field at 1000 Meters	51
2.20	Magnetic Field at 1000 Meters	52
2.21	Integration in Characteristic Surfaces for Algorithm "D"	55

1. INTRODUCTION

In the course of the work to be described in this report, a number of separate studies were undertaken. Because of the common aim of the investigations, certain comments and explanations generally apply to all of the studies. We will, therefore, attempt in this section to summarize a number of such aspects of the problem being investigated.

1.1 Basic Considerations

The overall objective of the study was to investigate a number of algorithms that could be useful in EMP field computations for off-the-ground bursts. The general problem of ground-burst EMP has been extensively discussed in many places^(1, 2, 3, 4, 5) and will not be discussed in great detail here. The basic problem of concern is sketched in Figure 1.1, which simply indicates a number of the factors which must be taken into account in computing the EMP environment due to a ground or near-ground burst. From an electromagnetic standpoint, one must simply compute the electromagnetic fields created within a prescribed geometry by a certain set of sources. The relevant geometry is, of course, the air-over-ground geometry shown in Figure 1.1; the electrical properties of both the air and the ground (ϵ , μ , and σ) are prescribed and are part of the problem. In EMP language, the sources are considered to be the driven Compton currents and transient conductivity created by nuclear radiation. Good physical models for these sources are still in the process of refinement. Further, interactions between sources and the fields that they generate are both physically important and a source of some practical difficulty in implementing accurate solutions to the field problem. We have nevertheless, assumed in this study that field and source problems can be moderately well separated, and have concentrated on the field algorithm problem.

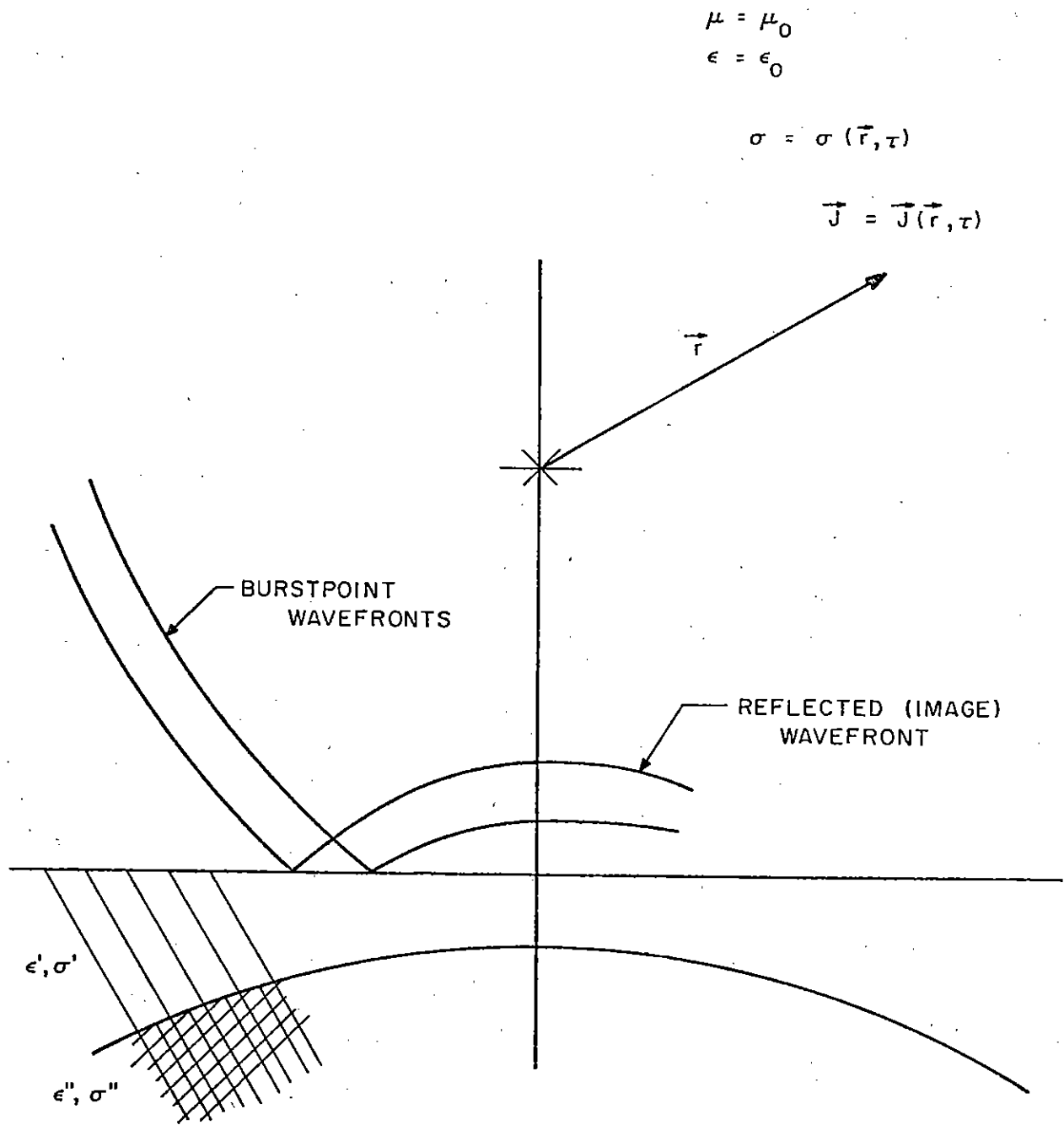


Figure 1.1. Sketch of Near-Ground EMP Problem

A number of ground-burst EMP codes have previously been developed. Many such codes take advantage of various physical approximations and important peculiarities of ground-burst EMP to handle particular aspects of the problem especially well. The G code,⁽¹⁾ ONDINE,⁽²⁾ and GLANC⁽³⁾ are examples of such special codes. The ground burst codes LEMP⁽⁴⁾ and SC⁽⁵⁾ handle solutions to a more general, two-dimensional field problem, but at some expense in other areas. For reasons that are not entirely clear (possible contributing factors are discussed later), neither the LEMP nor the SC field algorithms work well for bursts at a substantial height above the surface of the ground. The field algorithms to be discussed later were investigated for the purpose of providing a more general and adequate treatment of the off-the-ground EMP field problem. Substantial burst heights are presently handled only by one-dimensional field models. The validity of such models (as used in ONDINE or GLANC) is restricted to the close-in region. Some general considerations affecting the finite burst height field problem will be discussed next.

1.2 Major Problem Areas

1.2.1 Choice of Coordinate System

The problem sketched in Figure 1.1 is basically a two-dimensional one: a burst, at some finite height, a , above a ground plane, creates currents and conductivity that are axially symmetric about an axis through the burst and perpendicular to the ground. Ground electrical properties (ϵ , j , and σ) may be stratified and affected by nuclear radiation, but are also assumed to be axially symmetric about the z -axis.

The coordinate system chosen to describe the problem geometry is important because of the convenience that follows from a natural correspondence between coordinate surfaces and physical features of the problem. For example, the LEMP and SC ground-burst geometries use spherical coordinates above the plane containing the burst and cylindrical coordinates below (see Figure 1.2). For a burst directly at ground level, the choice is convenient, since both the sources and the radiated EMP signal are centered at the origin. For bursts above the ground, however, the propagating EMP wavefront (crudely described as originating at the below-ground image-point of the burst) travels obliquely through the composite grid, and is more difficult to conveniently describe.

One very convenient choice of coordinate system for the finite burst-height geometry was found to be the prolate-spheroidal (PS) coordinate system. Many important details of the PS coordinate system have been developed in detail elsewhere,⁽⁶⁾ and will not be re-derived here. Some basic features will, however, be summarized.

The coordinate system is shown in Figure 1.3. Two points on the z -axis, at $z = \pm a$, are identified; they correspond to the burst point and its image below the $z = 0$ ground-plane. Defining the vectors from burst and image points to some given point P by r and r' , respectively, the

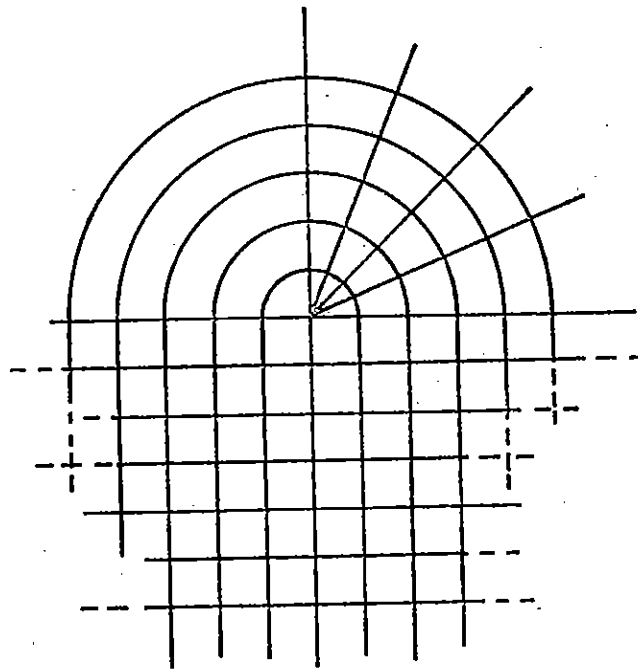


Figure 1.2. Coordinate Grid for Zero-Burst Height Computations

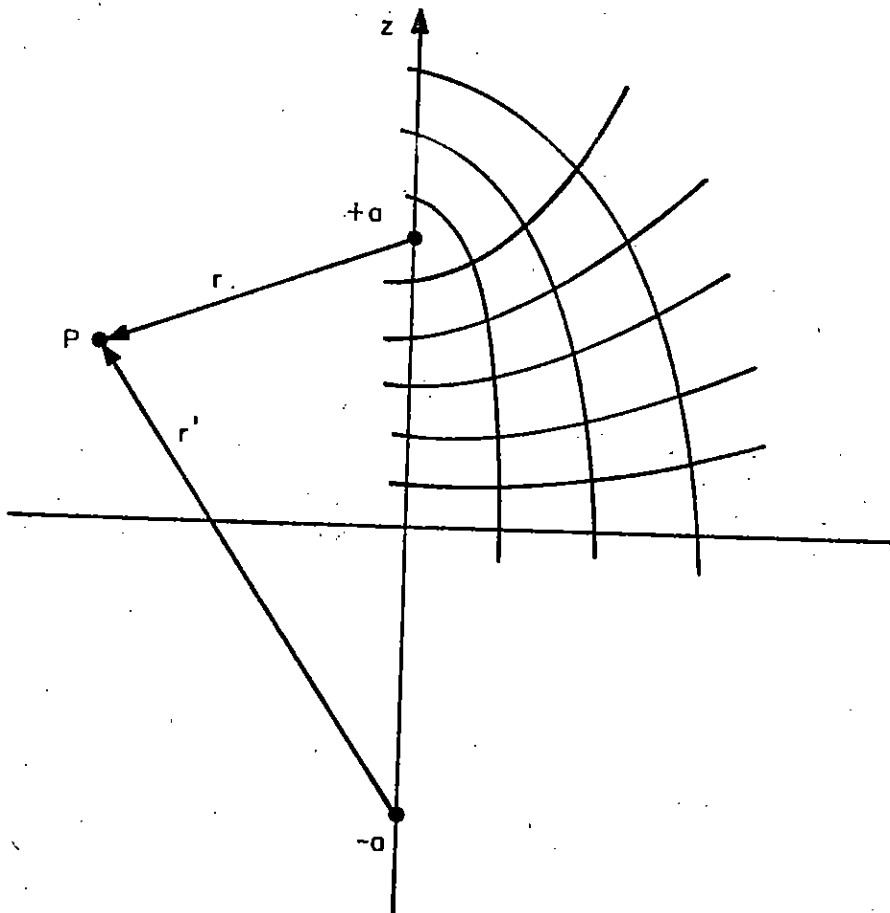


Figure 1.3. Prolate Spheroidal Coordinate Grid

PS coordinates of P are given by ξ , ζ , and φ . φ is the usual azimuthal angle, and

$$\xi = \frac{r' - r}{2a}$$
$$\zeta = \frac{r' + r}{2}$$
(1.2.1)

The surfaces defined by constant values of ζ are a set of confocal ellipsoids with foci at $z = \pm a$; surfaces of constant ξ are an orthogonal set of confocal hyperboloids.

The PS coordinate system is convenient for the following reasons:

1. The burst point (at $z = a$) and the ground surface (at $\xi = 0$) appear naturally in a single coordinate system.
2. Spheres centered about the foci are important auxiliary surfaces, and are easily represented as straight lines in (ξ, ζ) -space, since

$$r = \zeta - a\xi$$
$$r' = \zeta + a\xi$$
(1.2.2)

3. The problem of handling the waves reflected from the ground surface is also somewhat facilitated by PS coordinates. This will be discussed below.

1.2.2 Presence of Reflected Wave

The radiated EM signal is created, in a sense, at the air-ground interface. It resembles a spherical wave centered on the image

point of the burst. Another spherical wave (non-propagating, if the atmosphere is homogeneous) is centered about the burst itself, since excitation from the source expands in a wave moving with the velocity of light. Depending upon whether one chooses to do computations in real time t , or retarded time, τ ($\tau = (t - r/c)$), and whether the burst is at zero height or at a finite height, the problem of computing near outgoing wavefronts can be more or less complicated. At zero burst height, both outgoing wavefronts coincide, and computations using τ as a time variable may begin everywhere at once. In real time, computations at Δt only need extend to some range $R_{\max} = c\Delta t$. Because large spatial derivatives of the EMP fields occur near R_{\max} , spatial regridding may be required there. For bursts at a finite height, burst and burst-image wavefronts do not coincide, and real-time computations must track both. Computations in burst-point retarded time, $\tau = t - (r/c)$, may still need to track and regrid at the image-point wavefront. An additional attraction of PS coordinates in this regard is that surfaces of constant burst-image-point retarded time, $\tau' = t - (r'/c)$, lie (at fixed τ) along hyperboloids $\xi = \xi_0$ in the PS hyperboloidal coordinate surfaces, since $(r' - r) = 2a\xi$,

$$\xi_0 = c(\tau_0 - \tau'_0)/(2a) \quad (1.2.3)$$

1.2.3 Space-Structured σ and ϵ

In addition to drivers in the air, an important feature of the problem description is the presence of a finitely-conducting ground. A depth-dependent conductivity, the possible presence of subsurface currents, and radiation-enhanced conductivity, together with stratified dielectric properties, would be extremely important to include in an adequate treatment of the problem. Computations involving imaged sources may be contemplated as a partial solution, but are not strictly adequate in all regimes.

1.2.4 Outer Boundary Conditions

Fields beyond the boundaries of the immediate sources are an important part of the problem. Ideally, fields at extreme ranges are desired; either direct computations or extrapolations based on matching appropriate free-field solutions at the source region boundary are needed. In any event, conditions on the fields at the boundary of the volume of space considered must adequately account for outside fields without serious "mismatch". The kinds of boundary conditions that are adequate depend to some extent on the time duration of interest. For short times, simple $1/r$ extrapolations of fields have been shown to be adequate; at later times, the source is in a "near-field" region, and more complex extrapolation schemes, such as Babb and Granzow's time-domain treatment of multipoles,⁽⁷⁾ are needed.

1.2.5 Choice of Difference Scheme

In the present investigations, numerical field solutions, based on finite difference representations of the Maxwell field equations, are sought. The foregoing physical considerations were found to have considerable impact on the kinds of differencing schemes that were studied. Mathematical questions of accuracy and stability were also extremely important. Detailed aspects of these questions are discussed in the next section.

2. FIELD ALGORITHMS INVESTIGATED

2.1 Algorithm "A"

The field algorithm described in this section employs the first order exponential differencing method and evaluates spatial derivatives analogously to the scheme used in HAPS.⁽⁸⁾ The prolate spheroidal geometry and the transverse magnetic field equations are derived in appendix one. The final form of the field equations is

$$\frac{\partial E_{\zeta}}{\partial \tau} + \frac{z_0 \sigma}{\kappa} E_{\zeta} = \frac{1}{\kappa} \left(-z_0 j_{\zeta} + Q_{\tau} \frac{\partial H_{\varphi}}{\partial \tau} + \psi_2 \frac{\partial H_{\varphi}}{\partial v} \right) \quad (2.1.1)$$

$$\frac{\partial E_{\xi}}{\partial \tau} + \frac{z_0 \sigma}{\kappa} E_{\xi} = \frac{1}{\kappa} \left(-z_0 j_{\xi} + \frac{\partial H_{\varphi}}{\partial \tau} - \psi_1 \frac{\partial H_{\varphi}}{\partial u} \right) \quad (2.1.2)$$

$$Q_{\tau} G_2 \frac{\partial E_{\zeta}}{\partial \tau} + G_1 \frac{\partial E_{\xi}}{\partial \tau} - \kappa_m \frac{\partial H_{\varphi}}{\partial \tau} = G_1 \psi_1 \frac{\partial E_{\xi}}{\partial u} - G_2 \psi_2 \frac{\partial E_{\zeta}}{\partial v} \quad (2.1.3)$$

where

$$\tau = ct - r \quad (2.1.4)$$

$$G_1 = \frac{\zeta^2 - 1}{\zeta^2 - \xi^2} \quad G_2 = \frac{1 - \xi^2}{\zeta^2 - \xi^2} \quad (2.1.5)$$

The fields have been transformed as follows

$$\begin{pmatrix} E_{\zeta} \\ j_{\zeta} \end{pmatrix} = \sqrt{(\zeta^2 - \xi^2)(\zeta^2 - 1)} \begin{pmatrix} E'_{\zeta} \\ j'_{\zeta} \end{pmatrix} \quad (2.1.6)$$

$$\begin{pmatrix} E_{\xi} \\ j_{\xi} \end{pmatrix} = \sqrt{(\zeta^2 - \xi^2)(1 - \xi^2)} \begin{pmatrix} E'_{\xi} \\ j'_{\xi} \end{pmatrix} \quad (2.1.7)$$

$$H_{\varphi} = z_0 \sqrt{(\zeta^2 - 1)(1 - \xi^2)} H'_{\varphi} \quad (2.1.8)$$

in which the primed quantities are in mks units. The functions ψ_1 and ψ_2 in equations (2.1.1) through (2.1.3) are chosen to provide the desired spatial regridding in the code.

Equation (2.1.1) is of the form

$$\frac{\partial E_{\zeta}}{\partial \tau} + \gamma E_{\zeta} = \psi_1 \quad (2.1.9)$$

where

$$\gamma = \frac{z_0 \sigma}{\kappa} \quad (2.1.10)$$

$$\psi_1 = \frac{1}{\kappa} \left(-z_0 j_{\zeta} + Q_{\tau} \frac{\partial H_{\varphi}}{\partial \tau} + \psi_2 \frac{\partial H_{\varphi}}{\partial v} \right) \quad (2.1.11)$$

The finite difference approximation of the differential equation is

$$E_{\zeta i, j}^k = E_{\zeta i, j}^{k-1} e^{-\chi} + \Phi_1 \frac{1 - e^{-\chi}}{\chi} \quad (2.1.12)$$

where

$$\chi \equiv \bar{\gamma} \Delta \tau = \frac{z_0 \Delta \tau}{\kappa} \sigma_{i, j}^{k-1/2} \quad (2.1.13)$$

and where

$$\begin{aligned} \Phi_1 = & -\frac{z_0 \Delta \tau}{\kappa} j_{\zeta i, j}^{k-1/2} + \frac{Q_{\tau}}{\kappa} \left(H_{\varphi i, j}^k - H_{\varphi i, j}^{k-1} \right) + \frac{\Delta \tau}{2\kappa \Delta v} \psi_2^j \left(H_{\varphi i, j-1}^k - H_{\varphi i, j}^k \right. \\ & \left. + H_{\varphi i, j}^{k-1} - H_{\varphi i, j+1}^{k-1} \right) \end{aligned} \quad (2.1.14)$$

Equation (2.1.2) is of the form

$$\frac{\partial E_{\xi}}{\partial \tau} + \gamma E_{\xi} = \psi_2 \quad (2.1.15)$$

in which γ is the same as before and

$$\psi_2 = \frac{1}{\kappa} \left(-z_0 j_{\xi} + \frac{\partial H}{\partial \tau} \varphi - \psi_1 \frac{\partial H}{\partial u} \varphi \right) \quad (2.1.16)$$

The finite difference equation is

$$E_{\xi i, j}^k = E_{\xi i, j}^{k-1} e^{-\chi} + \Phi_2 \frac{1 - e^{-\chi}}{\chi} \quad (2.1.17)$$

where

$$\begin{aligned} \Phi_2 = & -\frac{z_0 \Delta \tau}{\kappa} j_{\xi i, j}^{k-1/2} + \frac{1}{\kappa} \left(H_{\varphi i, j}^k - H_{\varphi i, j}^{k-1} \right) - \frac{\Delta \tau}{2\kappa \Delta u} \psi_1 \left(H_{\varphi i, j}^k - H_{\varphi i-1, j}^k \right. \\ & \left. + H_{\varphi i+1, j}^{k-1} - H_{\varphi i, j}^{k-1} \right) \end{aligned} \quad (2.1.18)$$

Exponential differencing is not appropriate for equation (2.1.3). We simply write

$$\begin{aligned} Q_{\tau} G_2 \left(E_{\zeta i, j}^k - E_{\zeta i, j}^{k-1} \right) + G_1 \left(E_{\xi i, j}^k - E_{\xi i, j}^{k-1} \right) - \kappa_m \left(H_{\varphi i, j}^k - H_{\varphi i, j}^{k-1} \right) \\ = \frac{\Delta \tau}{2\Delta u} \psi_1 G_1 \left(E_{\xi i, j}^k - E_{\xi i-1, j}^k + E_{\xi i+1, j}^{k-1} - E_{\xi i, j}^{k-1} \right) \\ - \frac{\Delta \tau}{2\Delta v} \psi_2 G_2 \left(E_{\zeta i, j-1}^k - E_{\zeta i, j}^k + E_{\zeta i, j}^{k-1} - E_{\zeta i, j+1}^{k-1} \right) \end{aligned} \quad (2.1.19)$$

Equations (2.1.12), (2.1.17) and (2.1.19) form a set of explicit difference equations that can be solved simultaneously to obtain fields at the point (i, j, k). The boundary conditions are provided by the azimuthal symmetry at the z-axis, the continuity of E_z and H_ϕ across the air-ground interface, the vanishing of the fields at sufficient depth in the ground, and the radiation condition on the fields at the maximum zeta grid. Presently the latter condition is implemented by simply extrapolating the fields as $1/r$. At the air-ground interface, a difficulty arises in obtaining derivatives normal to the surface (i.e., $\frac{\partial H_\phi}{\partial v}$ and $\frac{\partial E_z}{\partial v}$). These derivatives are evaluated at two points above (or below) the interface and then linearly extrapolated to the interface.

2.2 Algorithm "B"

The second algorithm is set up in analogy to the differencing scheme used in the one-dimensional code, ONDINE. A number of variations on the basic approach were implemented, and will be described in this section. Either explicit or implicit versions are possible; a peculiarity of the implicit scheme requires that the time increment over which the fields are advanced be larger than the grid spacing. For this reason, one may be forced (with the basic approach) to perform early-time computations by an explicit method, and switch to its implicit counterpart at late times, when large time steps are desirable. An attractive feature of the basic scheme includes the possibility of handling a flexible and almost arbitrary stratification of ϵ and σ in the differencing grid without affecting the basic method of advancing the fields.

2.2.1 Theoretical Outline of Algorithm "B"

The "B" algorithm is based on Maxwell's equations as written for PS coordinates (described in Section 1) and retarded time of the burst point. We summarize for completeness the precise form used hereafter; standard RMKS notation is used unless otherwise specified. (For details, see Knight^(6,8).)

The "true" field components of interest (because of azimuthal symmetry) are the ξ - and ζ -components of D and E, and the φ -components of B and H. We define the permittivity and permeability constants by:

$$D = \epsilon \epsilon_0 E$$

and

$$B = \mu \mu_0 H$$

(2.2.1)

where, as usual, $c = (\epsilon_0 \cdot \mu_0)^{-1/2}$ and $Z_0 = (\mu_0 / \epsilon_0)^{1/2}$. The following field

transformations are introduced for convenience (primes now refer to old coordinates):

$$\begin{Bmatrix} E_{\xi} \\ j_{\xi} \end{Bmatrix} = \sqrt{(\zeta^2 - \xi^2 a^2)(1 - \xi^2)} \begin{Bmatrix} E'_{\xi} \\ j'_{\xi} \end{Bmatrix}$$

$$\begin{Bmatrix} E_{\zeta} \\ j_{\zeta} \end{Bmatrix} = \frac{1}{a} \sqrt{(\zeta^2 - \xi^2 a^2)(\zeta^2 - a^2)} \begin{Bmatrix} E'_{\zeta} \\ j'_{\zeta} \end{Bmatrix} \quad (2.2.2)$$

$$H_{\phi} = Z_0 \cdot \sqrt{(\zeta^2 - a^2)(1 - \xi^2)} H'_{\phi}$$

and the burst-point retarded time is defined by

$$\tau = ct - r \quad (2.2.3)$$

With these transformations, and with the further definition of the often-used geometrical factors γ_{ξ} and γ_{ζ} :

$$\gamma_{\xi} = \frac{a^2(1 - \xi^2)}{(\zeta^2 - \xi^2 a^2)} \quad (2.2.4)$$

$$\gamma_{\zeta} = \frac{(\zeta^2 - a^2)}{(\zeta^2 - \xi^2 a^2)}$$

we find the final form of the field equations to be differenced:

$$\frac{\partial E_{\xi}}{\partial \tau} = -\frac{Z_{0j}}{\epsilon} \xi - \frac{Z_{0\sigma}}{\epsilon} E_{\xi} + \frac{1}{\epsilon} \frac{\partial H_{\varphi}}{\partial \zeta} - \frac{1}{\epsilon} \frac{\partial H_{\varphi}}{\partial \tau} \quad (2.2.5)$$

$$\frac{\partial E_{\zeta}}{\partial \tau} = -\frac{Z_{0j}}{\epsilon} \zeta - \frac{Z_{0\sigma}}{\epsilon} E_{\zeta} - \frac{1}{\epsilon} \cdot \frac{1}{a} \frac{\partial H_{\varphi}}{\partial \xi} - \frac{1}{\epsilon} \frac{\partial H_{\varphi}}{\partial \tau} \quad (2.2.6)$$

$$\frac{\partial H_{\varphi}}{\partial \tau} = -\frac{1}{\mu} \gamma_{\xi} \left[\frac{1}{a} \cdot \frac{\partial E_{\zeta}}{\partial \xi} + \frac{\partial E_{\zeta}}{\partial \tau} \right] + \frac{1}{\mu} \cdot \gamma_{\zeta} \left[\frac{\partial E_{\xi}}{\partial \zeta} - \frac{\partial E_{\xi}}{\partial \tau} \right] \quad (2.2.7)$$

2.2.2 Differencing Scheme for Algorithm "B"

The differencing procedure for equations (2.2.5) through (2.2.7) is based on the grid and fields defined in the sketch of Figure 2.1. The (i, j) grid structure is constructed so that the grid lines fall at $\zeta_j = a + (j - \frac{1}{2}) \Delta \zeta$ and $\xi_i = 1 - (i - \frac{1}{2}) \Delta \xi$. The fields are defined and indexed at various spatial positions as shown:

$$\begin{aligned} H_{\varphi ij}^1 &= H_{\varphi}(\xi_i, \zeta_j, \tau_1) \\ E_{\zeta ij}^1 &= E_{\zeta}(\xi_{i-1/2}, \zeta_j, \tau_1) \\ E_{\xi ij}^1 &= E_{\xi}(\xi_i, \zeta_{j-1/2}, \tau_1) \end{aligned} \quad (2.2.8)$$

The "1" superscripts refer the fields to their values at the "old" time, τ_1 ; new values at the time $\tau_2 = \tau_1 + \Delta \tau$ are denoted by 2-superscripts.

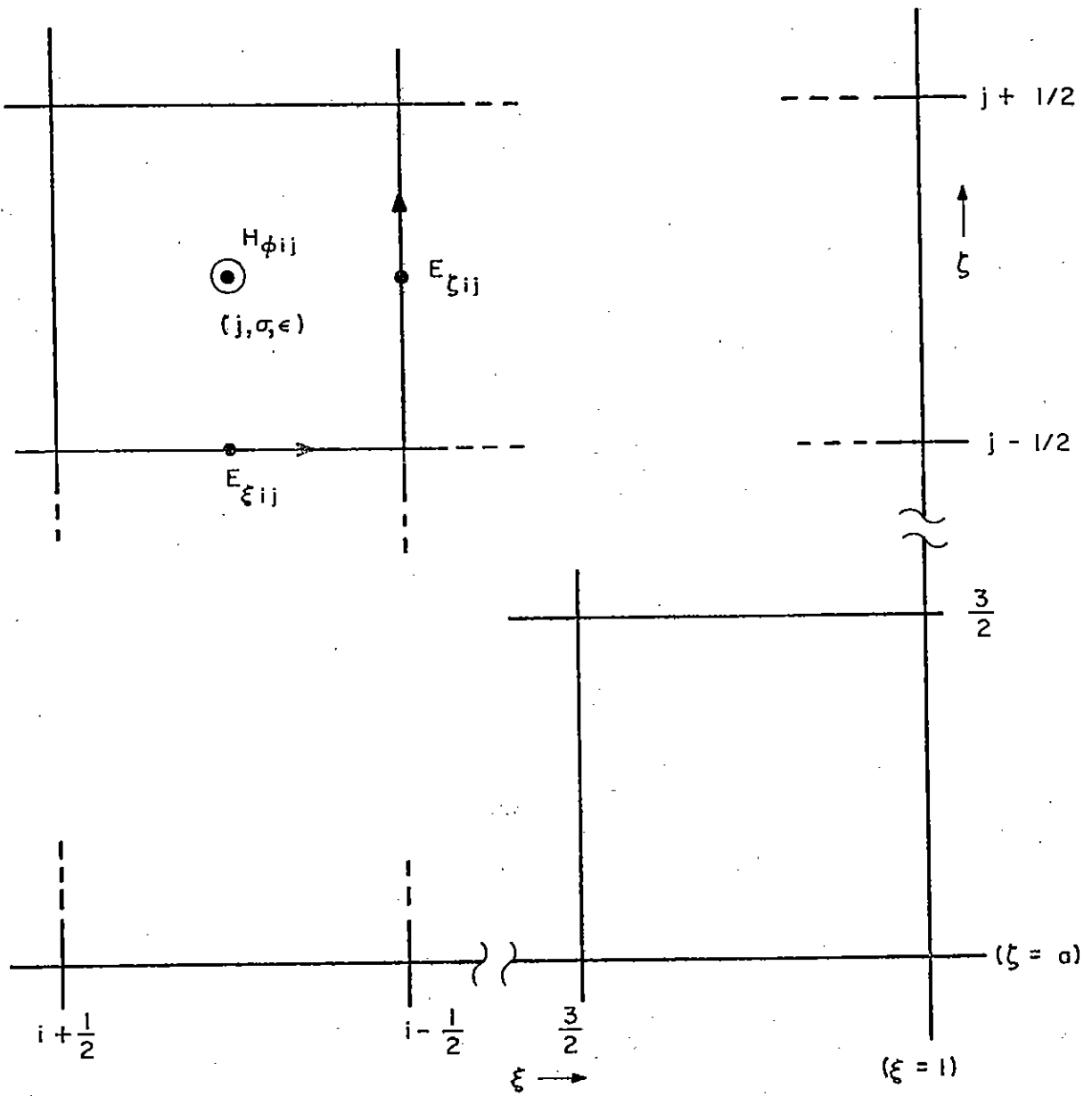


Figure 2.1. Algorithm "B" Differencing Conventions

The spatial cell in which H_{ij} is centered is also indexed by i and j , together with values for the Compton current drivers, J_ξ and J_ζ , the conductivity σ , and the dielectric constant ϵ . The detailed procedure followed in differencing equations (2.2.5) through (2.2.7) is perhaps best explained by reference to Figure 2.2. We will first consider equation (2.2.7) (the \dot{H} -equation), which is differenced identically for each of the (i, j) -th cells in the mesh. Figure 2.2 (a) shows the fields involved in the differenced form of the \dot{H} -equation, which is centered at $(\xi_i, \zeta_j, \tau_1 + \frac{1}{2}\Delta\tau)$. Straightforward algebraic manipulation leads to an expression for H_{ij}^2 of the form

$$H_{ij}^2 = H_C^2 + A_0 E_{\zeta i, j}^2 + A_1 E_{\zeta i+1, j}^2 + B_0 E_{\xi i, j}^2 + B_1 E_{\xi i, j+1}^2 \quad (2.2.9)$$

where

$$\begin{aligned} A_0 &= -\frac{\gamma_\xi}{2} \left(1 + \frac{\Delta\tau}{a\Delta\xi}\right) \\ A_1 &= -\frac{\gamma_\xi}{2} \left(1 - \frac{\Delta\tau}{a\Delta\xi}\right) \\ B_0 &= -\frac{\gamma_\zeta}{2} \left(1 + \frac{\Delta\tau}{\Delta\zeta}\right) \\ B_1 &= -\frac{\gamma_\zeta}{2} \left(1 - \frac{\Delta\tau}{\Delta\zeta}\right) \end{aligned} \quad (2.2.10)$$

and

$$H_C = H_{ij}^1 - A_1 E_{\zeta ij}^1 - A_0 E_{\zeta i+1, j}^1 - B_1 E_{\xi i, j}^1 - B_0 E_{\xi i, j+1}^1$$

The \dot{E}_ξ - and \dot{E}_ζ -equations (equations (2.2.5) and (2.2.6), respectively) are differenced by putting them into the form:

$$\frac{\partial \mathbf{E}}{\partial \tau} + k(\tau)\mathbf{E} = S(\tau) \quad (2.2.11)$$

The solution of equation (2.2.11) above (for $k(\tau)$ and $S(\tau)$ approximated by constants evaluated at mid-timestep) is used to advance the \mathbf{E} 's:

$$\mathbf{E}^2 = \mathbf{E}^1 e^{-\bar{k}\Delta\tau} + (1 - e^{-\bar{k}\Delta\tau}) \frac{\bar{S}}{\bar{k}} \quad (2.2.12)$$

The \dot{E}_ξ -equation and \dot{E}_ζ -equation are handled in exactly analogous fashions; we will give the details for the \dot{E}_ξ -equation. First, equation (2.2.5) is put into the form of equation (2.2.11). We use equation (2.2.12) to advance $(E_{\xi ij} + E_{\xi i, j+1})/2$ from τ_1 to τ_2 . Source terms are centered at mid-time in the (i, j) -th cell, as is the evaluation of $\partial H/\partial \tau$. The spatial derivative of H is handled as indicated in Figure 2.2. (b), explicitly, we use:

$$\left[\frac{\partial H}{\partial \tau} - \frac{\partial H}{\partial \zeta} \right] = \left\{ \frac{(H_{ij}^2 - H_{ij}^1)}{\Delta\tau} - \frac{1}{2} \left[\frac{(H_{i, j+1}^1 - H_{i, j}^1)}{\Delta\zeta u} + \frac{(H_{ij}^2 - H_{i, j-1}^2)}{\Delta\zeta L} \right] \right\} \quad (2.2.13)$$

At the z -axis boundary (i. e., $j = 1$ for the \dot{E}_ξ -equation or $i = 1$ for the \dot{E}_ζ -equation), one may wish to use a form of equation (2.2.13) for which $H_\varphi = 0$ along the z -axis. In that case (see Figure 2.2. (c)):

$$\left[\frac{\partial H}{\partial \tau} - \frac{\partial H}{\partial \zeta} \right] = \left\{ \frac{(H_{ij}^2 - H_{ij}^1)}{\Delta\tau} - \frac{1}{2} \left[\frac{(H_{i, j+1}^1 - H_{ij}^1)}{\Delta\zeta u} + \frac{H_{ij}^2 - (0)}{\left(\frac{\Delta\zeta}{2}\right)} \right] \right\} \quad (2.2.14)$$

Using either of the above forms for the H -field derivative terms in equation (2.2.5), we can manipulate equation (2.2.12) (as applied to the advanced \mathbf{E}_ξ^2 's) into the form:

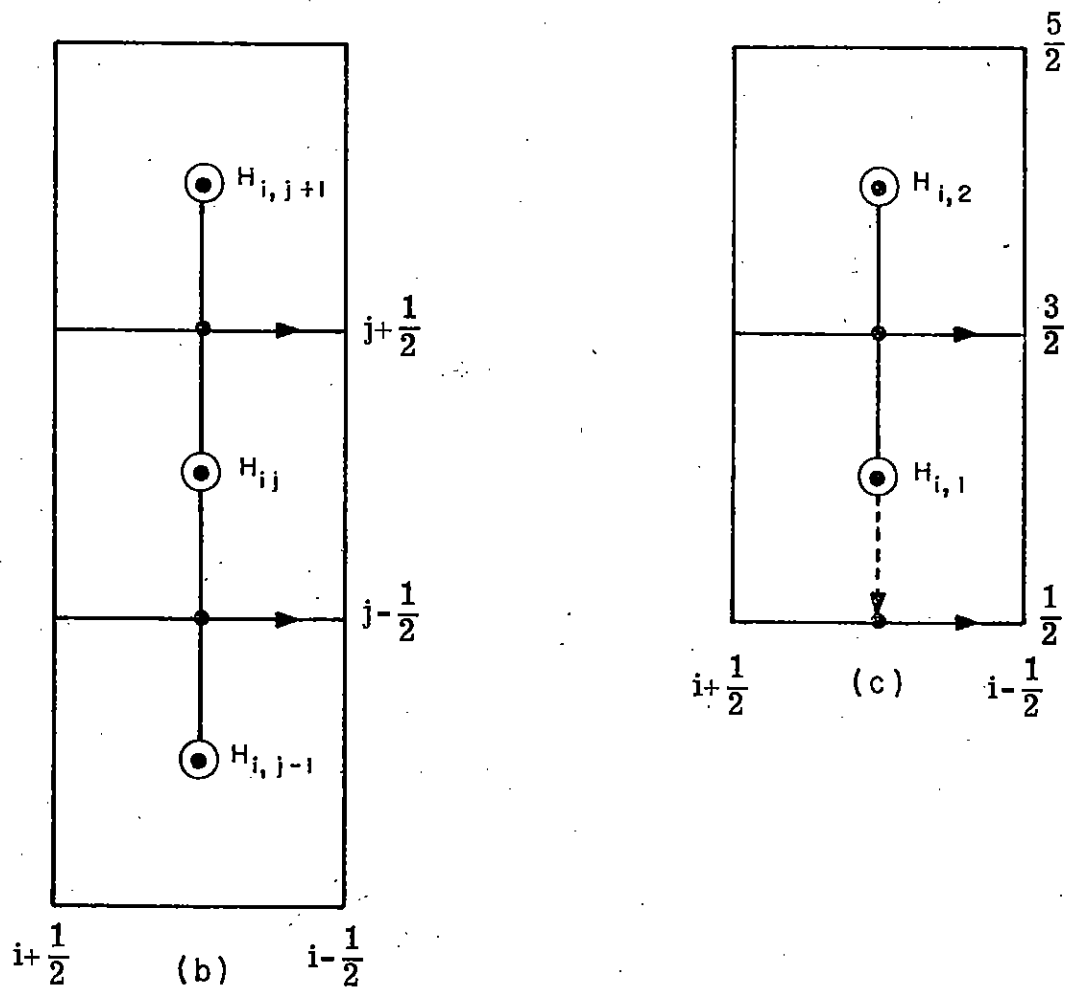
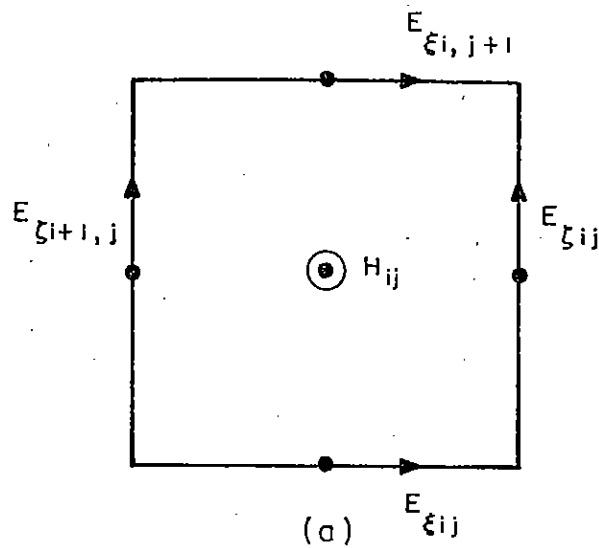


Figure 2.2. Specific Fields Involved in Typical Differencing for Equations 2.2.5 and 2.2.7.

$$E_{\xi i, j}^2 + E_{\xi i, j+1}^2 = E_{\xi c} + C_{1L} H_{ij}^2 + r_{\zeta L} H_{i, j-1}^2 \quad (2.2.15)$$

As before, the constants are functions of the old fields and known parameters. In particular, let us define

$$P = -2 \frac{(1 - e^{-k\Delta\tau})}{Z_0 \sigma \Delta\tau} \quad (2.2.16)$$

Then

$$C_{1L} = \begin{cases} P \cdot \left(1 - \frac{\Delta\tau}{2\Delta\zeta_L}\right), & \text{if } j > 1 \\ P \cdot \left(1 - \frac{\Delta\tau}{\Delta\zeta}\right), & \text{if } j = 1 \end{cases}$$

$$C_{1u} = P \cdot \left(1 - \frac{\Delta\tau}{2\Delta\zeta_u}\right)$$

$$r_{\zeta L} = \begin{cases} P \cdot \left(\frac{\Delta\tau}{2\Delta\zeta_L}\right), & \text{if } j > 1 \\ 0, & \text{if } j = 1 \end{cases}$$

$$r_{\zeta u} = P \cdot \left(\frac{\Delta\tau}{2\Delta\zeta_u}\right)$$

$$E_{\xi C} = \left(E_{\xi ij}^1 + E_{\xi i, j+1}^1\right) e^{-k\Delta\tau} - \frac{(1 - e^{-k\Delta\tau})}{\sigma} \cdot 2j_{\xi} - r_{\zeta u} H_{i, j+1}^1 - C_{1u} H_{ij}^1 \quad (2.2.17)$$

Exactly analogous results are obtained for the E_{ζ}^2 's, so that we must consider a set of equations which, for a typical cell, has the following appearance:

$$H_{ij} = H_c + A_0 E_{\zeta ij}^2 + A_1 E_{\zeta i+1, j}^2 + B_0 E_{\xi ij}^2 + B_1 E_{\xi i, j+1}^2 \quad (2.2.18)$$

$$E_{\zeta ij}^2 + E_{\zeta i+1, j}^2 = E_{\zeta c} + D_{1L} H_{ij}^2 + r_{\xi L} H_{i-1, j}^2 \quad (2.2.19)$$

$$E_{\xi i, j}^2 + E_{\xi ij+1}^2 = E_{\xi c} + C_{1L} H_{ij}^2 + r_{\zeta L} H_{i, j-1}^2 \quad (2.2.20)$$

2.2.3 Summary of Computational Procedure

The above equations can be used in an explicit manner, if $H_{i, j-1}^2$, $H_{i-1, j}^2$, $E_{\zeta i, j}^2$, and $E_{\xi i, j}^2$ are known, since equations (2.2.18) through (2.2.20) then become three equations in the three unknown fields $H_{i, j}^2$, $E_{\zeta i+1, j}^2$ and $E_{\xi i, j+1}^2$. The process is started from values of E and H along the z-axis and proceeds to some outer boundary, where outermost values of either E or H are assumed known from some boundary condition.

A variation can be made implicit in either direction (we will choose the ξ -direction). We disregard equation (2.2.19) and $H_{i-1, j}^2$ for $i = 1$ (rather than using a form of (2.2.19) with $H_{1/2, j}^2$ set at zero, as it is for the explicit method), and obtain a tridiagonal set of simultaneous equations for the E_{ζ} 's. One can readily obtain such a set by using equation (2.2.18) (for H_{ij}^2 and $H_{i-1, j}^2$) and (2.2.20) (for $E_{\xi i, j+1}^2$ and $E_{\xi i+1, j+1}^2$) in equation (2.2.19), eliminating unknown E_{ξ} 's and H_{ϕ} 's to obtain a relation involving E_{ζ} 's at $i-1$, i , and $i+1$. The computational procedure thus involves stepping from one j -value to another; at each value of j , one sweeps through a range of i to find the new fields at points along a given ellipsoidal coordinate surface.

2.2.4 Implementation of Algorithm "B"

Algorithm "B" was implemented by adaptation of another two-dimensional code, ARIADNE. ARIADNE was originally constructed to solve the prolate-spheroidal Maxwell's equations for a high-altitude burst situation. The new auxiliary machinery (necessary to set up problem geometry parameters, initialize source and field computations, furnish peripheral functions necessary to supply updated sources to the field algorithm, and output results) was readily programmed for the ground-burst situation by minor changes in ARIADNE, so that the field algorithm subroutine was the most significant aspect of the programming problems.

The algorithm was checked by the device of providing "invented" sources that corresponded to known fields. The procedure involved an initially assumed analytical form for $E_{\zeta}(\xi, \zeta, \tau)$ and $E_{\xi}(\xi, \zeta, \tau)$. Equation (2.2.7) may be used to find $H(\xi, \zeta, \tau)$, and equations (2.2.5) and (2.2.6) then solved (together with assumptions for $\sigma(\xi, \zeta, \tau)$) to give explicit expressions for the sources J_{ξ} and J_{ζ} . Using such invented sources, the algorithm should then numerically produce fields that closely correspond to the analytical form initially assumed. Results of such check comparisons for moderately-realistic geometry, sources, and time variation of the fields showed agreement to within about 5% over approximately 5 orders of magnitude of field variation. Detailed results will be discussed in Section 2.2.5.

Consistent with experience with ground-burst codes now in use, it was found that poor computational results were obtained unless source representations were smoothly varying in space and time. For this reason, analytic representations of current and conductivity were used as a convenient means to drive the field algorithm. Results for a sample problem show fields that vary with space and time in a physically reasonable way. Detailed results will be presented in the following section.

The details of the algorithm, as programmed, are given in Appendix B, which contains a FORTRAN listing of the field subroutine MARCH, together with a brief explanation of the subroutine structure and the variables used.

2.2.5 Some Sample Computational Results

Some computations were carried out for a rather simple, "toy" problem; a burst at HOB = 40 meters (near $I = 1$, $J = 1$) was considered, with purely radial Compton currents (and associated conductivity) given by a simple analytic form. Sources were considered to be zero beyond the surface $\zeta = 640$ meters; the ground was assumed to have constant conductivity (.01 mho/m) and dielectric constant $\epsilon = 5$. The computation grid in (ξ_I, ζ_J) -space is sketched in Figure 2.3, where the positions of points at which output was requested are indicated. The source region is restricted to the gridpoints (I, J) for which $1 \leq I \leq 40$ and $1 \leq J \leq 30$. The ground lies in the interval $40 < I \leq 45$ for all J in the grid. Field intensities and sources are tabulated, as a function of time, in Figures 2.4 through 2.8, the positions are indicated in the grid. The point labelled "9" is far up in the source region, and only a purely radial E-field is found there. Closer to the ground, the image-point wavefront can be seen moving upward perpendicular to the I-surfaces, as retarded time progresses.

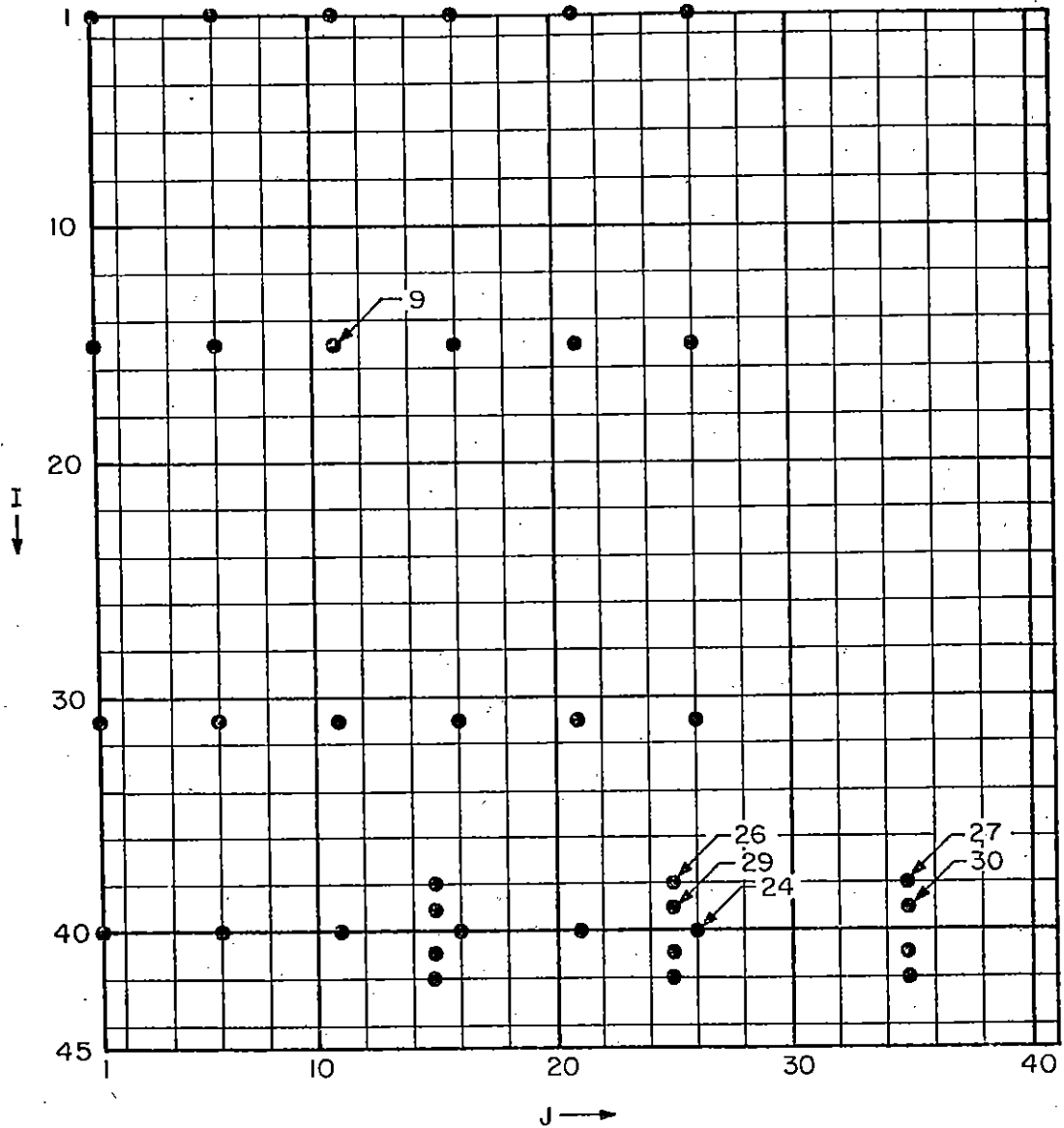


Figure 2.3. (I, J) Computation Grid for Sample Problem

CUMULATIVE TIME HISTORY AT 25-TH SAMPLE POINT

TIME	E-R	E-T	9-F	JG-R	JG-T	SIGMA
+1.600E-08	1.277E-13	-1.458E-07	-1.458E-07	2.003E-13	-1.410E-23	2.003E-16
+1.200E-08	2.025E-09	-1.792E-06	-1.792E-06	2.204E-12	8.078E-23	2.204E-15
-3.800E-08	2.358E-08	-1.985E-05	-1.985E-05	2.426E-11	-1.292E-26	2.426E-14
-3.400E-08	2.620E-07	-2.137E-04	-2.137E-04	2.669E-10	-1.034E-25	2.669E-13
-3.100E-08	2.832E-06	-2.400E-03	-2.400E-03	2.938E-09	-1.654E-24	2.938E-12
-2.600E-08	3.494E-05	-2.566E-02	-2.566E-02	3.233E-08	0.	3.233E-11
-2.200E-08	2.522E-04	-2.170E-01	-2.170E-01	3.558E-07	-1.059E-22	3.558E-10
-1.800E-08	5.096E-03	-8.611E-01	-8.611E-01	3.915E-06	0.	3.915E-09
-1.400E-08	-1.091E-02	4.802E-01	4.802E-01	4.308E-05	-2.711E-20	4.308E-08
-1.000E-08	-1.169E-01	-3.549E-02	-3.326E-02	4.737E-04	-4.337E-19	4.737E-07
-6.000E-09	-1.286E+00	1.337E-01	1.053E-01	5.148E-03	-1.735E-18	5.148E-06
-2.000E-09	-1.278E+01	2.397E-02	2.657E-02	4.817E-02	0.	4.817E-05
2.000E-09	-6.735E+01	1.823E-03	8.593E-03	1.713E-01	-1.665E-16	1.713E-04
6.000E-09	-1.423E+02	5.989E-03	1.136E-02	1.801E-01	-3.551E-17	1.801E-04
1.000E-08	-2.016E+02	6.275E-03	1.280E-02	1.452E-01	0.	1.452E-04
1.400E-08	-2.455E+02	8.261E-03	1.589E-02	1.144E-01	-5.551E-17	1.144E-04
1.800E-08	-2.784E+02	4.613E-02	5.820E-02	9.003E-02	-2.776E-17	9.003E-05
2.200E-08	-3.031E+02	2.794E-01	3.080E-01	7.084E-02	-5.551E-17	7.084E-05
2.600E-08	-3.217E+02	1.173E+00	1.257E+00	5.573E-02	-5.551E-17	5.573E-05
3.000E-08	-3.322E+02	3.780E+00	3.994E+00	4.385E-02	-2.776E-17	4.385E-05
3.400E-08	-3.444E+02	1.336E+01	1.656E+01	3.450E-02	-2.776E-17	3.450E-05
3.800E-08	-3.494E+02	2.388E+01	2.411E+01	2.714E-02	0.	2.714E-05
+2.00E-08	-3.531E+02	4.595E+01	4.886E+01	2.135E-02	-6.939E-18	2.135E-05
4.600E-08	-3.462E+02	8.627E+01	8.948E+01	1.680E-02	0.	1.680E-05
5.000E-08	-3.375E+02	1.451E+02	1.501E+02	1.322E-02	-1.388E-17	1.322E-05

Figure 2.4. Fields Near 530 Meters Ground Range and 33 Meters Above the Ground

CUMULATIVE TIME HISTORY AT 29-TH SAMPLE POINT

TIME	E-R	E-T	B-P	JC-R	JC-T	SIGMA
-4.600E-03	3.561E-11	-1.397E-07	-1.397E-07	1.985E-13	-1.010E-28	1.985E-16
-4.200E-08	1.631E-19	-1.723E-06	-1.723E-06	2.185E-12	-8.078E-28	2.185E-13
-3.800E-08	2.279E-18	-1.309E-05	-1.909E-05	2.403E-11	-6.462E-27	2.404E-14
-3.400E-08	2.623E-17	-2.101E-04	-2.101E-04	2.546E-10	1.134E-25	2.644E-13
-3.000E-08	2.898E-16	-2.306E-03	-2.306E-03	2.912E-09	-1.654E-24	2.912E-12
-2.600E-08	3.124E-15	-2.466E-02	-2.466E-02	3.205E-08	-1.323E-23	3.205E-11
-2.200E-08	2.832E-14	-2.093E-01	-2.093E-01	3.527E-07	-1.059E-22	3.527E-10
-1.800E-08	1.364E-03	-8.445E-01	-8.445E-01	3.381E-06	0.0	3.881E-09
-1.400E-08	-1.367E-13	+1.988E-01	4.205E-01	4.271E-05	0.0	4.271E-08
-1.000E-08	-8.608E-02	2.581E-01	2.606E-01	7.696E-04	-2.168E-19	4.696E-07
-6.000E-09	-1.252E+00	1.443E-01	1.472E-01	5.102E-03	-1.735E-18	5.102E-06
-2.000E-09	-1.266E+01	9.732E-03	1.314E-02	4.774E-02	0.0	4.774E-05
2.000E-09	-6.678E+01	-7.856E-03	-7.856E-03	1.698E-01	0.0	1.698E-04
6.000E-09	-1.412E+02	-9.638E-03	-5.782E-03	1.785E-01	-5.551E-17	1.785E-04
1.000E-08	-1.999E+02	3.384E-02	3.378E-02	1.439E-01	0.0	1.439E-04
1.400E-08	-2.433E+02	3.995E-01	4.414E-01	1.134E-01	-1.110E-16	1.134E-04
1.800E-08	-2.753E+02	1.862E+00	2.607E+00	8.925E-02	0.0	8.925E-05
2.200E-08	-2.983E+02	3.957E+00	3.356E+00	7.122E-02	-2.776E-17	7.022E-05
2.600E-08	-3.141E+02	1.516E+01	1.606E+01	3.524E-02	-2.776E-17	3.524E-05
3.000E-08	-3.236E+02	3.285E+01	3.466E+01	4.346E-02	-2.776E-17	4.346E-05
3.400E-08	-3.273E+02	6.281E+01	6.591E+01	3.419E-02	0.0	3.419E-05
3.800E-08	-3.256E+02	1.080E+02	1.136E+02	2.699E-02	-1.388E-17	2.699E-05
4.200E-08	-3.191E+02	1.727E+02	1.799E+02	2.117E-02	0.0	2.117E-05
4.600E-08	-3.686E+02	2.551E+02	2.649E+02	1.665E-02	6.939E-18	1.665E-05
5.000E-08	-2.951E+02	3.533E+02	3.659E+02	1.319E-02	-6.939E-18	1.319E-05

Figure 2.5. Fields Near 530 Meters Ground Range and 20 Meters Above the Ground

CUMULATIVE TIME HISTORY AT 24-TH SAMPLE POINT

TIME	E-R	E-T	B-P	JC-R	JC-T	SIGMA
-4.500E-08	1.692E-19	-1.3+7E-07	-1.3+6E-07	1.654E-13	0.	1.654E-16
-4.200E-18	2.073E-18	-1.606E-06	-1.605E-16	1.820E-12	8.678E-28	1.820E-15
-3.800E-08	2.4+0E-07	-1.771E-05	-1.771E-05	2.003E-11	1.292E-25	2.003E-14
-3.+00E-18	2.704E-16	-1.949E-04	-1.9+7E-04	2.204E-10	1.034E-25	2.204E-13
-3.000E-18	2.975E-15	-2.139E-03	-2.137E-03	2.+25E-09	8.272E-25	2.425E-12
-2.600E-08	3.2+0E-04	-2.285E-02	-2.283E-02	2.669E-08	1.323E-23	2.669E-11
-2.200E-08	3.216E-03	-1.921E-01	-1.919E-01	2.937E-07	0.	2.937E-10
-1.800E-08	2.655E-12	-7.326E-01	-7.312E-01	3.232E-06	8.470E-22	3.232E-09
-1.+00E-08	3.38E-12	8.953E-01	8.936E-01	3.57E-05	1.355E-20	3.557E-08
-1.000E-08	-7.211E-12	1.611E-01	1.63+E-01	3.911E-04	0.	3.911E-07
-6.000E-09	-1.054E+11	-3.329E-02	-3.176E-02	4.249E-03	1.735E-19	4.249E-06
-2.000E-09	-1.025E+11	-4.823E-02	-4.661E-02	3.976E-02	0.	3.976E-05
2.000E-09	-3.581E+11	2.537E-02	3.51E-02	1.+1+E-01	0.	1.414E-04
5.000E-09	-1.184E+12	5.737E-01	6.37+E-01	1.+87E-01	5.551E-17	1.+87E-04
1.000E-08	-1.675E+12	3.17+E+01	3.431E+01	1.199E-01	0.	1.199E-04
1.400E-08	-2.028E+12	1.008E+01	1.079E+01	9.+46E-02	8.327E-17	9.446E-05
1.800E-08	-2.274E+12	2.37+E+01	2.529E+01	7.+33E-02	2.776E-17	7.433E-05
2.200E-08	-2.+35E+12	4.551E+01	4.932E+01	5.348E-02	0.	5.848E-05
2.600E-08	-2.529E+12	8.120E+01	8.470E+01	4.601E-02	0.	4.601E-05
3.000E-08	-2.672E+12	1.257E+02	1.322E+02	3.620E-02	2.776E-17	3.620E-05
3.400E-08	-2.576E+12	1.828E+02	1.915E+02	2.848E-02	1.388E-17	2.848E-05
3.800E-08	-2.55+E+12	2.+99E+02	2.6J8E+02	2.241E-02	6.939E-18	2.241E-05
4.200E-08	-2.518E+12	3.2+3E+12	3.378E+02	1.763E-02	0.	1.763E-05
4.600E-08	-2.+48E+12	4.025E+02	4.157E+02	1.387E-02	6.939E-18	1.387E-05
5.000E-08	-2.+48E+12	4.0J8E+02	4.958E+02	1.391E-02	0.	1.991E-05

Figure 2.6. Fields Near 550 Meters Ground Range and 7 Meters Above the Ground

CUMULATIVE TIME HISTORY AT 27-TH SAMPLE POINT

TIME	E-R	E-T	3-F	JC-R	JC-T	SIGMA
-4.500E-08	9.227E-11	-1.993E-07	-1.993E-07	0.	0.	0.
-4.200E-08	1.392E-09	-1.344E-06	-1.344E-06	0.	0.	0.
-3.800E-08	1.587E-08	-1.487E-05	-1.487E-05	0.	0.	0.
-3.400E-08	1.752E-07	-1.637E-04	-1.637E-04	0.	0.	0.
-3.000E-08	1.939E-06	-1.797E-03	-1.797E-03	0.	0.	0.
-2.600E-08	2.199E-05	-1.921E-02	-1.921E-02	0.	0.	0.
-2.200E-08	1.879E-04	-1.619E-01	-1.619E-01	0.	0.	0.
-1.800E-08	7.855E-04	-6.324E-01	-6.324E-01	0.	0.	0.
-1.400E-08	-3.162E-04	3.757E-01	3.757E-01	0.	0.	0.
-1.000E-08	1.344E-03	1.915E-02	1.915E-02	0.	0.	0.
-6.000E-09	8.261E-03	3.692E-02	3.737E-02	0.	0.	0.
-2.000E-09	1.150E-02	-6.997E-02	-6.910E-02	0.	0.	0.
-2.000E-09	1.642E-02	-7.406E-01	-7.395E-01	0.	0.	0.
6.000E-09	9.422E-03	-1.965E+00	-1.564E+00	0.	0.	0.
1.000E-08	9.254E-03	-2.410E+00	-2.409E+00	0.	0.	0.
1.400E-08	1.473E-02	-2.968E+00	-2.966E+00	0.	0.	0.
1.800E-08	4.415E-02	-3.319E+00	-3.316E+00	0.	0.	0.
2.200E-08	1.471E-01	-3.281E+00	-3.272E+00	0.	0.	0.
2.600E-08	3.855E-01	-2.375E+00	-2.351E+00	0.	0.	0.
3.000E-08	9.032E-01	3.132E-01	3.742E-01	0.	0.	0.
3.400E-08	1.853E+00	5.249E+00	6.370E+00	0.	0.	0.
3.800E-08	3.451E+00	1.742E+01	1.755E+01	0.	0.	0.
4.200E-08	5.896E+00	3.514E+01	3.652E+01	0.	0.	0.
4.600E-08	9.262E+00	6.459E+01	6.517E+01	0.	0.	0.
5.000E-08	1.359E+01	1.142E+02	1.051E+02	0.	0.	0.

Figure 2.7. Fields Near 730 Meters Ground Range and 45 Meters Above the Ground

CUMULATIVE TIME HISTORY AT 30-TH SAMPLE POINT

TIME	E-R	E-T	9-P	JC-R	JC-T	SIGMA
-4.600E-08	5.481E-11	-1.345E-07	-1.6+6E-07	0.	0.	0.
-4.200E-08	1.149E-09	-1.291E-06	-1.291E-06	0.	0.	0.
-3.800E-08	1.550E-08	-1.439E-05	-1.439E-05	0.	0.	0.
-3.400E-08	1.765E-07	-1.574E-04	-1.574E-04	0.	0.	0.
-3.000E-08	1.949E-06	-1.727E-03	-1.727E-03	0.	0.	0.
-2.600E-08	2.109E-05	-1.846E-02	-1.846E-02	0.	0.	0.
-2.200E-08	1.985E-04	-1.563E-01	-1.563E-01	0.	0.	0.
-1.800E-08	1.228E-03	-6.222E-01	-6.222E-01	0.	0.	0.
-1.400E-08	5.164E-03	3.491E-01	3.494E-01	0.	0.	0.
-1.000E-08	1.647E-02	1.569E-01	1.679E-01	0.	0.	0.
-6.000E-09	1.814E-02	1.629E-01	1.641E-01	0.	0.	0.
-2.000E-09	1.201E-02	-1.350E-01	-1.341E-01	0.	0.	0.
2.000E-09	9.216E-03	-7.350E-01	-7.843E-01	0.	0.	0.
6.000E-09	1.172E-02	-1.680E+00	-1.679E+00	0.	0.	0.
1.000E-08	3.521E-02	-2.341E+00	-2.339E+00	0.	0.	0.
1.400E-08	1.186E-01	-2.486E+00	-2.479E+00	0.	0.	0.
1.800E-08	3.235E-01	-1.562E+00	-1.542E+00	0.	0.	0.
2.200E-08	7.295E-01	1.352E+00	1.395E+00	0.	0.	0.
2.600E-08	1.422E+00	7.519E+00	7.598E+00	0.	0.	0.
3.000E-08	2.475E+00	1.842E+01	1.854E+01	0.	0.	0.
3.400E-08	5.922E+00	3.552E+01	3.568E+01	0.	0.	0.
3.800E-08	5.723E+00	5.993E+01	6.008E+01	0.	0.	0.
4.200E-08	7.741E+00	9.213E+01	9.212E+01	0.	0.	0.
4.600E-08	9.722E+00	1.312E+02	1.311E+02	0.	0.	0.
5.000E-08	1.131E+01	1.756E+02	1.751E+02	0.	0.	0.

Figure 2.8. Fields Near 730 Meters Ground Range and 27 Meters Above the Ground

2.3 Real-time Fields Algorithm in Cylindrical Coordinates for an Infinitely Conducting Ground: Algorithm "C"

2.3.1 Theoretical Considerations

The Maxwell curl equations in MKS units are

$$\nabla \times \vec{E} = - \frac{\partial \vec{B}}{\partial t} \quad (2.3.1)$$

$$\nabla \times \vec{B} = \mu \vec{J} + \mu \sigma \vec{E} + \mu \epsilon \frac{\partial \vec{E}}{\partial t} \quad (2.3.2)$$

with the implied constituent relations

$$\vec{B} = \mu \vec{H} \quad \vec{D} = \epsilon \vec{E}$$

for μ, ϵ constant.

Figure 2.9 shows the coordinate system which is to be considered.

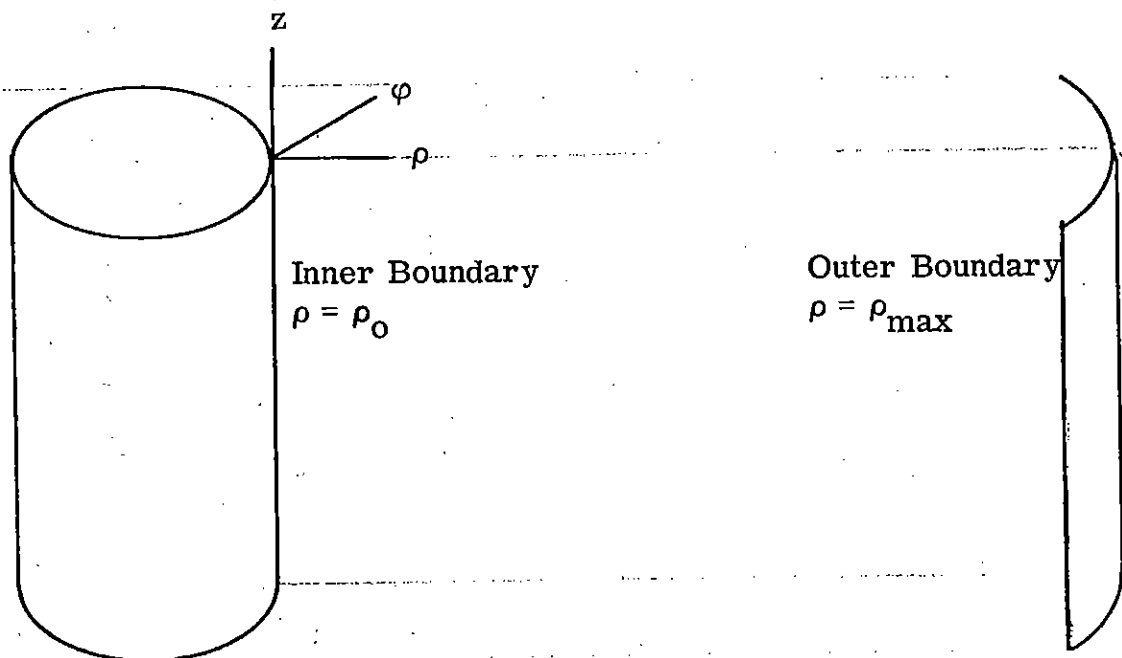


Figure 2.9. Coordinate Grid for Algorithm "C"

The near surface burst problem is azimuthally symmetric if the source is. In this case none of the variables are a function of $\hat{\phi}$ and the curl equation becomes

$$-\frac{\partial E_{\phi}}{\partial z} \hat{\rho} + \left(\frac{\partial E_{\rho}}{\partial z} - \frac{\partial E_z}{\partial \rho} \right) \hat{\phi} + \frac{1}{\rho} \frac{\partial(\rho E_{\rho})}{\partial \rho} = -\frac{\partial B_{\rho}}{\partial t} \hat{\phi} - \frac{\partial B_{\phi}}{\partial t} \hat{\rho} - \frac{\partial B_z}{\partial t} \hat{z} \quad (2.3.3)$$

$$-\frac{\partial B_{\phi}}{\partial z} \hat{\rho} + \left(\frac{\partial B_{\rho}}{\partial z} - \frac{\partial B_z}{\partial \rho} \right) \hat{\phi} + \frac{1}{\rho} \frac{\partial(\rho B_{\phi})}{\partial \rho} \hat{z} = \left(\mu J_{\rho} + \mu \sigma E_{\rho} + \mu \epsilon \frac{\partial E_{\rho}}{\partial t} \right) \hat{\rho} \\ + \left(\mu J_{\phi} + \mu \sigma E_{\phi} + \mu \epsilon \frac{\partial E_{\phi}}{\partial t} \right) \hat{\phi} + \left(\mu J_z + \mu \sigma E_z + \mu \epsilon \frac{\partial E_z}{\partial t} \right) \hat{z} \quad (2.3.4)$$

It is to be noted that due to azimuthal symmetry the equation may be separated into two sets which are coupled only by the dependence of the air chemistry parameter on the total electric field.

The TM equations are

$$\frac{\partial E_{\rho}}{\partial t} = -\frac{J_{\rho}}{\epsilon} - \frac{\sigma}{\epsilon} E_{\rho} - \frac{1}{\sqrt{\mu\epsilon}} \frac{\partial B_{\phi}}{\partial z} \quad (2.3.5)$$

$$\frac{\partial E_z}{\partial t} = -\frac{J_z}{\epsilon} - \frac{\sigma}{\epsilon} E_z - \frac{1}{\rho\sqrt{\mu\epsilon}} \frac{\partial(\rho B_{\phi})}{\partial \rho} \quad (2.3.6)$$

$$\frac{\partial B_{\phi}}{\partial t} = \frac{\partial E_z}{\partial \rho} - \frac{\partial E_{\rho}}{\partial z} \quad (2.3.7)$$

The TE equations are

$$\frac{\partial B_{\rho}}{\partial t} = \frac{\partial E_{\phi}}{\partial z} \quad (2.3.8)$$

$$\frac{\partial B_z}{\partial t} = -\frac{1}{\rho} \frac{\partial}{\partial \rho} (\rho E_{\phi}) \quad (2.3.9)$$

$$\frac{\partial E_{\phi}}{\partial t} = -\frac{J_{\phi}}{\epsilon} - \frac{\sigma}{\epsilon} E_{\phi} + \frac{1}{\sqrt{\mu\epsilon}} \left(\frac{\partial B_{\rho}}{\partial z} - \frac{\partial B_z}{\partial \rho} \right) \quad (2.3.10)$$

If B_{ρ} , B_z and E_{ϕ} are initially zero and J_{ϕ} is zero for all time, then these components of the fields will remain zero. Only the TM set of equations needs to be solved.

Make the substitution $z = -n$ in the TM equation

$$\frac{\partial E_{\rho}}{\partial t} = -\frac{J_{\rho}}{\epsilon} - \frac{\sigma}{\epsilon} E_{\rho} + \frac{1}{\sqrt{\mu\epsilon}} \frac{\partial B_{\phi}}{\partial n} \quad (2.3.11)$$

$$\frac{\partial E_z}{\partial t} = -\frac{J_z}{\epsilon} - \frac{\sigma}{\epsilon} E_z + \frac{1}{\rho\sqrt{\mu\epsilon}} \frac{\partial(\rho B_{\phi})}{\partial \rho} \quad (2.3.12)$$

$$\frac{\partial B_{\phi}}{\partial t} = \frac{\partial E_z}{\partial \rho} + \frac{\partial E_{\rho}}{\partial n} \quad (2.3.13)$$

Let

$$B_{\rho} = B'_{\phi}$$

$$E_{\rho} = -E'_{\rho}$$

$$E_z = E'_z$$

$$J_{\rho} = -J'_{\rho}$$

$$J_z = J'_z$$

Then we obtain

$$\frac{\partial E'_{\rho}}{\partial t} = -\frac{J'_{\rho}}{\epsilon} - \frac{\sigma}{\epsilon} E'_{\rho} - \frac{1}{\sqrt{\mu\epsilon}} \frac{\partial B'_{\phi}}{\partial n} \quad (2.3.14)$$

$$\frac{\partial E'_{z}}{\partial t} = -\frac{J'_{z}}{\epsilon} + \frac{1}{\sqrt{\mu\epsilon}\rho} \frac{\partial(\rho B'_{\phi})}{\partial \rho} \quad (2.3.15)$$

$$\frac{\partial B'_{\phi}}{\partial t} = \frac{\partial E'_{z}}{\partial \rho} - \frac{\partial E'_{\rho}}{\partial n} \quad (2.3.16)$$

The boundary condition on E'_{ρ} is the same as that on E_{ρ} , namely

$$E'_{\rho} \rightarrow 0 \text{ as } \rho \rightarrow \infty$$

The field E'_{ρ} , E'_{z} , B'_{ϕ} produced by the source J'_{ρ} , J'_{z} at the point ρ, n, t is identical to the field E_{ρ} , E_z , B_{ϕ} produced by the source J_{ρ} , J_z at r, z, t .

To obtain fields above the earth due to a perfectly conducting earth, add the two sets of fields calculated subject to the condition that $J = 0$ for $z < 0$ and $J' = 0$ for $z > 0$. Then at the plane $z = 0$, the ρ component of the electric field is zero, which is precisely the required boundary condition, subject to the condition

$$\mu'(\rho, z, t) = \mu(\rho, -z, t)$$

$$\epsilon'(\rho, z, t) = \epsilon(\rho, -z, t)$$

$$\sigma'(\rho, z, t) = \sigma(\rho, -z, t)$$

For ease in later implementing a varying grid size, make the following transformations

$$x = f(\rho) \quad \rho = F(x)$$

$$y = y(z) \quad Z = G(\mu)$$

so that the corresponding partial derivatives transform according to

$$\frac{\partial}{\partial \rho} \rightarrow \frac{\partial f}{\partial \rho} \frac{\partial}{\partial x}$$

$$\frac{\partial}{\partial z} \rightarrow \frac{\partial g}{\partial z} \frac{\partial}{\partial y}$$

With $FP = \partial f / \partial \rho$ and $GP = \partial g / \partial z$ the TM set of equations becomes

$$\frac{\partial E_{\rho}}{\partial t} = -\frac{J_{\rho}}{\epsilon} - \frac{\sigma}{\epsilon} E_{\rho} - \frac{GP}{\sqrt{\mu\epsilon}} \frac{\partial B_{\varphi}}{\partial y} \quad (2.3.17)$$

$$\frac{\partial E_z}{\partial t} = -\frac{J_z}{\epsilon} - \frac{\sigma}{\epsilon} E_z - \frac{1}{\sqrt{\mu\epsilon}} \left(FP \frac{\partial B_{\varphi}}{\partial x} + \frac{B_{\varphi}}{F} \right) \quad (2.3.18)$$

$$\frac{\partial B_{\varphi}}{\partial t} = FP \frac{\partial E_z}{\partial x} - GP \frac{\partial E_{\rho}}{\partial y} \quad (2.3.19)$$

The above equations are the ones to be finite differenced as described in the next section.

2.3.2 Finite Difference Methods

The following notation will be used on all the diagrams. The values of E_{ρ} used at the i, j step are denoted by \diamond , values of E_z by Δ and values of B_{φ} by \circ . It is to be noted that E_z and B_{φ} are defined at the grid points, E_{ρ} midway between the grid points. The superscripts 1 refer to time (t) and superscripts 2 refer to time ($t + \Delta t$).

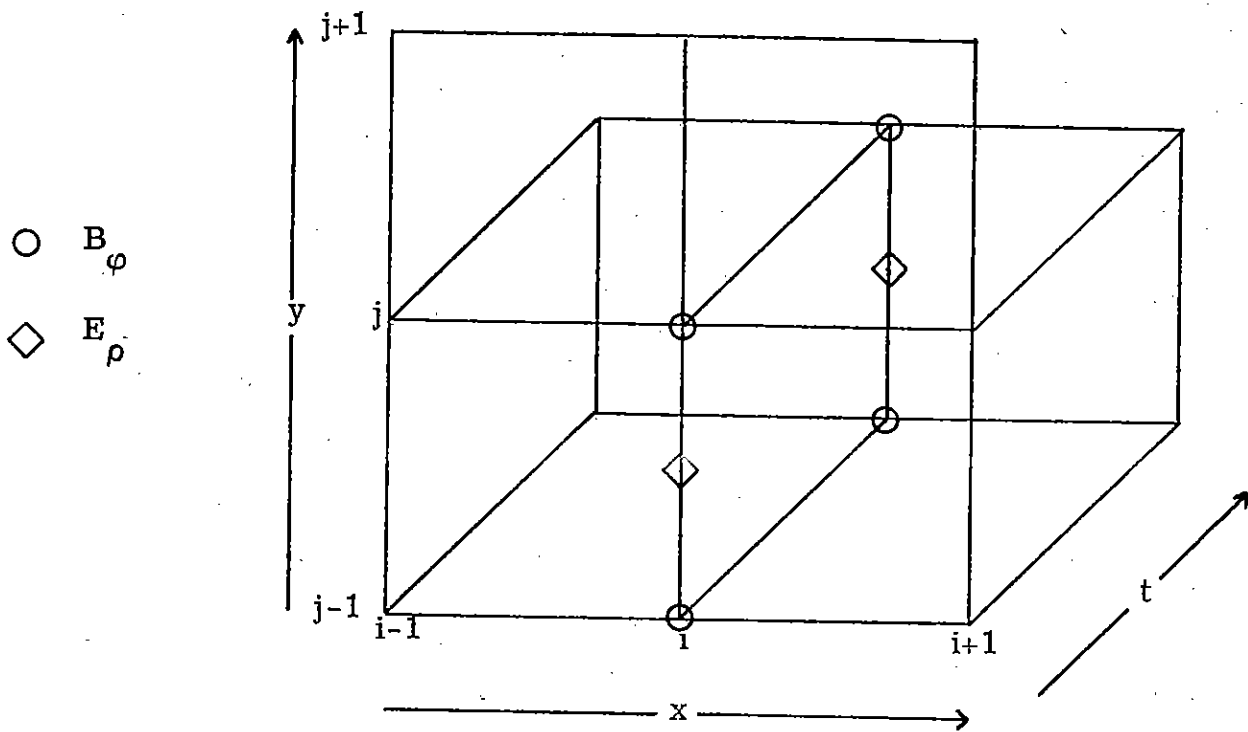


Figure 2.10. Differencing for Equation 2.3.17

Equation (2.3.17)

$$\frac{\partial E_{\rho}}{\partial t} + \frac{\sigma}{\epsilon} E_{\rho} = -\frac{J_{\rho}}{\epsilon} - \frac{GP}{\sqrt{\mu\epsilon}} \frac{\partial B_{\phi}}{\partial y}$$

will be differenced centered at $(i, j-1/2, t+\Delta t/2)$. Both equations (2.3.17) and (2.3.18) are of the form

$$\frac{dF}{dt} + AF = B \tag{2.3.20}$$

This equation has an exact solution given by

$$F(\ell) = F_0 e^{-\int_0^\ell A(\ell') d\ell'} + e^{-\int_0^\ell A(\ell') d\ell'} \int_0^\ell e^{\int_0^{\ell'} A(\ell'') d\ell''} B(\ell') d\ell'$$

A first order approximation to solution valid for variations in A and B is

$$F(\ell) = F(0) e^{-A(\ell/2)\ell} + \left(1 - e^{-A(\ell/2)\ell}\right) \frac{B(\ell/2)}{A(\ell/2)}$$

Equation (2.3.17) differenced in this form is

$$E_{\rho ij-1}^2 = E_{\rho ij-1}^1 e^{-\theta} + (1 - e^{-\theta}) \left[\frac{\psi_1}{\gamma_1} \right]_{ij-1/2}^{1/2} \quad (2.3.21)$$

where

$$\theta_1 = \gamma_1 \Delta t$$

$$\gamma_1 = \sigma/\epsilon \Big|_{t=t+\Delta t/2}$$

$$\psi_1 = -\frac{J_{rij-1}^{1/2}}{\epsilon} - \frac{GP_{ij-1}}{2\sqrt{\mu\epsilon} \Delta y} \left[B_{\phi ij}^1 - B_{\phi ij-1}^1 + B_{\phi ij}^2 - B_{\phi ij-1}^2 \right]$$

Define the following constant

$$A_1 = \frac{(1 - e^{-\theta_1})}{\gamma_1} \frac{GP_{ij-1}}{2\sqrt{\mu\epsilon} \Delta y}$$

$$C_1 = E_{\rho ij-1}^1 e^{-\theta_1} + \frac{(1 - e^{-\theta_1})}{\gamma_1} \left[-\frac{J_{\rho ij-1}}{\epsilon} - \frac{GP_{ij}}{2\sqrt{\mu\epsilon} \Delta y} \left(B_{\phi ij}^1 - B_{\phi ij-1}^1 \right) \right]$$

Equation (2.3.21) can be written

$$E_{\rho ij-1}^2 + A_1 B_{\phi ij}^2 - A_1 B_{\phi ij-1}^2 = C_1 \quad (2.3.22)$$

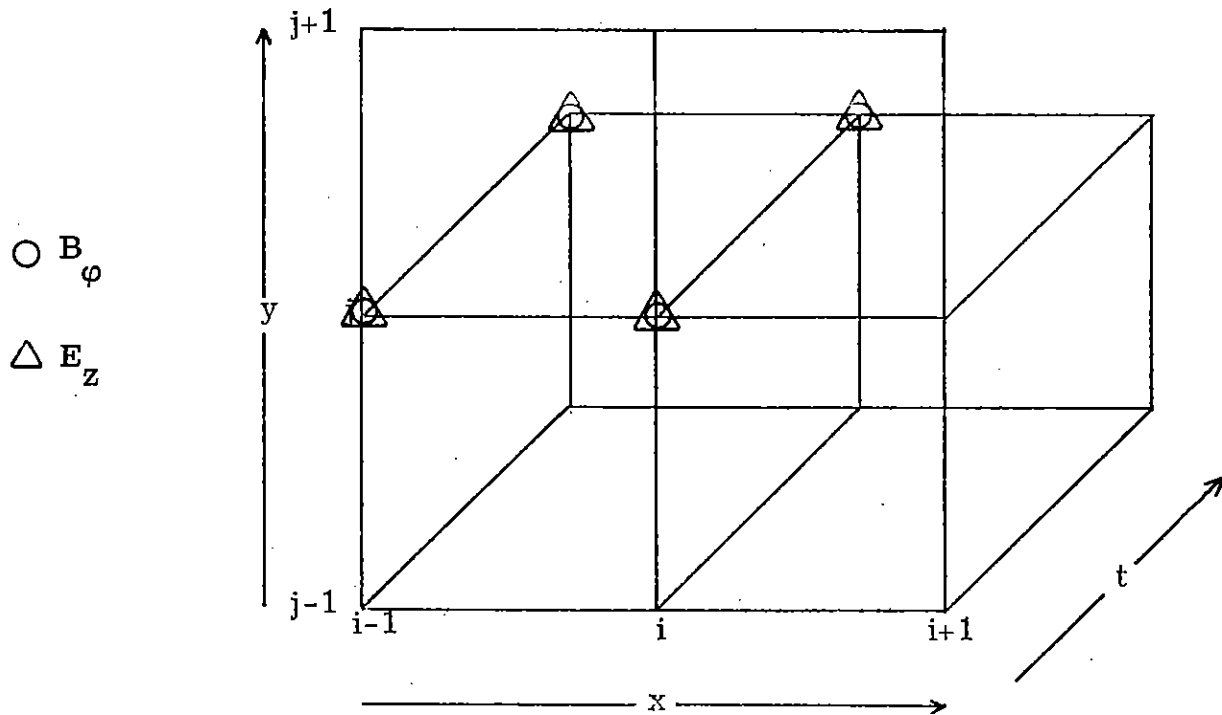


Figure 2.11. Differencing for Equation 2.3.18

Equation (2.3.18)

$$\frac{\partial E_z}{\partial t} + \frac{\sigma}{\epsilon} E_z = -\frac{J_z}{\epsilon} - \frac{FP}{\sqrt{\mu\epsilon}} \frac{\partial B_\phi}{\partial x} - \frac{1}{F\sqrt{\mu\epsilon}} B_\phi$$

will be centered differenced at $(i-1/2, j, t+\Delta t/2)$. The finite difference form of equation (2.3.18) is

$$\frac{E_{zi-1j}^2 + E_{zij}^2}{2} = \frac{(E_{zi-1j}^1 + E_{zij}^1)}{2} e^{-\theta} + (1 - e^{-\theta}) \left[\frac{\psi_2}{\gamma} \right]_{i-1/2j}^{t+\Delta t/2} \quad (2.3.23)$$

where

$$\theta_2 = \gamma_2 \Delta t$$

$$\gamma_2 = \sigma / \epsilon$$

$$\begin{aligned} \psi_2 = & -\frac{J_{zi-1j}^{1/2}}{\epsilon} - \frac{FP_{i-1j}}{2\sqrt{\mu\epsilon}\Delta x} \left[B_{\phi ij}^1 - B_{\phi i-1j}^1 + B_{\phi ij}^2 - B_{\phi i-1j}^2 \right] \\ & - \frac{1}{4F_{i-1/2j}\sqrt{\mu\epsilon}} \left[B_{\phi i-1j}^2 + B_{\phi i-1j}^1 + B_{\phi ij}^2 + B_{\phi ij}^1 \right] \end{aligned}$$

Define the following constants

$$A_2 = \left[\frac{(1 - e^{-\theta_2})}{\gamma_2} \cdot 2 \left(\frac{FP_{i-1j}}{2\sqrt{\mu\epsilon}\Delta x} + \frac{1}{2F_{i-1j}\sqrt{\mu\epsilon}} \right) \right]$$

$$\begin{aligned} C_2 = & E_{zi-1j}^2 + (E_{zi-1j}^1 + E_{zij}^1) e^{-\theta_2} + \frac{2(1 - e^{-\theta_2})}{\gamma_2} \left[\frac{-J_{zi-1j}}{\epsilon} - \frac{FP_{i-1j}}{2\sqrt{\mu\epsilon}\Delta x} \right. \\ & \left. (B_{\phi ij}^1 - B_{\phi i-1j}^1 - B_{\phi i-1j}^2) - \frac{1}{2F_{i-1j}\sqrt{\mu\epsilon}} (B_{\phi i-1j}^2 + B_{\phi i-1j}^1 + B_{\phi ij}^1) \right] \end{aligned}$$

Equation (2.3.23) becomes

$$E_{zij}^2 + A_2 B_{\phi ij}^2 = C_2 \quad (2.3.24)$$

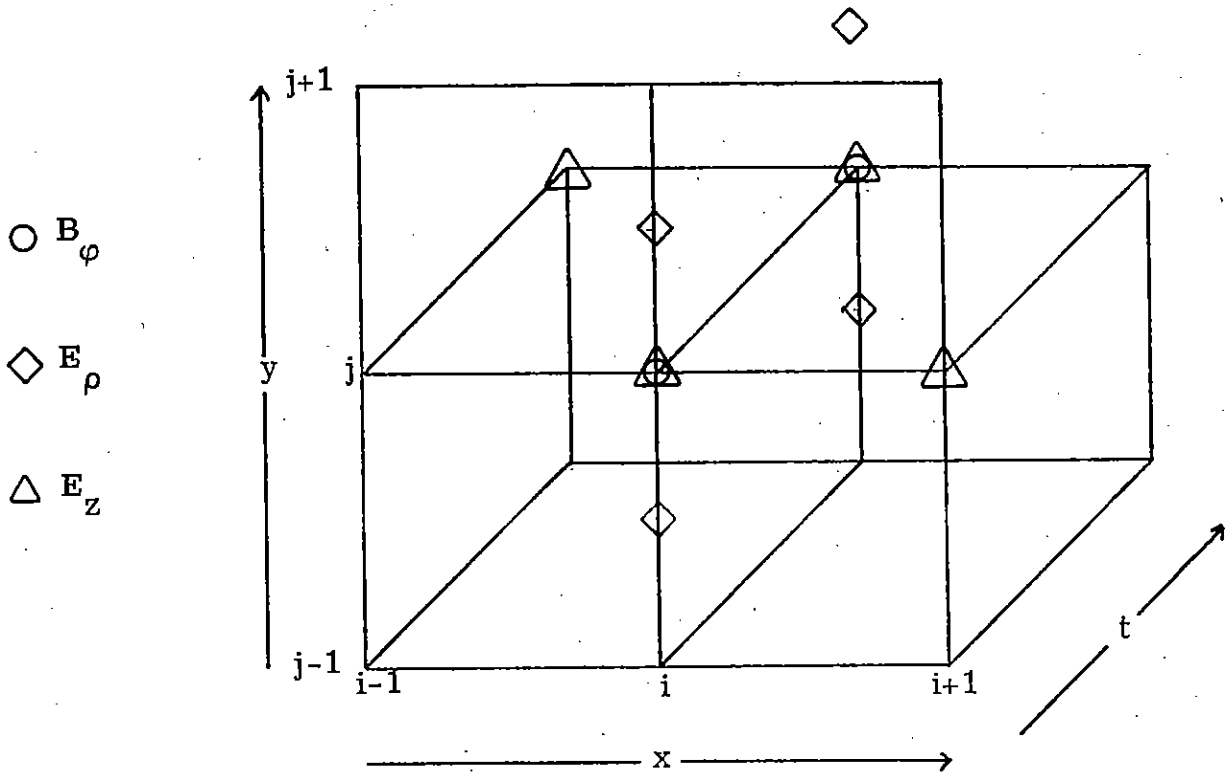


Figure 2.12. Differencing for Equation 2.3.19

Equation (2.3.19)

$$\frac{\partial B_{\phi}}{\partial t} = FP \frac{\partial E_z}{\partial x} - GP \frac{\partial E_{\rho}}{\partial y}$$

will be differenced, centered at $(i, j, t + \Delta t/2)$. The finite difference form of equation (2.3.19) is

$$\frac{B_{ij}^2 - B_{ij}^1}{\Delta t} = \frac{FP_{ij}}{2\Delta x} \left[E_{zij}^2 - E_{i-1j}^2 + E_{zi+1j}^1 - E_{zij}^1 \right] - \frac{GP}{2\Delta y} \left[E_{\rho ij}^1 - E_{\rho ij-1}^1 + E_{\rho ij}^2 - E_{\rho ij-1}^2 \right] \quad (2.3.25)$$

Define the following constants

$$A_3 = \frac{FP_{ij} \Delta t}{2\Delta x}$$

$$A_4 = \frac{GP_{ij} \Delta t}{2\Delta y}$$

$$C_3 = B_{\rho ij}^1 + \frac{FP_{ij} \Delta t}{2\Delta x} \left[E_{zi+1j}^1 - E_{ij}^1 - E_{zi-1j}^2 \right] - \frac{GP_{ij} \Delta t}{2\Delta y} \left[E_{\rho ij}^1 - E_{\rho ij-1}^1 \right]$$

With these definitions equation (2.3.25) becomes

$$B_{\phi ij}^2 + A_3 E_{zij}^2 + A_4 E_{\rho ij}^2 - A_4 E_{\rho ij-1}^2 = C_3 \quad (2.3.26)$$

Substitute the expression for E_{zij}^2 from equation (2.3.24) into (2.3.26) and collect the terms

$$B_{\phi ij}^2 (1 - A_3 A_2) + A_4 E_{\rho ij}^2 - A_4 E_{\rho ij-1}^2 = C_3 - A_3 C_2 \quad (2.3.27)$$

Now substitute the expression for $E_{\rho ij-1}^2$ from equation (2.3.22) into (2.3.27) and collect

$$(1 - A_3 A_2 + A_1 A_4) B_{\phi ij}^2 + A_4 E_{\gamma ij}^2 - A_1 A_4 B_{\phi ij-1}^2 = C_3 - A_3 C_2 + A_4 C_1 \quad (2.3.28)$$

Rewrite equation (2.3.22) to center the equation at $(i, j+1/2, t+\Delta t/2)$

$$E_{\rho ij}^2 - a_1 B_{\phi ij+1}^2 + a_1 B_{\phi ij}^2 = c_1 \quad (2.3.29)$$

Substitute equation (2.3.29) into (2.3.28) and collect like terms

$$\begin{aligned} (1 - A_3 A_2 + A_1 A_4 - a_1 A_4) B_{\phi ij}^2 - A_1 A_4 B_{\phi ij-1}^2 - A_4 a_1 B_{\phi ij+1}^2 \\ = C_3 - A_3 C_2 + A_4 C_1 - A_4 c_1 \end{aligned}$$

Define the following constants

$$\begin{aligned} B_1 &= + A_4 a_1 \\ B_2 &= 1 - A_3 A_2 + A_1 A_4 - a_1 A_4 \\ B_3 &= - A_1 A_4 \\ B_4 &= C_3 - A_4 C_2 + A_4 C_1 - A_1 c_1 \\ & B_1 B_{\phi ij+1}^2 + B_2 B_{\phi ij}^2 + B_3 B_{\phi ij-1}^2 \end{aligned}$$

Assume that the B_{ϕ} can be calculated recursively, that is

$$B_{\phi j}^2 = E_j B_{\phi j+1}^2 + FF_j$$

or

$$B_{\phi j-1}^2 = E_{j-1} B_{\phi j}^2 + FF_{j-1}$$

then

$$B_1 B_{\phi ij+1}^2 + (B_2 + B_3 E_{j-1}) B_{\phi ij}^2 = B_4 - B_3 FF_{j-1}$$

We define the E_j 's and FF_j 's as

$$E_j = \frac{B_1}{B_2 + B_3 E_{j-1}}$$

$$FF_j = \frac{B_4 - B_3 FF_{j-1}}{B_2 + B_3 E_{j-1}}$$

A possible set of boundary conditions for the recursive relation is $B_\phi = 0$ at $j = 1$ and $j = j_{\max}$. This implies $E_1 = FF_1 = 0$.

2.3.3 Computational Procedure

The computer code is composed of a main routine, which is responsible for supervising activity of a number of subroutines. The main routine IG2D reads input data, defines calculational grids and some constants. IG2D then calls SETPT which defines the constants for the simple analytical sources. RDS is then called by IG2D to print a summary of the input data and constants for this run.

The calculation is stepped in time a Δt , SIGMA is called to calculate the conductivity and CURRENT is called to calculate the current densities. The calculation is then stepped in range and the fields are calculated over all altitudes explicitly as described in the section on finite differencing. At the end of the time loop, the fields are extrapolated in range to the last range grid point. OVTPVT is called for all output functions. PROFILE is called by OVTPVT to graph the sources and fields at a constant time and range as a function of altitude. RANGER is called to graph the source and field at a constant time and altitude as a function of range.

2.3.4 General Considerations

Since this algorithm is a real time algorithm, the grid spacing must be kept rather small to resolve the fast rise of the probe as it propagates through the grid. To make a real time code run to very late

times, it would be necessary to incorporate into the code some form of regridding.

The particular implicit scheme used to advance the calculation over altitude has been used with good success in several retarded time codes, such as SCX and ONDINE. The scheme seen to be very stable as long as the Courant condition is used to select the rate of the sizes of the grid steps.

Since the algorithm assumed an infinite conductivity for the ground, the results can be expected to agree well with other calculations when the air conductivity is much less than the ground conductivity. For close-in, early time regions, however, the code can not be expected to perform as well as other codes which assume a finite conductivity. Since the pulse which is observed far from the sources is produced on the outer edge of the source region where the air conductivity is low, the code should be able to predict the radiated signal fairly accurately.

2.3.5 Conclusion

Representative data is given for two ground ranges, 500 meters and 1000 meters with a source height of 50 meters. The sources are not for a particular weapon but were chosen as values which might typically be encountered. The time axes on the plots are in retarded time of the burst point. The two observers plotted are located just above the infinitely conducting ground. It is to be noted that the jitter in the vertical electric field is due to the lack of transverse currents and can be expected to go away if the transverse is installed.

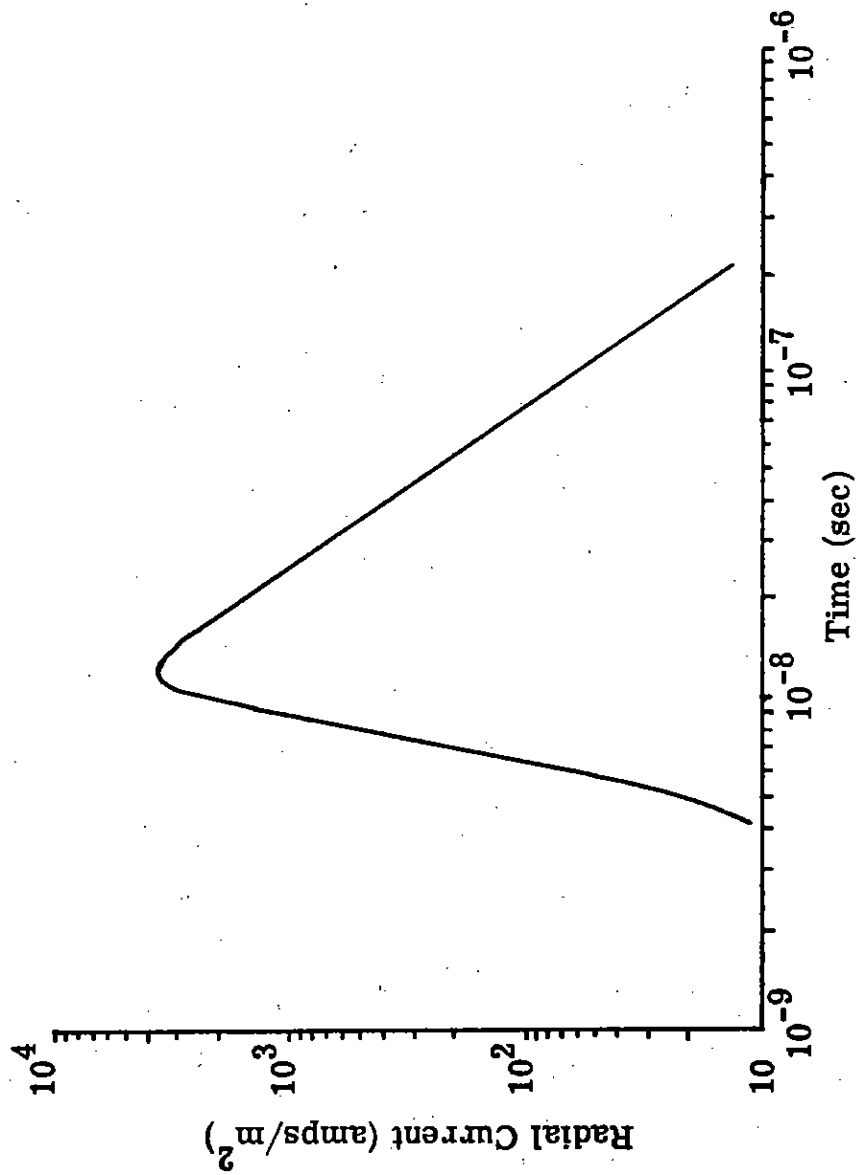


Figure 2.13. Radial Current at 500 Meters

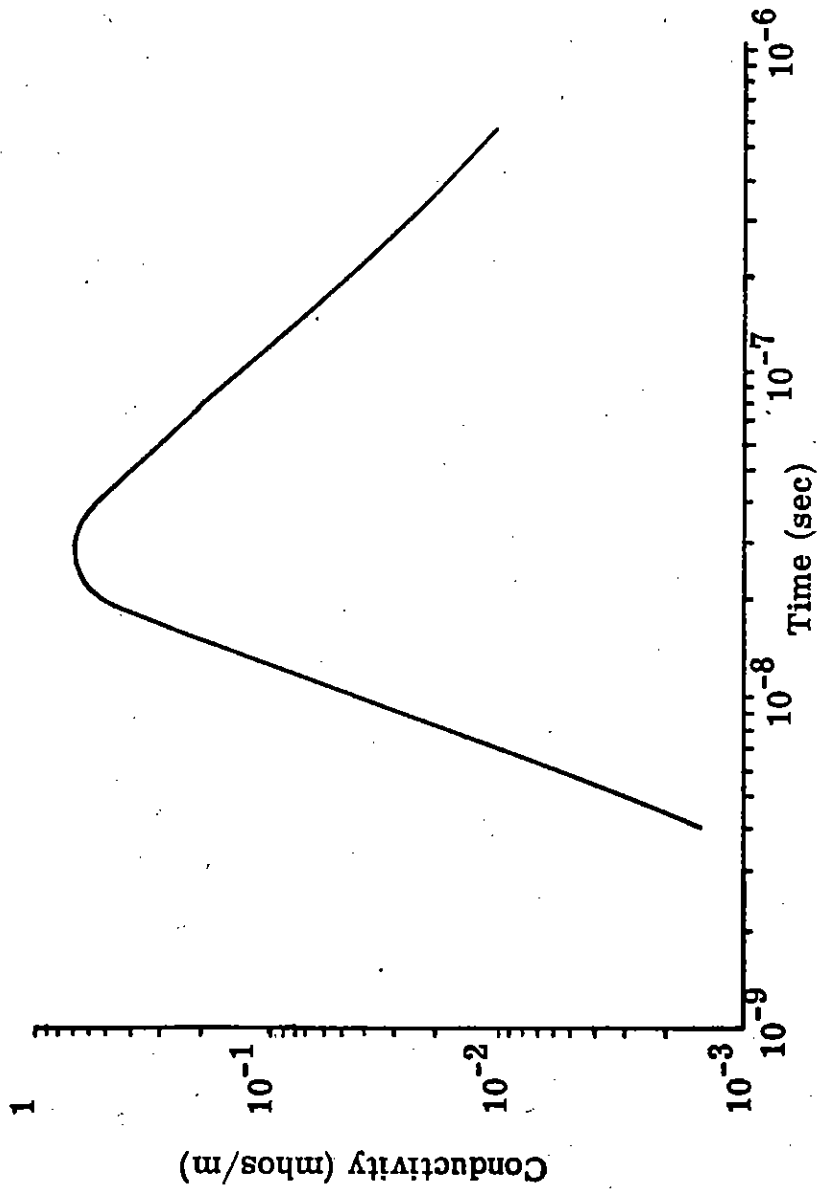


Figure 2.14. Conductivity at 500 Meters

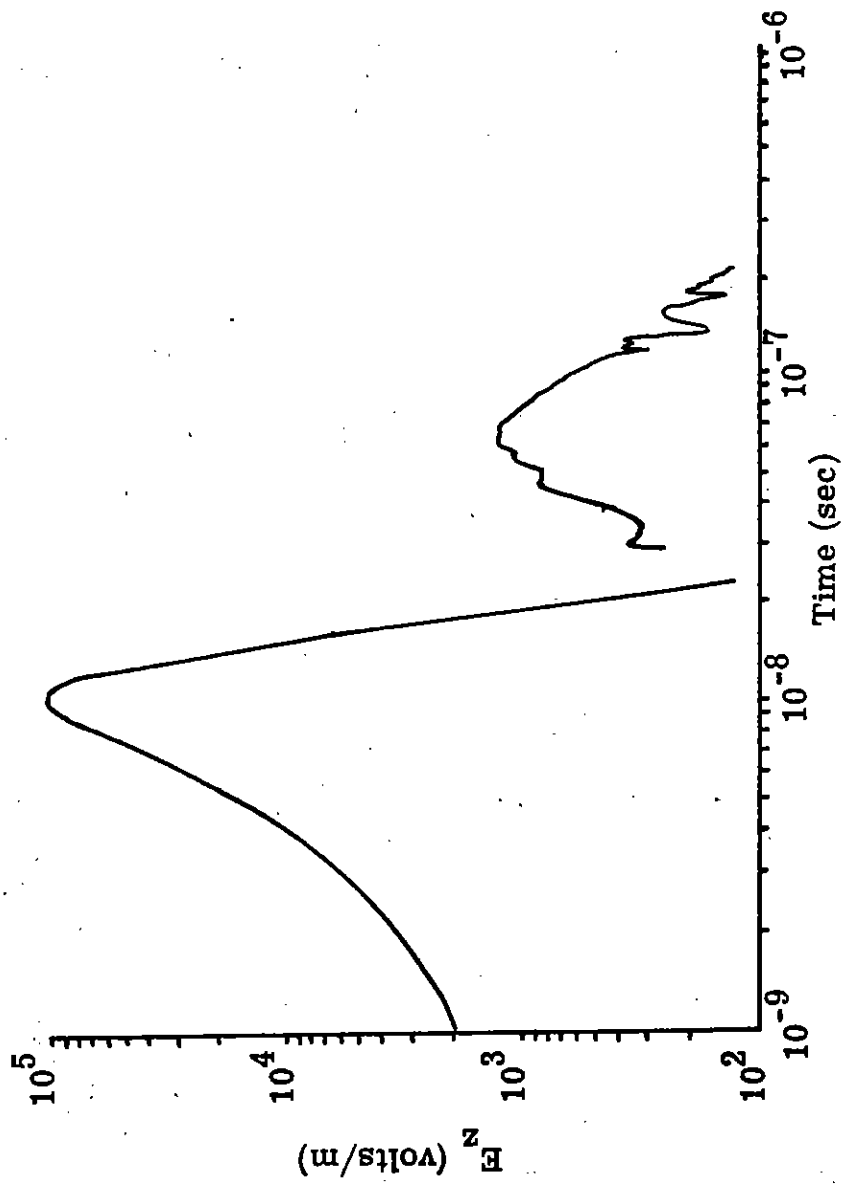


Figure 2. 15. Vertical Electric Field at 500 Meters

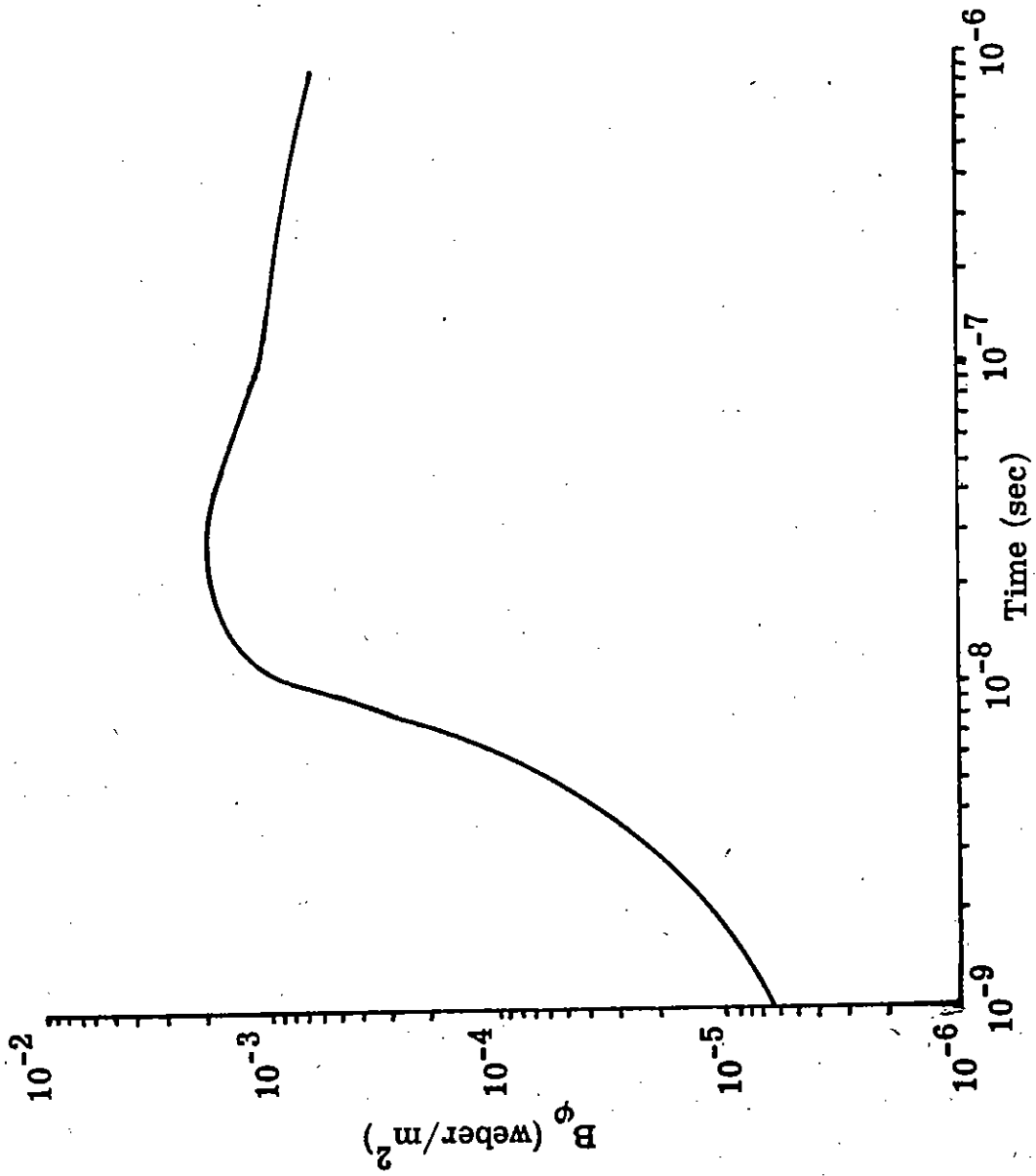


Figure 2.16. Magnetic Field at 500 Meters

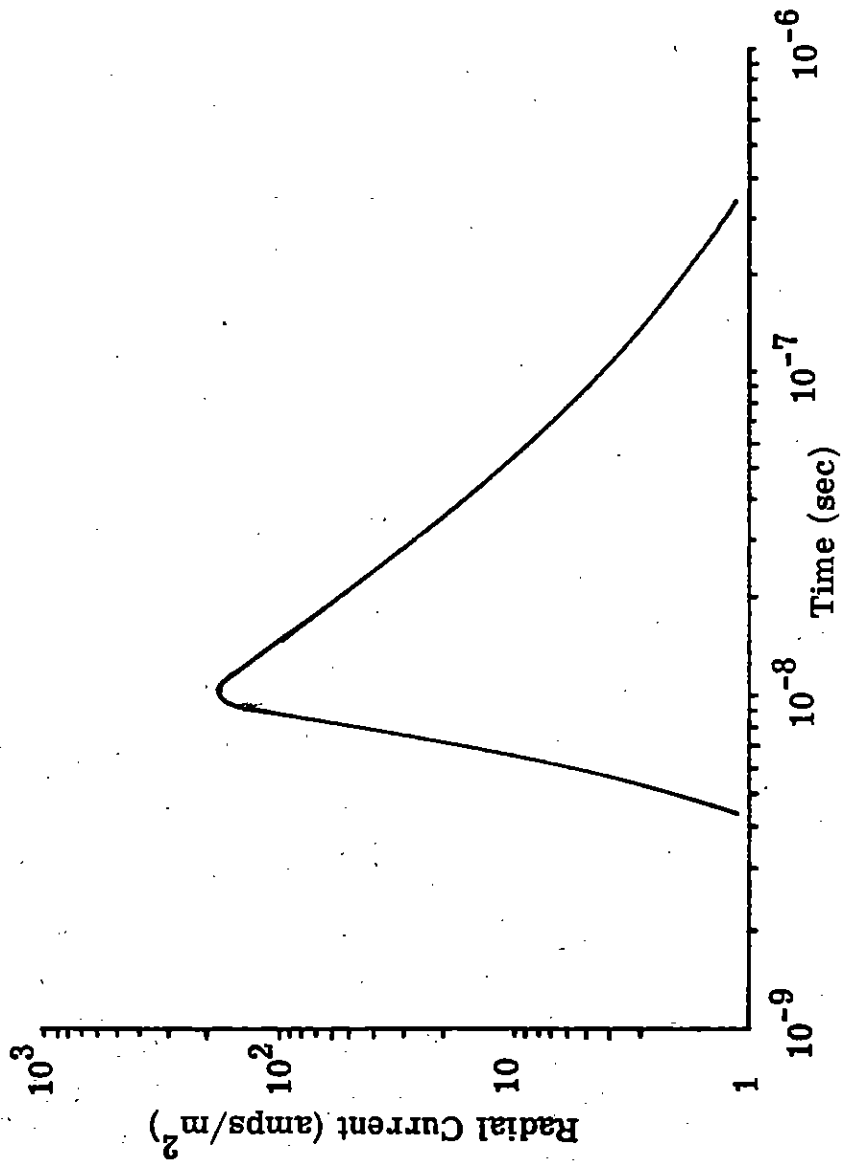


Figure 2.17. Radial Current at 1000 Meters

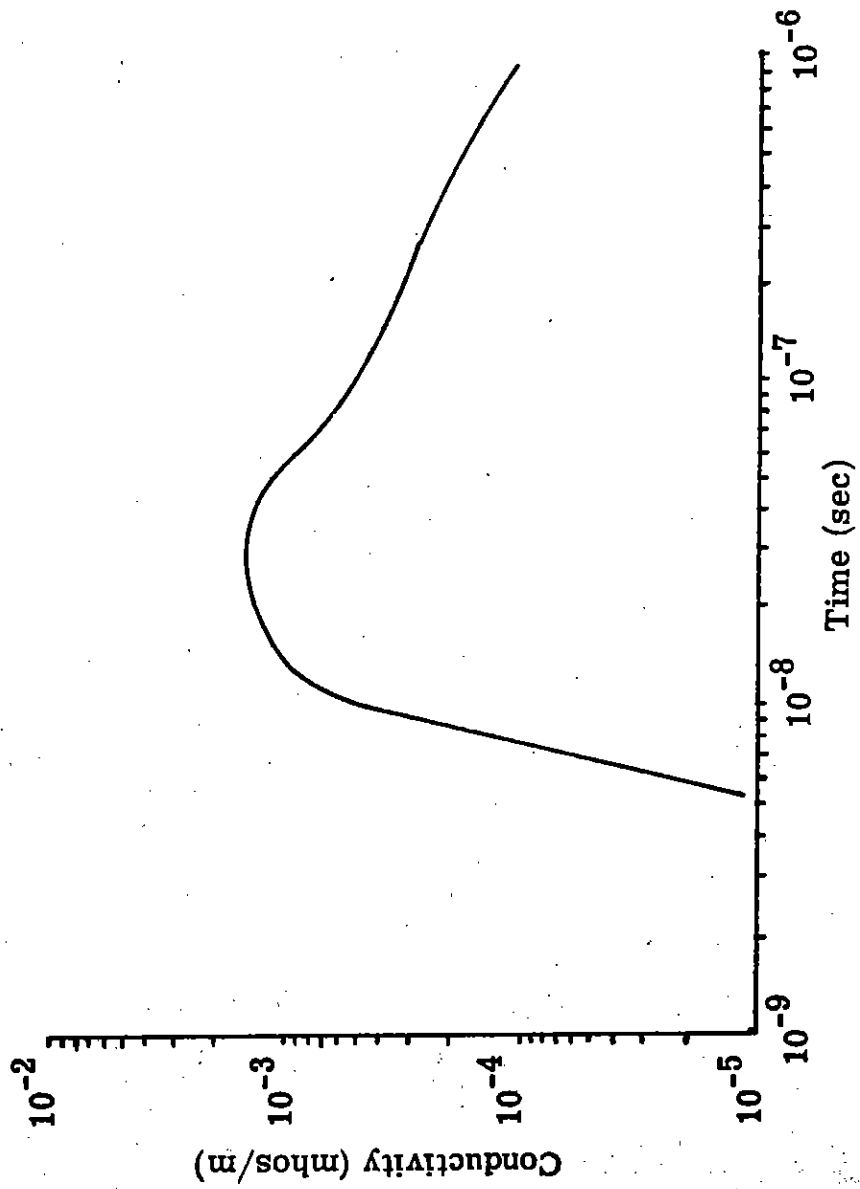


Figure 2.18. Conductivity at 1000 Meters

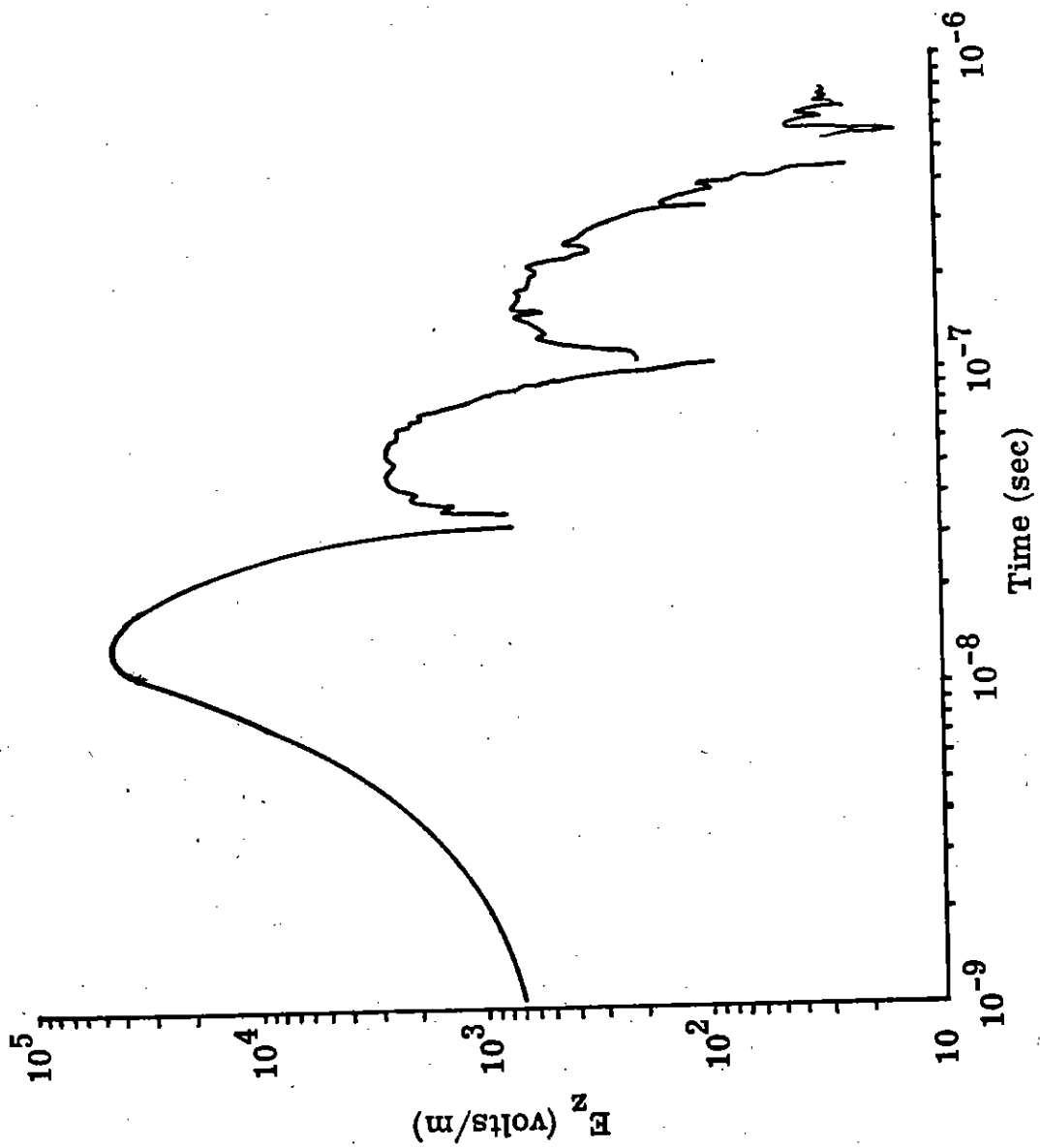
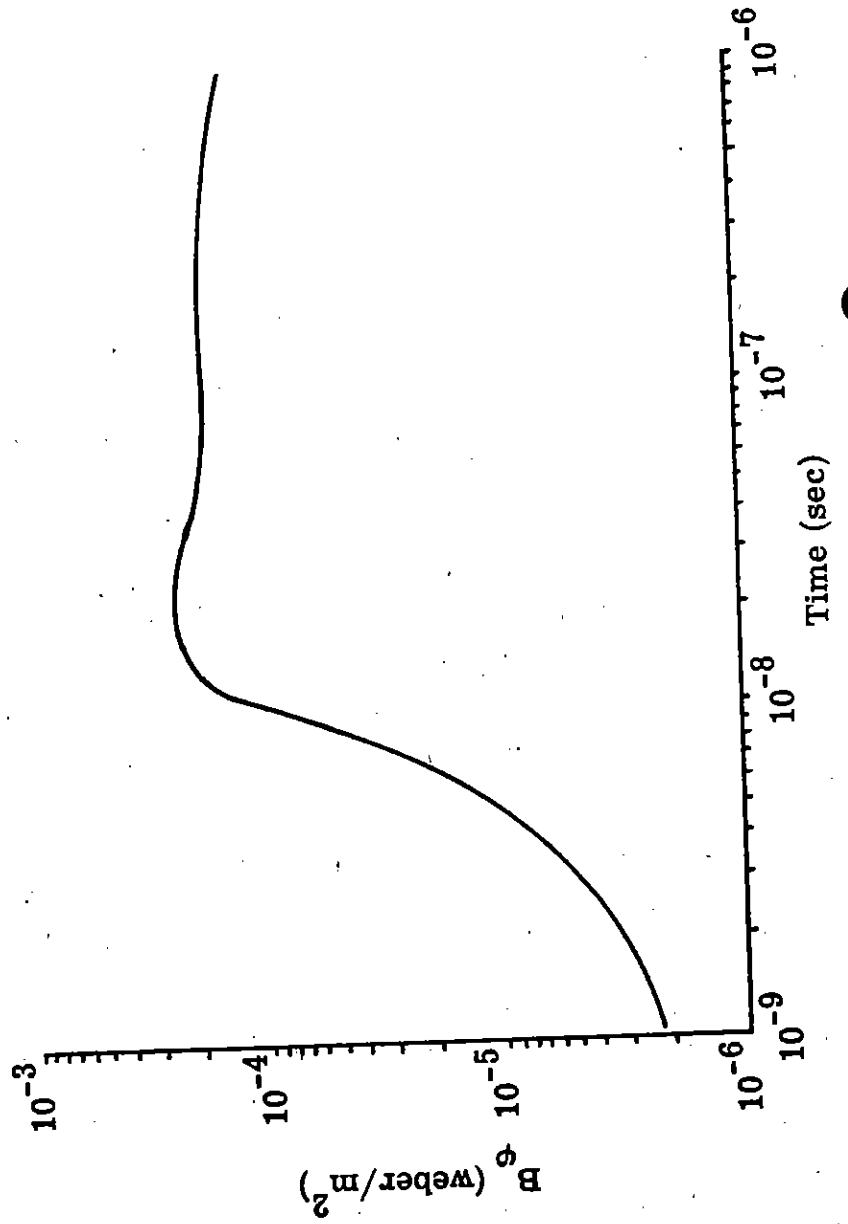


Figure 2.19. Vertical Electric Field at 1000 Meters



2.4 Algorithm "D"

An approach that was briefly investigated near the end of the effort covered by this report involved the development of an algorithm requiring integration of the field equations along characteristics. Unfortunately, there was insufficient time to program an algorithm for machine computation, but the approach nevertheless appeared to be quite promising; a brief description of the general scheme was therefore felt to be justified.

The use of characteristics methods has been extensively described in the literature, ^(9, 10, 11) and will not be presented in detail here. Briefly, characteristics for systems of hyperbolic partial differential equations are curves or surfaces associated with the propagation of wavefronts. The process of "integrating along characteristics" is attractive from a physical standpoint because it is connected with notions of causality, and attractive from a numerical standpoint because the original partial differential equations take on the form of very convenient relations (called "characteristic conditions") for the variations of fields along the directions of characteristics. Peebles⁽¹²⁾ has presented a solution technique using characteristics for an EMP problem with two independent variables: one space dimension, \underline{r} , and time, \underline{t} . In that case, the characteristics were families of straight lines ($r \pm ct = \text{constant}$, and $r = \text{constant}$), and the characteristic conditions had the form of ordinary differential equations. An analogous result appears for the three-independent-variable EMP problem, except that the characteristics then become surfaces, and the characteristic conditions involve derivatives in two directions along the characteristic surfaces. We can summarize the detailed results of a characteristics analysis of Maxwell's equations, as written in prolate-spheroidal coordinates and retarded time, as follows:

We may rewrite equations (2.2.5) through (2.2.7) in the following form:

$$\epsilon \frac{\partial E_{\xi}}{\partial \tau} + \left[\frac{\partial H_{\varphi}}{\partial \tau} - \frac{\partial H_{\varphi}}{\partial \zeta} \right] = -J_{\xi} \quad (2.4.1)$$

$$\epsilon \frac{\partial E_{\zeta}}{\partial \tau} + \left[\frac{\partial H_{\varphi}}{\partial \tau} + \frac{1}{a} \frac{\partial H_{\varphi}}{\partial \xi} \right] = -J_{\zeta} \quad (2.4.2)$$

$$\gamma_{\zeta} \left[\frac{\partial E_{\xi}}{\partial \tau} - \frac{\partial E_{\xi}}{\partial \zeta} \right] + \gamma_{\xi} \left[\frac{\partial E_{\zeta}}{\partial \tau} + \frac{1}{a} \frac{\partial E_{\zeta}}{\partial \xi} \right] + \frac{\partial H_{\varphi}}{\partial \tau} = 0 \quad (2.4.3)$$

For $\epsilon = 1$ (as an example) we can identify three convenient characteristic surfaces:

- A. $\tau = \text{const}$
B. $\tau - 2a\xi = \text{const}$
C. $\xi = \text{const}$

The characteristic conditions associated with each of the above surfaces are differential relations amongst the field variables within the surfaces A., B., and C.

For A.,

$$\gamma_{\zeta} D_{+} (E_{\xi} - H_{\varphi}) - \gamma_{\xi} D_{A} (E_{\zeta} - H_{\varphi}) = -\gamma_{\zeta} J_{\xi} - \gamma_{\xi} J_{\zeta} \quad (2.4.4)$$

For B.,

$$\gamma_{\zeta} D_{+} (E_{\xi} - H_{\varphi}) - \gamma_{\xi} D_{B} (E_{\zeta} + H_{\varphi}) = -\gamma_{\zeta} J_{\xi} + \gamma_{\xi} J_{\zeta} \quad (2.4.5)$$

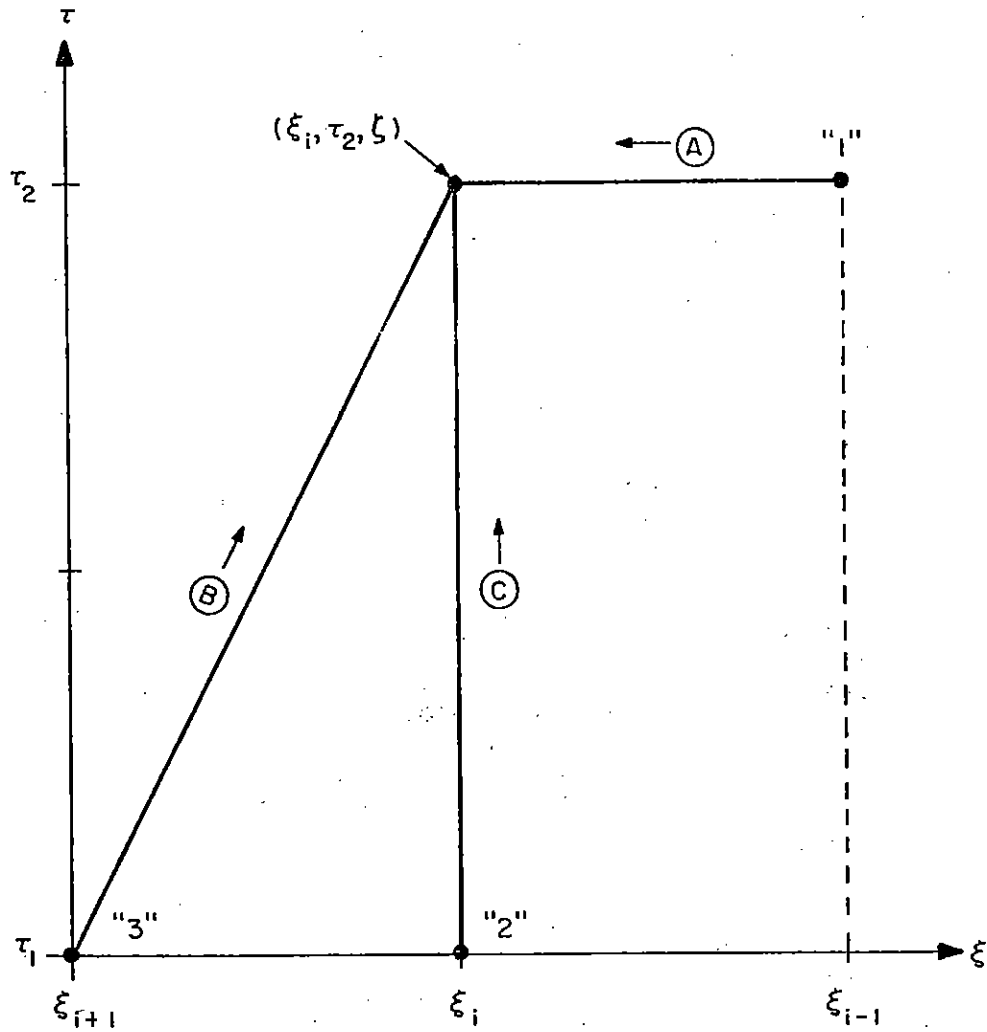


Figure 2.21. Integration in Characteristic Surfaces for Algorithm "D"

and for C,

$$-D_{\perp} H_{\varphi} + D_C (E_{\xi} + H_{\varphi}) = -J_{\xi} \quad (2.4.6)$$

The D-operators in equations (2.4.4) through (2.4.6) are readily defined:

$$D_{\perp} = \frac{\partial}{\partial \xi} \quad (2.4.7)$$

$$D_A = \frac{1}{a} \frac{\partial}{\partial \xi} \quad (2.4.8)$$

$$D_B = \frac{1}{a} \frac{\partial}{\partial \xi} + 2 \frac{\partial}{\partial \tau} \quad (2.4.9)$$

$$D_C = \frac{\partial}{\partial \tau} \quad (2.4.10)$$

D_A , D_B , and D_C simply represent derivatives taken parallel to the directions of the A, B, and C-characteristics in the (ξ, τ) -plane.

The three characteristic conditions (2.4.4) through (2.4.6) thus can replace the original set of field equations, and can be used, as suggested in Figure 2.21, to find fields along the line through ξ_1 and τ_2 , once the fields along the lines "1", "2", and "3" are known. The sets of implicit equations obtained from this procedure can be solved by standard methods, and are likely to be more satisfactory, because of the causality considerations implicit in their development, than equations generated by more straightforward difference representations of the original field equations. It is felt that this approach is attractive enough to warrant more detailed consideration.

3. SUMMARY

Several finite difference algorithms for the calculation of low altitude EMP environments were investigated. These algorithms were programmed and run on a CDC 6600 computer. The results were checked for two test problems. The first test was to input a radial current and then to determine how nearly radial the resultant fields were. The second test problem employed the Maxwell equations to calculate currents for an assumed set of fields, then these currents were put into the codes and the resulting fields were compared with the assumed ones. A third test problem was developed. This consisted of a real-time air burst code and an image calculation to incorporate the effects of a perfectly conducting earth. This code is complete and is running. However, comparison of it and the low altitude environment codes has not yet been made.

Comparison of the algorithms studied with the test problems indicated that the two explicit algorithms described in Sections 2.1 and 2.2 above worked considerably better than any of the several implicit methods studied. Details of a few of the implicit calculations are given in Appendix D.

A new approach to the problem using the method of characteristics is discussed in Section 2.4. Although this method appears very promising, it was developed near the end of the contract and has not yet been programmed for the computer.

APPENDIX A

I. FIELD EQUATIONS

Define modified MKS units by redefining \vec{E} and \vec{H} according to

$$\vec{E} = c \vec{E} \text{ MKS}, \quad \vec{H} = \mu_0 c \vec{H} \text{ MKS} \quad (1)$$

Maxwell's equations become

$$\nabla \cdot \vec{D} = \rho \quad (2)$$

$$\nabla \cdot \vec{B} = 0 \quad (3)$$

$$\nabla \times \vec{E} = - \frac{1}{c} \frac{\partial \vec{B}}{\partial t} \quad (4)$$

$$\nabla \times \vec{H} = z_0 \left(\vec{j} + \frac{\partial \vec{D}}{\partial t} \right) \quad (5)$$

where the definition

$$z_0 = \sqrt{\frac{\mu_0}{\epsilon_0}} = \mu_0 c \quad (6)$$

has been used. The constitutive equations become

$$\vec{D} = \epsilon \vec{E}, \quad \vec{B} = \kappa_m \vec{H}, \quad \epsilon = \kappa \epsilon_0, \quad \mu = \kappa_m \mu_0 \quad (7)$$

Then, define

$$z = \sqrt{\frac{\kappa_m}{\kappa}} z_0 \quad (8)$$

We transform to retarded time defined by

$$\tau = ct - r = ct - a(\zeta - \xi) \quad (9)$$

The transformations of derivatives are

$$\frac{\partial}{\partial t} = c \frac{\partial}{\partial \tau} \quad (10)$$

$$\nabla_t = \nabla_\tau - \hat{r} \frac{\partial}{\partial \tau} \quad (11)$$

where ∇_t and ∇_τ are the gradient operators at constant t and constant τ .

Maxwell's equations become

$$(\nabla_\tau - \hat{r} \frac{\partial}{\partial \tau}) \cdot \vec{E} = \frac{\rho}{\kappa \epsilon_0} \quad (12)$$

$$(\nabla_\tau - \hat{r} \frac{\partial}{\partial \tau}) \cdot \vec{H} = 0 \quad (13)$$

$$(\nabla_\tau - \hat{r} \frac{\partial}{\partial \tau}) \times \vec{E} = -\kappa_m \frac{\partial \vec{H}}{\partial \tau} \quad (14)$$

$$(\nabla_\tau - \hat{r} \frac{\partial}{\partial \tau}) \times \vec{H} = z_0 \vec{j} + \kappa \frac{\partial \vec{E}}{\partial \tau} \quad (15)$$

The divergence equations are initial conditions for the problem. The fields are thus determined by the curl equations. Now:

$$\hat{r} = \alpha_{11} \hat{\zeta} + \alpha_{21} \hat{\xi} \quad (16)$$

The coordinates are cyclic in the order (ζ, ξ, φ) , thus:

$$\hat{r} \times \frac{\partial \vec{E}}{\partial \tau} = \alpha_{21} \frac{\partial E_\varphi}{\partial \tau} \hat{\zeta} - \alpha_{11} \frac{\partial E_\varphi}{\partial \tau} \hat{\xi} + \left(\alpha_{11} \frac{\partial E_\xi}{\partial \tau} - \alpha_{21} \frac{\partial E_\zeta}{\partial \tau} \right) \hat{\varphi} \quad (17)$$

A similar equation holds for the magnetic field. For an azimuthally symmetric problem, Maxwell's equations become

$$\alpha_{11} \frac{\partial E_{\zeta}}{\partial \tau} + \alpha_{21} \frac{\partial E_{\xi}}{\partial \tau} = -\frac{\rho}{\kappa \epsilon_0} + \frac{1}{a(\zeta^2 - \xi^2)} \left[\frac{\partial}{\partial \zeta} \left(\sqrt{(\zeta^2 - \xi^2)(\zeta^2 - 1)} E_{\zeta} \right) + \frac{\partial}{\partial \xi} \left(\sqrt{(\zeta^2 - \xi^2)(1 - \xi^2)} E_{\xi} \right) \right] \quad (18)$$

$$\alpha_{11} \frac{\partial H_{\zeta}}{\partial \tau} + \alpha_{21} \frac{\partial H_{\xi}}{\partial \tau} = \frac{1}{a(\zeta^2 - \xi^2)} \left[\frac{\partial}{\partial \zeta} \left(\sqrt{(\zeta^2 - \xi^2)(\zeta^2 - 1)} H_{\zeta} \right) + \frac{\partial}{\partial \xi} \left(\sqrt{(\zeta^2 - \xi^2)(1 - \xi^2)} H_{\xi} \right) \right] \quad (19)$$

$$\begin{aligned} & \alpha_{21} \frac{\partial E_{\varphi}}{\partial \tau} \hat{\xi} - \alpha_{11} \frac{\partial E_{\varphi}}{\partial \tau} \hat{\xi} + \left(\alpha_{11} \frac{\partial E_{\xi}}{\partial \tau} - \alpha_{21} \frac{\partial E_{\zeta}}{\partial \tau} \right) \hat{\varphi} - \kappa_m \frac{\partial}{\partial \tau} (H_{\zeta} \hat{\xi} + H_{\xi} \hat{\xi} + H_{\varphi} \hat{\varphi}) \\ &= \frac{\hat{\xi}}{a\sqrt{(\zeta^2 - \xi^2)(\zeta^2 - 1)}} \frac{\partial}{\partial \xi} \left(\sqrt{(\zeta^2 - 1)(1 - \xi^2)} E_{\varphi} \right) - \frac{\hat{\xi}}{a\sqrt{(\zeta^2 - \xi^2)(1 - \xi^2)}} \\ & \frac{\partial}{\partial \zeta} \left(\sqrt{(\zeta^2 - 1)(1 - \xi^2)} E_{\varphi} \right) + \frac{\hat{\varphi} \sqrt{(\zeta^2 - 1)(1 - \xi^2)}}{a(\zeta^2 - \xi^2)} \\ & \left[\frac{\partial}{\partial \zeta} \left(\sqrt{\frac{\zeta^2 - \xi^2}{1 - \xi^2}} E_{\xi} \right) - \frac{\partial}{\partial \xi} \left(\sqrt{\frac{\zeta^2 - \xi^2}{\zeta^2 - 1}} E_{\zeta} \right) \right] \quad (20) \end{aligned}$$

$$\begin{aligned}
& \alpha_{21} \frac{\partial H_{\varphi}}{\partial \tau} \hat{\zeta} - \alpha_{11} \frac{\partial H_{\varphi}}{\partial \tau} \hat{\xi} + \left(\alpha_{11} \frac{\partial H_{\xi}}{\partial \tau} - \alpha_{21} \frac{\partial H_{\zeta}}{\partial \tau} \right) \hat{\phi} + \kappa \frac{\partial}{\partial \tau} (E_{\zeta} \hat{\zeta} + E_{\xi} \hat{\xi} + E_{\varphi} \hat{\phi}) \\
& = -z_0 (j_{\zeta} \hat{\zeta} + j_{\xi} \hat{\xi} + j_{\varphi} \hat{\phi}) + \frac{\hat{\zeta}}{a \sqrt{(\zeta^2 - \xi^2)(\zeta^2 - 1)}} \frac{\partial}{\partial \xi} \left(\sqrt{(\zeta^2 - 1)(1 - \xi^2)} H_{\varphi} \right) \\
& \quad - \frac{\hat{\xi}}{a \sqrt{(\zeta^2 - \xi^2)(1 - \xi^2)}} \frac{\partial}{\partial \zeta} \left(\sqrt{(\zeta^2 - 1)(1 - \xi^2)} H_{\varphi} \right) \\
& \quad + \frac{\hat{\phi} \sqrt{(\zeta^2 - 1)(1 - \xi^2)}}{a(\zeta^2 - \xi^2)} \left[\frac{\partial}{\partial \zeta} \left(\sqrt{\frac{\zeta^2 - \xi^2}{1 - \xi^2}} H_{\xi} \right) - \frac{\partial}{\partial \xi} \left(\sqrt{\frac{\zeta^2 - \xi^2}{\zeta^2 - 1}} H_{\zeta} \right) \right] \quad (21)
\end{aligned}$$

In component form, these separate into two sets of equations, the TM and TE field equations.

TM Equations

$$\kappa \frac{\partial E_{\zeta}}{\partial \tau} + \alpha_{21} \frac{\partial H_{\varphi}}{\partial \tau} = -z_0 j_{\zeta} + \frac{1}{a \sqrt{(\zeta^2 - \xi^2)(\zeta^2 - 1)}} \frac{\partial}{\partial \xi} \left(\sqrt{(\zeta^2 - 1)(1 - \xi^2)} H_{\varphi} \right) \quad (22)$$

$$\kappa \frac{\partial E_{\xi}}{\partial \tau} - \alpha_{11} \frac{\partial H_{\varphi}}{\partial \tau} = -z_0 j_{\xi} - \frac{1}{a \sqrt{(\zeta^2 - \xi^2)(1 - \xi^2)}} \frac{\partial}{\partial \zeta} \left(\sqrt{(\zeta^2 - 1)(1 - \xi^2)} H_{\varphi} \right) \quad (23)$$

$$\begin{aligned}
\alpha_{11} \frac{\partial E_{\xi}}{\partial \tau} - \alpha_{21} \frac{\partial E_{\zeta}}{\partial \tau} - \kappa_m \frac{\partial H_{\varphi}}{\partial \tau} &= \frac{\sqrt{(\zeta^2 - 1)(1 - \xi^2)}}{a(\zeta^2 - \xi^2)} \left[\frac{\partial}{\partial \zeta} \left(\sqrt{\frac{\zeta^2 - \xi^2}{1 - \xi^2}} E_{\xi} \right) \right. \\
&\quad \left. - \frac{\partial}{\partial \xi} \left(\sqrt{\frac{\zeta^2 - \xi^2}{\zeta^2 - 1}} E_{\zeta} \right) \right] \quad (24)
\end{aligned}$$

TE Equations

$$\alpha_{21} \frac{\partial E_{\phi}}{\partial \tau} - \kappa_m \frac{\partial H_{\zeta}}{\partial \tau} = \frac{1}{a \sqrt{(\zeta^2 - \xi^2)(\zeta^2 - 1)}} \frac{\partial}{\partial \xi} \left(\sqrt{(\zeta^2 - 1)(1 - \xi^2)} E_{\phi} \right) \quad (25)$$

$$\alpha_{11} \frac{\partial E_{\phi}}{\partial \tau} + \kappa_m \frac{\partial H_{\xi}}{\partial \tau} = \frac{1}{a \sqrt{(\zeta^2 - \xi^2)(1 - \xi^2)}} \frac{\partial}{\partial \zeta} \left(\sqrt{(\zeta^2 - 1)(1 - \xi^2)} E_{\phi} \right) \quad (26)$$

$$\alpha_{11} \frac{\partial H_{\xi}}{\partial \tau} - \alpha_{21} \frac{\partial H_{\zeta}}{\partial \tau} + \kappa \frac{\partial E_{\phi}}{\partial \tau} = -z_0 j_{\phi} + \frac{\sqrt{(\zeta^2 - 1)(1 - \xi^2)}}{a(\zeta^2 - \xi^2)} \left[\frac{\partial}{\partial \zeta} \left(\sqrt{\frac{\zeta^2 - \xi^2}{1 - \xi^2}} H_{\xi} \right) - \frac{\partial}{\partial \xi} \left(\sqrt{\frac{\zeta^2 - \xi^2}{\zeta^2 - 1}} H_{\zeta} \right) \right] \quad (27)$$

For the low altitude burst problem j_{ϕ} is zero. Thus the TE mode is not excited and we confine our investigation to the TM fields. The matrix elements in equation (16) are

$$\alpha_{11} = \frac{a}{h_{\zeta}} = \sqrt{\frac{\zeta^2 - 1}{\zeta^2 - \xi^2}} \quad (28)$$

$$\alpha_{21} = \frac{-a}{h_{\xi}} = -\sqrt{\frac{1 - \xi^2}{\zeta^2 - \xi^2}} \quad (29)$$

The TM equations become

$$\kappa \frac{\partial E_{\zeta}}{\partial \tau} - \sqrt{\frac{1 - \xi^2}{\zeta^2 - \xi^2}} \frac{\partial H_{\phi}}{\partial \tau} = -z_0 j_{\zeta} + \frac{1}{a \sqrt{(\zeta^2 - \xi^2)(\zeta^2 - 1)}} \frac{\partial}{\partial \xi} \left(\sqrt{(\zeta^2 - 1)(1 - \xi^2)} H_{\phi} \right) \quad (30)$$

$$\kappa \frac{\partial E_{\xi}}{\partial \tau} - \sqrt{\frac{\zeta^2 - 1}{\zeta^2 - \xi^2}} \frac{\partial H_{\varphi}}{\partial \tau} = -z_0 j_{\xi} - \frac{1}{a \sqrt{(\zeta^2 - \xi^2)(1 - \xi^2)}} \frac{\partial}{\partial \xi} \left(\sqrt{(\zeta^2 - 1)(1 - \xi^2)} H_{\varphi} \right) \quad (31)$$

$$\sqrt{\frac{\zeta^2 - 1}{\zeta^2 - \xi^2}} \frac{\partial E_{\xi}}{\partial \tau} + \sqrt{\frac{1 - \xi^2}{\zeta^2 - \xi^2}} \frac{\partial E_{\zeta}}{\partial \tau} - \kappa_m \frac{\partial H_{\varphi}}{\partial \tau} = \frac{\sqrt{(\zeta^2 - 1)(1 - \xi^2)}}{a(\zeta^2 - \xi^2)} \left[\frac{\partial}{\partial \zeta} \left(\sqrt{\frac{\zeta^2 - \xi^2}{1 - \xi^2}} E_{\xi} \right) - \frac{\partial}{\partial \xi} \left(\sqrt{\frac{\zeta^2 - \xi^2}{\zeta^2 - 1}} E_{\zeta} \right) \right] \quad (32)$$

The field equations are simplified by the following transformation of dependent variables

$$\begin{pmatrix} E_{\zeta} \\ j_{\zeta} \end{pmatrix} = \sqrt{(\zeta^2 - \xi^2)(\zeta^2 - 1)} \begin{pmatrix} E'_{\zeta} \\ j'_{\zeta} \end{pmatrix} \quad (33)$$

$$\begin{pmatrix} E_{\xi} \\ j_{\xi} \end{pmatrix} = \sqrt{(\zeta^2 - \xi^2)(1 - \xi^2)} \begin{pmatrix} E'_{\xi} \\ j'_{\xi} \end{pmatrix} \quad (34)$$

$$H_{\varphi} = \sqrt{(\zeta^2 - 1)(1 - \xi^2)} H'_{\varphi} \quad (35)$$

where the primed variables are those used previously. We obtain

$$\kappa \frac{\partial E'_{\zeta}}{\partial \tau} - \frac{\partial H'_{\varphi}}{\partial \tau} = -z_0 j'_{\zeta} + \frac{1}{a} \frac{\partial H'_{\varphi}}{\partial \xi} \quad (36)$$

$$\kappa \frac{\partial E_{\xi}}{\partial \tau} - \frac{\partial H_{\varphi}}{\partial \tau} = -z_0 j_{\xi} - \frac{1}{a} \frac{\partial H_{\varphi}}{\partial \zeta} \quad (37)$$

$$G_2 \frac{\partial E_{\zeta}}{\partial \tau} + G_1 \frac{\partial E_{\xi}}{\partial \tau} - \kappa_m \frac{\partial H_{\varphi}}{\partial \tau} = \frac{G_1}{a} \frac{\partial E_{\xi}}{\partial \zeta} - \frac{G_2}{a} \frac{\partial E_{\zeta}}{\partial \xi} \quad (38)$$

where

$$G_1 = \frac{\zeta^2 - 1}{\zeta^2 - \xi^2} = \frac{a^2}{h_1^2} \quad (39)$$

$$G_2 = \frac{1 - \xi^2}{\zeta^2 - \xi^2} = \frac{a^2}{h_2^2} \quad (40)$$

To facilitate regriding in the three coordinate directions, (ζ, ξ, τ) we introduce the following transformations

$$\frac{1}{a} \frac{\partial}{\partial \zeta} = \psi_1 \frac{\partial}{\partial u} \quad (41)$$

$$\frac{1}{a} \frac{\partial}{\partial \xi} = \psi_2 \frac{\partial}{\partial v} \quad (42)$$

We assume that the conduction current can be described by a scalar conductivity, then

$$\vec{j} \Rightarrow \vec{j} + \sigma \vec{E} \quad (43)$$

A derivation similar to the one above can be done in which the retarded time of the image point is used. The resulting differential equations differ only by sign changes on some terms. Let $Q_{\tau} = -1$ signify retarded time of the image point, then the final form of the field equations is

$$\kappa \frac{\partial E_{\zeta}}{\partial \tau} - Q_{\tau} \frac{\partial H_{\varphi}}{\partial \tau} = -z_0 j_{\zeta} - z_0 \sigma E_{\zeta} + \psi_2 \frac{\partial H_{\varphi}}{\partial v} \quad (44)$$

$$\kappa \frac{\partial E_{\xi}}{\partial \tau} - \frac{\partial H_{\varphi}}{\partial \tau} = -z_0 j_{\xi} - z_0 \sigma E_{\xi} - \psi_1 \frac{\partial H_{\varphi}}{\partial u} \quad (45)$$

$$Q_{\tau} G_2 \frac{\partial E_{\zeta}}{\partial \tau} + G_1 \frac{\partial E_{\xi}}{\partial \tau} - \kappa_m \frac{\partial H_{\varphi}}{\partial \tau} = G_1 \psi_1 \frac{\partial E_{\xi}}{\partial u} - G_2 \psi_2 \frac{\partial E_{\zeta}}{\partial v} \quad (46)$$

II. GEOMETRY

Define:

$$\zeta \equiv \frac{1}{2a} (r' + r); \quad \xi \equiv \frac{1}{2a} (r' - r) \quad (1)$$

then

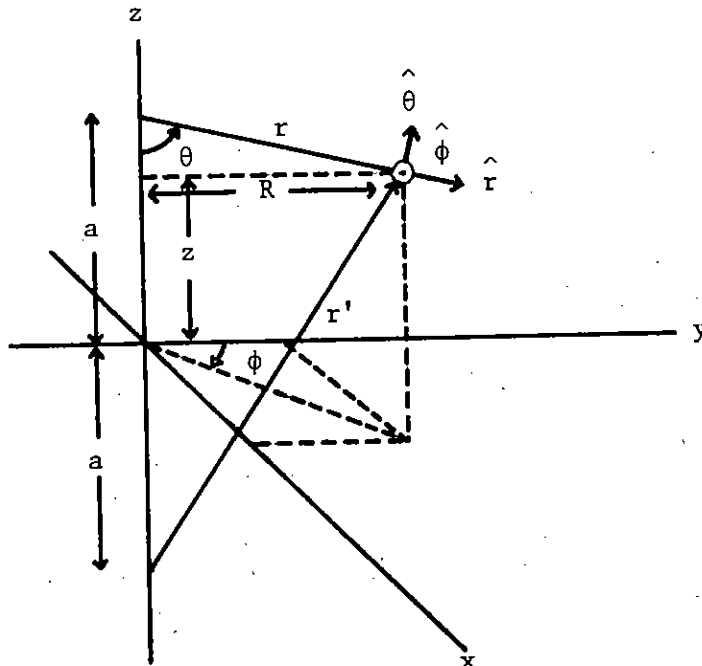
$$r' = a(\zeta + \xi); \quad r = a(\zeta - \xi) \quad (2)$$

Choose the prolate spheroidal coordinates to be cyclic in the order (ζ, ξ, φ) . Note that:

$$\cos \theta = \frac{1 - \xi\zeta}{\zeta - \xi} \quad (3)$$

$$\sin \theta = \frac{\sqrt{(\zeta^2 - 1)(1 - \xi^2)}}{\zeta - \xi} \quad (4)$$

$$R = a\sqrt{(\zeta^2 - 1)(1 - \xi^2)} \quad (5)$$



The transformations to Cartesian coordinates are

$$x = R \sin \varphi = a \sqrt{(\zeta^2 - 1)(1 - \xi^2)} \sin \varphi \quad (6)$$

$$y = R \cos \varphi = a \sqrt{(\zeta^2 - 1)(1 - \xi^2)} \cos \varphi \quad (7)$$

$$z = a \xi \zeta \quad (8)$$

The inverse transformations are:

$$\zeta = \frac{1}{2a} \left[\sqrt{x^2 + y^2 + (a + z)^2} + \sqrt{x^2 + y^2 + (a - z)^2} \right] \quad (9)$$

$$\xi = \frac{1}{2a} \left[\sqrt{x^2 + y^2 + (a + z)^2} - \sqrt{x^2 + y^2 + (a - z)^2} \right] \quad (10)$$

$$\varphi = \tan^{-1} \left(\frac{x}{y} \right) \quad (11)$$

The radicals in equations (9) and (10) are just:

$$r = \sqrt{x^2 + y^2 + (a - z)^2} \quad (12)$$

$$r' = \sqrt{x^2 + y^2 + (a + z)^2} \quad (13)$$

the transformation to the spherical polar system in Figure 1 is given by

$$r = a(\zeta - \xi) \quad (14)$$

$$\theta = \cos^{-1} \left(\frac{1 - \xi \zeta}{\zeta - \xi} \right) \quad (15)$$

The inverse transformations are

$$\zeta = \frac{1}{2a} \left[r + \sqrt{r^2 + 4a(a - r \cos \theta)} \right] \quad (16)$$

$$\xi = \frac{1}{2a} \left[-r + \sqrt{r^2 + 4a(a - r \cos \theta)} \right] \quad (17)$$

where

$$r' = \sqrt{r^2 + 4a(a - r \cos \theta)} \quad (18)$$

We now wish to determine scale factors h_ζ , h_ξ , h_φ such that

$$ds^2 = h_\zeta^2 d\zeta^2 + h_\xi^2 d\xi^2 + h_\varphi^2 d\varphi^2 \quad (19)$$

To obtain these, differentiate equations (14) and (15) and substitute into

$$ds^2 = dr^2 + r^2 d\theta^2 + r^2 \sin^2 \theta d\varphi^2 \quad (20)$$

We find

$$ds^2 = a^2 \frac{\zeta^2 - \xi^2}{\zeta^2 - 1} d\zeta^2 + a^2 \frac{\zeta^2 - \xi^2}{1 - \xi^2} d\xi^2 + a^2 (\zeta^2 - 1)(1 - \xi^2) d\varphi^2 \quad (21)$$

The following relations were used

$$\frac{\partial \theta}{\partial \zeta} = \frac{1}{\zeta - \xi} \sqrt{\frac{1 - \xi^2}{\zeta^2 - 1}} \quad (22)$$

$$\frac{\partial \theta}{\partial \xi} = \frac{1}{\zeta - \xi} \sqrt{\frac{\zeta^2 - 1}{1 - \xi^2}} \quad (23)$$

Finally,

$$h_{\zeta} = a \sqrt{\frac{\zeta^2 - \xi^2}{\zeta^2 - 1}} \quad (24)$$

$$h_{\xi} = a \sqrt{\frac{\zeta^2 - \xi^2}{1 - \xi^2}} \quad (25)$$

$$h_{\varphi} = a \sqrt{(\zeta^2 - 1)(1 - \xi^2)} \quad (26)$$

Some useful vector operators are defined by:

$$\nabla f = \frac{1}{a} \sqrt{\frac{\zeta^2 - 1}{\zeta^2 - \xi^2}} \frac{\partial f}{\partial \zeta} \hat{\zeta} + \frac{1}{a} \sqrt{\frac{1 - \xi^2}{\zeta^2 - \xi^2}} \frac{\partial f}{\partial \xi} \hat{\xi} + \frac{1}{a \sqrt{(\zeta^2 - 1)(1 - \xi^2)}} \frac{\partial f}{\partial \varphi} \hat{\varphi} \quad (27)$$

$$\begin{aligned} \nabla \cdot \vec{f} = \frac{1}{a(\zeta^2 - \xi^2)} & \left[\frac{\partial}{\partial \zeta} \left(\sqrt{(\zeta^2 - \xi^2)(\zeta^2 - 1)} f_{\zeta} \right) + \frac{\partial}{\partial \xi} \left(\sqrt{(\zeta^2 - \xi^2)(1 - \xi^2)} f_{\xi} \right) \right. \\ & \left. + \frac{\partial}{\partial \varphi} \left(\frac{\zeta^2 - \xi^2}{\sqrt{(\zeta^2 - 1)(1 - \xi^2)}} f_{\varphi} \right) \right] \quad (28) \end{aligned}$$

$$\begin{aligned} \nabla \times \vec{f} = & \frac{\hat{\zeta}}{a \sqrt{(\zeta^2 - \xi^2)(\zeta^2 - 1)}} \left[\frac{\partial}{\partial \xi} \left(\sqrt{(\zeta^2 - 1)(1 - \xi^2)} f_{\varphi} \right) - \frac{\partial}{\partial \varphi} \left(\sqrt{\frac{\zeta^2 - \xi^2}{1 - \xi^2}} f_{\xi} \right) \right] \\ & + \frac{\hat{\xi}}{a \sqrt{(\zeta^2 - \xi^2)(1 - \xi^2)}} \left[\frac{\partial}{\partial \varphi} \left(\sqrt{\frac{\zeta^2 - \xi^2}{\zeta^2 - 1}} f_{\zeta} \right) - \frac{\partial}{\partial \zeta} \left(\sqrt{(\zeta^2 - 1)(1 - \xi^2)} f_{\varphi} \right) \right] \\ & + \frac{\hat{\varphi} \sqrt{(\zeta^2 - 1)(1 - \xi^2)}}{a(\zeta^2 - \xi^2)} \left[\frac{\partial}{\partial \zeta} \left(\sqrt{\frac{\zeta^2 - \xi^2}{1 - \xi^2}} f_{\xi} \right) - \frac{\partial}{\partial \xi} \left(\sqrt{\frac{\zeta^2 - \xi^2}{\zeta^2 - 1}} f_{\zeta} \right) \right] \quad (29) \end{aligned}$$

We now consider the transformation of vectors. In the following, the unprimed variables are in the prolate spheroidal system and the primed ones are in another orthogonal system. Define a transformation matrix (α_{ij}) by:

$$\hat{e}_i = \sum_j \alpha_{ij} \hat{e}'_j \quad (30)$$

The inverse transformation is

$$\hat{e}'_i = \sum_j \alpha_{ji} \hat{e}_j \quad (31)$$

The orthogonality relations associated with the transformation are

$$\sum_k \alpha_{ki} \alpha_{kj} = \delta_{ij} \quad (32)$$

$$\sum_k \alpha_{ik} \alpha_{jk} = \delta_{ij} \quad (33)$$

For any vector, \vec{f} , we have

$$f_i = \sum_j \alpha_{ij} f'_j \quad (34)$$

$$f'_i = \sum_j \alpha_{ji} f_j \quad (35)$$

To determine the matrix elements (α_{ij}) , we note that

$$\hat{\zeta} = h_\zeta \nabla_\zeta, \quad \hat{\xi} = h_\xi \nabla_\xi \quad (36)$$

Now, for an azimuthally symmetric problem

$$\nabla\zeta = \frac{\partial\zeta}{\partial r} \hat{r} + \frac{1}{r} \frac{\partial\zeta}{\partial\theta} \hat{\theta} \quad (37)$$

or,

$$\nabla\zeta = \frac{a}{h_\zeta^2} \hat{r} + \frac{a}{h_\xi h_\zeta} \hat{\theta} \quad (38)$$

∴

$$\hat{\zeta} = \frac{a}{h_\zeta} \hat{r} + \frac{a}{h_\xi} \hat{\theta} \quad (39)$$

Similarly,

$$\nabla\xi = \frac{\partial\xi}{\partial r} \hat{r} + \frac{1}{r} \frac{\partial\xi}{\partial\theta} \hat{\theta} \quad (40)$$

or,

$$\nabla\xi = \frac{-a}{h_\xi^2} \hat{r} + \frac{a}{h_\zeta h_\xi} \hat{\theta} \quad (41)$$

∴

$$\hat{\xi} = -\frac{a}{h_\xi} \hat{r} + \frac{a}{h_\zeta} \hat{\theta} \quad (42)$$

Comparing equations (30), (39), and (42) yields the desired matrix elements

$$(\alpha_{ij}) = a \begin{pmatrix} \frac{1}{h_\zeta} & \frac{1}{h_\xi} \\ -\frac{1}{h_\xi} & \frac{1}{h_\zeta} \end{pmatrix} \quad (43)$$

The transformation is orthogonal. Its inverse is:

$$(\alpha_{ij})^{-1} = a \begin{pmatrix} \frac{1}{h_{\zeta}} & -\frac{1}{h_{\xi}} \\ \frac{1}{h_{\xi}} & \frac{1}{h_{\zeta}} \end{pmatrix} \quad (44)$$

The equations inverse to equations (39) and (42) are:

$$\hat{r} = \frac{a}{h_{\zeta}} \hat{\zeta} - \frac{a}{h_{\xi}} \hat{\xi} \quad (45)$$

$$\hat{\theta} = \frac{a}{h_{\xi}} \hat{\zeta} + \frac{a}{h_{\zeta}} \hat{\xi} \quad (46)$$

Note that

$$\frac{1}{h_{\xi}^2} + \frac{1}{h_{\zeta}^2} = \frac{1}{a^2} \quad (47)$$

The transformation of vectors to the spherical polar system centered at the image point of the weapon is given by

$$(\alpha'_{ij}) = \begin{pmatrix} \frac{a}{h_{\zeta}} & -\frac{a}{h_{\xi}} \\ \frac{a}{h_{\xi}} & \frac{a}{h_{\zeta}} \end{pmatrix} \quad (48)$$

The inverse transformation is:

$$(\alpha'_{ij})^{-1} = \begin{pmatrix} \frac{a}{h_\zeta} & \frac{a}{h_\xi} \\ -\frac{a}{h_\xi} & \frac{a}{h_\zeta} \end{pmatrix} \quad (49)$$

The equations analogous to equations (45) and (46) are:

$$\hat{r}' = \frac{a}{h_\zeta} \hat{\zeta} + \frac{a}{h_\xi} \hat{\xi} \quad (50)$$

$$\theta' = -\frac{a}{h_\xi} \hat{\zeta} + \frac{a}{h_\zeta} \hat{\xi} \quad (51)$$

APPENDIX B: PROGRAMMING DETAILS OF ALGORITHM "B"

B.1 General Description

A good deal of machinery is required to operate prior to the exercising of Subroutine MARCH, as it is used to implement Algorithm "B". As noted in Section 2.2.4, the overall computational procedure is organized much as in ARIADNE,⁽¹³⁾ with MARCH performing the specific function of advancing the fields by one timestep. The total procedure, in brief, may be assumed to consist of repeated cycles (one for each field-timestep) in which current and conductivity sources are updated and supplied to MARCH via a set of labelled COMMON data blocks. MARCH is called to complete a timestep cycle by advancing the fields to their "new" values, using the sources supplied from elsewhere in the procedure. Section B.2 contains a summary of important physical variables in MARCH, together with their FORTRAN equivalents, and references to the appropriate equations in Section 2.2. Section B.3 contains a FORTRAN listing of the MARCH subroutine itself. Details of the MARCH internal computational procedure are felt to be best explained by the fairly complete commentary that is supplied as part of the FORTRAN listing.

B.2 Important Variables In MARCH

B.2.1 Input/Output Data

Data is exchanged with MARCH via the five labelled COMMON blocks /PHYS1/, /PHYS2/, /PHYS3/, /DRIVR3/, and /DRIVR4/. Vital elements of these data are listed and briefly explained in the table below.

Table B.1

COMMUNICATION WITH MARCH

<u>Variable</u>	<u>Analytic Equivalent</u>	<u>Description</u>
TAUED1	τ_1	Value of time at timestep beginning
TAUED2	τ_2	Value of time at timestep end
AAA	a	PS coordinate system parameter, equation (1.2)
DXI	$\Delta\xi_i$	---
DZETA	$\Delta\zeta_j$	---
NXIS, NZETAS, IM, IM1, JM, JM1, etc. are indexing limits on subscripts		
XI	ξ_i	---
X2A2	$\xi^2 a^2$	---
XNUM	$a^2(1 - \xi^2)$	---
SRXNUM	---	$XNUM^{1/2}$
ZETA	ζ_j	---
Z2	ζ^2	---
ZNUM	$(\zeta^2 - a^2)$	---

Table B. 1 (Cont'd.)

<u>Variable</u>	<u>Analytic Equivalent</u>	<u>Description</u>
SRZNUM	---	ZNUM ^{1/2}
EPS	ϵ	(See 2.2.1)
EXI	E_{ξ}	TM Components of the EM field. (See equation (2.2.2))
EZETA	E_{ζ}	
BPHI	H_{φ}	
XJXI	J_{ξ}	Compton current sources. (See equation (2.2.2))
XJZETA	J_{ζ}	
SIGMA	σ	
XBJX	J_{ξ}	Sources along z-axis, at $\zeta = a$
XBSIG	σ	
ZBJZ	J_{ζ}	Sources along z-axis, at $\xi = 1$
ZBSIG	σ	

B.2.2 Internal Variables

Geometrical parameters, source input data, and field output data are listed in the table above. Most of the remainder of the variables are internally-defined in an obvious way. Important exceptions are the basic coefficients mentioned in Section 2.2 and the variables used in the implicit variation of the field solution mentioned in Section 2.2.3.

Table B.2
INTERNAL MARCH VARIABLES

<u>Variable</u>	<u>Analytic Equivalent</u>	<u>Description</u>
A0	A_0	See equations (2.2.10)
A1	A_1	
B0	B_0	
B1	B_1	
C1L	C_{1L}	See equations (2.2.17)
C1U	C_{1U}	
RZL	$r_{\zeta L}$	
RZU	$r_{\zeta U}$	
D1L	D_{1L}	Analogues of equations (2.2.17) for
D1U	D_{1U}	
RXL	$r_{\xi L}$	
RXU	$r_{\xi U}$	
HPA	---	See equations (2.2.9) and (2.2.10)
EXA	---	See equations (2.2.17) and (2.2.20)
EZA	---	Analogous to EXA. See equation (2.2.19)
EU	E	Recursion coefficients used in implicit solution of difference equations for E_{ζ}
FU	F	

Table B.2 (Cont'd.)

<u>Variable</u>	<u>Analytic Equivalent</u>	<u>Description</u>
Q___	---	A variety of variables are used as intermediate storage of constants needed to obtain remaining fields from E_{ζ}
EXAS	---	
C1S	---	

B.3 FORTRAN Listing of MARCH

	SUBROUTINE MARCH	ACH	348
C		ACH	349
C	MARCH IS THE ELECTRODYNAMIC ALGORITHM. IT SOLVES THE C.M.F.E.	ACH	350
C	FROM THE SOURCES THAT HAVE BEEN PREPARED AND INSERTED INTO	ACH	351
C	COMMON /DRIVR3/.	ACH	352
C		ACH	353
C		MRCH	7
000001	COMMON /PHYS1/ TAUED1, TAUED2, TSRC3, TSRC1, TSRC2	MRCH	8
000001	COMMON /PHYS2/ AAA, DXI(200), DZETA(200), NXIS, NZETAS,	ACH	354
1	IM, IM1, IM2, IM3, JM, JM1, JM2, JM3,	MRCH	10
2	XI(200), X2A2(200), XNUM(200), SRXNUM(200),	MRCH	11
3	ZETA(100), Z2(100), ZNUM(100), SRZNUM(100)	MRCH	12
4	,EPS(200),SIG(200)	ACH	355
C		BIGGY	2
C	THIS SECTION CONTAINS THE SOURCE AND FIELD ARRAYS. THE	ACH	1
C	SOURCES ARE UPDATED IN SPSRC AND USED IN MARCH TO UPDATE	ACH	2
C	THE FIELDS. EGS STORAGE OR LARGE STORAGE MAY BE USED FOR	ACH	3
C	VARIABLES HERE, BECAUSE OF THE LARGE ARRAY SIZE.	ACH	4
C		ACH	5
000001	COMMON /PHYS3/ EXI(50,50), EZETA(50,50), EPHI(5, 5),	ACH	6
1	BXI(5, 5), BZETA(5, 5), BPHI(50,100)	ACH	7
C	1 BXI(5, 5), BZETA(5, 5), BPHI(50,50)	ACH	8
C		ACH	9
000001	COMMON /DRIVR3/ XJXI(50,50), XJZETA(50,50), XJPHI(5, 5),	ACH	10
1	SIGMA(50,50)	ACH	11
000001	COMMON /DRIVR4/ XBJX(50), XBSIG(50), ZBJZ(50), ZBSIG(50)	ACH	12
C		9IGGY	14
C		ACH	356
000001	DIMENSION AX2(200), AXM(200), AZP(200), AZM(200), GXN(200), GZN(200)	ACH	357
000001	DIMENSION EX29(200), EZ29(200), HP29(200), SIGRC(200), QSO(200),	ACH	358
1	QS1(200), QS2(200), EU(200), FU(200), C1S(200), EXAS(200),	ACH	359
2	D1S(200), EZBS(200), CJX(50,50), CJZ(50,50)	ACH	360
000001	DIMENSION EX(50, 50), EZ(50, 50), HP(50, 50)	ACH	361
000001	DIMENSION DTODXU(200), AXMU(200), DTODZU(200), AZMU(200)	ACH	362
C		ACH	363
000001	EQUIVALENCE (GXN,XNUM), (GZN,ZNUM), (EZ,EZETA), (EX,EXI), (HP,BPHI)	ACH	364
000001	EQUIVALENCE (CJX,XJXI), (CJZ,XJZETA)	ACH	365
C		ACH	366
C	FUNDAMENTAL CONSTANTS	ACH	367
C		ACH	368
000001	DATA CL /2.997925E+18/	ACH	369
000001	DATA ZJ /376.7304/	ACH	370
000001	DATA KIMP /-1/	ACH	371
000001	DATA KCX3, KCZ3 /1, -1/	ACH	372
000001	IF(TAUED2.GT.5.E-8) KIMP=1	ACH	373
C		ACH	374
C		ACH	375
C	A FEW FACTORS USEFUL THROUGHOUT THIS TIMESTEP.	ACH	376
C		ACH	377
000005	DTAU=CL*(TAUED2-TAUED1)	ACH	378
000007	ZJDTAU = ZJ*DTAU	ACH	379
000011	SIG3=2./ZJDTAU	ACH	380
C		ACH	381
C	I-DEPENDENT FACTORS.	ACH	382
C	(EPSILON IS PRESENTLY STRATIFIED ONLY IN I.)	ACH	383
C		ACH	384
000013	DO 19 I = 1, IM1	ACH	385
000022	DTODX = DTAU/(AAA*DXI(I))	ACH	386

000024	AXP(I) = (1. + DTODX)	ACH	397
000025	AXM(I) = (1. - DTODX)	ACH	388
000027	DTODXU(I) = DTAU / (AAA*(DXI(I)+DXI(I+1)))	ACH	399
000032	AXMU(I) = (1. - DTODXU(I))	ACH	392
000033	SIGR(I) = ZC9TAU/EPS(I)	ACH	391
000034	19 CONTINUE	ACH	392
C		ACH	393
C	J-DEPENDENT FACTORS	ACH	394
C		ACH	395
000036	DO 29 J = 1, JM1	ACH	396
000046	DTODZ = DTAU/DZETA(J)	ACH	397
000047	AZP(J) = (1. + DTODZ)	ACH	398
000050	AZM(J) = (1. - DTODZ)	ACH	399
000051	DTODZU(J) = DTAU / (DZETA(J)+DZETA(J+1))	ACH	400
000053	AZMU(J) = (1. - DTODZU(J))	ACH	401
000053	29 CONTINUE	ACH	402
C		ACH	403
C	THIS IS THE PROCEDURE ITSELF. HERE, ROWS	ACH	404
C	OF FIELD VALUES ALONG SUCCESSIVE	ACH	405
C	ELLIPSOIDS (FIXED VALUE OF *J*) ARE	ACH	406
C	UPDATED VIA AN EXPLICIT OR IMPLICIT SCHEME. J	ACH	407
C	IS MARCHED OUT FROM J=1 (THE LOWER	ACH	408
C	Z-AXIS) TO JM2, THE J-INDEX OF AN	ACH	409
C	OUTER ELLIPSOIDAL SHELL. H-PHI=D AT	ACH	410
C	ALL POINTS ALONG THE Z-AXIS (I=1 OR J=1)	ACH	411
C	AND RADIAL-FIELD BOUNDARY CONDITIONS	ACH	412
C	DETERMINE E-XI AT J=1 AND S-ZETA	ACH	413
C	AT I=1.	ACH	414
C		ACH	415
C	UPDATE SOURCES FOR THIS CYCLE.	ACH	416
C		ACH	417
000054	CALL SOURCE(1,2)	ACH	418
C		ACH	419
C	BEGIN BY INITIALIZING ROW-BELOW VECTORS OF HP AND EX TO Z-AXIS	ACH	420
C	VALUES.	ACH	421
C		ACH	422
000056	101 DO 109 I=1, IM2	ACH	423
C		ACH	424
000061	HP29(I) = 0.	ACH	425
C		ACH	426
C	EX IS A RADIAL FIELD AT THE POINT THAT EACH HYPERBOLOID	ACH	427
C	INTERSECTS THE LOWER Z-AXIS.	ACH	428
C		ACH	429
000061	XKDT = X3SIG(I)*SIGR(I)	ACH	430
000063	IF(XKDT .LE. 1.E-5) GO TO 107	ACH	431
000065	EXKDT = EXP(-XKDT)	ACH	432
000071	EXKDTP = (1. - EXKDT)	ACH	433
000072	SRA = -EXKDTP/X3SIG(I)	ACH	434
000075	GO TO 108	ACH	435
000077	107 SPHACT = (1. - .5*XKDT)	ACH	436
000101	EXKOTP = XKDT*SPHACT	ACH	437
000102	EXKDT = (1. - EXKOTP)	ACH	438
000103	SRA = -SIGR(I)*SPHACT	ACH	439
000106	108 EX29(I) = EX(I,1)*EXKDT + SRA*XBIX(I)	ACH	440
000113	109 CONTINUE	ACH	441
C		ACH	442
C	NOW, PROCEED TO MARCH OUT IN I AT EACH OF THE	ACH	443
C	APPROPRIATE J-VALUES.	ACH	444

000115	C	DO 1+3 J=1, JN2	ACH	445
	C		ACH	446
	C	PREPARE A FEW I-INDEPENDENT CONSTANTS USEFUL AT THIS J-VALUE.	ACH	447
	C		ACH	448
000116		AZPJ = AZP(J)	ACH	449
000121		AZMJ = AZM(J)	ACH	450
000122		ZURJ=DTODZU(J)	ACH	451
000123		AZMUJ=AZMU(J)	ACH	452
000125		IF(J.EQ.1) GO TO 115	ACH	453
000130		ZLRJ=DTODZU(J-1)	ACH	454
000131		AZMLJ=AZMU(J-1)	ACH	455
000133		GO TO 116	ACH	456
000133	115	ZLRJ=J.	ACH	457
000134		AZMLJ=AZMJ	ACH	458
000137	116	GZMJ=GZM(J)	ACH	459
000140		ZZJ = Z2(J)	ACH	460
	C		ACH	461
	C	INITIALIZE CELL-TO-THE-RIGHT VALUES OF NEW	ACH	462
	C	E-ZETA AND H-PHI BEFORE PROCEEDING AT NEW J.	ACH	463
	C		ACH	464
000142		HF2R=J.	ACH	465
	C		ACH	466
	C	EZ AT THE TOP CENTER OF EACH ELLIPSOID IS FOUND FROM THE RADIAL	ACH	467
	C	E-FIELD BOUNDARY CONDITION ALONG THE UPPER Z-AXIS.	ACH	468
	C		ACH	469
000142		XKDT = ZBSIG(J)*SIGR0(1)	ACH	470
000144		IF(XKDT .LE. 1.E-5) GO TO 117	ACH	471
000147		EXKDT = EXP(-XKDT)	ACH	472
000153		EXKDTP = (1. - EXKDT)	ACH	473
000154		SRA=-EXKOTP/ZBSIG(J)	ACH	474
000160		GO TO 118	ACH	475
000161	117	SPHACT=(1.-J.5*XKDT)	ACH	476
000163		EXKDTP=EXKDT*SPHACT	ACH	477
000164		EXKDT = (1. - EXKDTP)	ACH	478
000165		SRA=-SIGR0(1)*SPHACT	ACH	479
000167	118	EZ2R=EZ1(J)*EXKDT+SRA*ZBJZ(J)	ACH	480
	C		ACH	481
	C	BEGINNING WITH I=1, FIND NEW	ACH	482
	C	E-FIELDS AT OUTER EDGES OF (I,J)-TH	ACH	483
	C	CELL. AND NEW H-FIELD WITHIN (I,J)-TH CELL.	ACH	484
	C		ACH	485
000175		DO 129 I=1, IN2	ACH	486
	C		ACH	487
	C	(REMAINING FACTORS NEEDED AS BASIC COEFFICIENTS IN THE (I,J)-TH	ACH	488
	C	RING)	ACH	489
	C		ACH	490
000177		AXFI = AXF(I)	ACH	491
000202		AXMI = AXM(I)	ACH	492
000203		XURI=DTODXU(I)	ACH	493
000204		AXMUI=AXMU(I)	ACH	494
000206		IF(I.EQ.1) GO TO 123	ACH	495
000211		XLRI=DTODXU(I-1)	ACH	496
000212		AXMLI=AXMU(I-1)	ACH	497
000214		GO TO 124	ACH	498
000214	123	XLRI=J.	ACH	499
000215		AXMLI=AXMI	ACH	500
000224	124	GOPH=-1./(2.*(Z2J-X2A2(I)))	ACH	501
			ACH	502

000227	GX = GOPH*GXN(I)	ACH	503
000230	GZ = GOPH*GZNJ	ACH	504
	C	ACH	505
000232	XKDT = SIGMA(I,J)*SIGR(I)	ACH	506
000233	IF(XKDT .LE. 1.E-5) GO TO 125	ACH	507
000236	EXKDT = EXP(-XKDT)	ACH	508
000245	EXKDTP = (1. - EXKDT)	ACH	509
000247	SIGR=-EXKDTP/SIGMA(I,J)	ACH	510
000250	GO TO 125	ACH	511
000252	125 SPHACT=(1.-J,3*XKDT)	ACH	512
000254	EXKDTP=XKDT*SPHACT	ACH	513
000255	EXKDT = (1. - EXKDTP)	ACH	514
000256	SIGR=-SIGR(I)*SPHACT	ACH	515
000270	126 PHACTR=SIGR*SIGR	ACH	516
	C	ACH	517
	C	ACH	518
	C	ACH	519
	C	ACH	520
000271	A0 = GX*AXPI	ACH	521
000272	A1 = GX*AXMI	ACH	522
000274	B0 = GZ*AZPJ	ACH	523
000276	B1 = GZ*AZMJ	ACH	524
000277	C1L=PHACTR*AZMLJ	ACH	525
000301	C1U=PHACTR*AZMUJ	ACH	526
000302	RZL=PHACTR*ZLRJ	ACH	527
000304	RZU=PHACTR*ZURJ	ACH	528
000305	D1L=PHACTR*AXMLI	ACH	529
000307	D1U=PHACTR*AXMUI	ACH	530
000310	RXL=PHACTR*XLRI	ACH	531
000312	RXU=PHACTR*XURI	ACH	532
	C	ACH	533
000313	HPA = HP(I,J)-A1*EZ(I,J)-A2*EZ(I+1,J)-B1*EX(I,J)	ACH	534
	-B2(EX(I,J+1)-EX2B(I))	ACH	535
000325	EXA = (EX(I,J+1)+EX(I,J))*EXKDT-EX2B(I)+2.*SIGR*CJX(I,J)	ACH	536
	*-C1U*HP(I,J)-RZU*HP(I,J+1)+RZL*HP2B(I)	ACH	537
000337	EZA = (EZ(I+1,J)+EZ(I,J))*EXKDT+2.*SIGR*CJZ(I,J)-D1U*HP(I,J)	ACH	538
	*-RXU*HP(I+1,J)	ACH	539
	C	ACH	540
	C	ACH	541
	C	ACH	542
	C	ACH	543
000350	IF(KIME .GT. 0) GO TO 127	ACH	544
	C	ACH	545
	C	ACH	546
	C	ACH	547
	C	ACH	548
	C	ACH	549
000353	IF (I.GT.1) HP(I-1,J)=HP2R	ACH	550
000361	IF(I.EQ.IM2.AND.KCX9.EQ.1) A1=0.	ACH	551
000370	IF(J.EQ.JM2.AND.KCZ9.EQ.1) B1=0.	ACH	552
000405	EZAR=EZA+RXL*HP2R	ACH	553
000407	HP2R = ((A0-A1)*EZ2R+HPA+A1*EZAR+B1*EXA) /	ACH	554
	*(1.-A1*D1L-B1*C1L)	ACH	555
000423	HP2B(I)=HP2R	ACH	556
000424	EX(I,J)=EX2B(I)	ACH	557
000425	EX2B(I) = EXA+C1L*HP2R	ACH	558
000427	IF(J.EQ.JM2.AND.KCZ8.EQ.1) EX2B(I)=0.	ACH	559
000444	EZ(I,J) = EZ2R	ACH	560
000445	EZ2R = EZAR+D1L*HP2R-EZ2R	ACH	560

00050		IF(I.EQ.IM2.AND.KCX9.EQ.1) EZ2R=0.	ACH	551
00051		GO TO 129	ACH	552
00052	127	EXAS(I)=EXA	ACH	563
00053		C1S(I)=C1L	ACH	564
00054		IF(J.EQ.JM2.AND.KCZ9.EQ.1) B1=C.	ACH	565
	C		ACH	566
000500		QDEN=1./(1.-31*C1L)	ACH	567
000503		QUJ=QDEN*A0	ACH	568
000504		QU1=QDEN*A1	ACH	569
000505		QU2=QDEN*(HFA+91*EXA)	ACH	570
	C		ACH	571
000511		QS3(I)=QUJ	ACH	572
000512		QS1(I)=QU1	ACH	573
000513		QS2(I)=QU2	ACH	574
	C		ACH	575
000516		IF(I.GT.1) GO TO 1281	ACH	576
	C		ACH	577
	C	BOTTOM-MOST RECURSION COEFFICIENTS	ACH	578
	C		ACH	579
000521		EU(1)=0.	ACH	580
000521		FU(1)=EZ2R	ACH	581
000523		GO TO 1282	ACH	582
	C		ACH	583
	C	REGULAR RECURSION COEFFICIENTS	ACH	584
	C		ACH	585
000523	1281	QPLS=(1.-D1L*QU1)	ACH	586
000526		QZRO=(1.-D1L*QU2-RXL*QL1)	ACH	587
000532		QMIN=-RXL*QL0	ACH	588
	C		ACH	589
000533		PUR=EZA+D1L*QU2+RXL*QL2	ACH	590
000543		IF(I.NE.I02.OR.KCXB.NE.1) GO TO 1283	ACH	591
	C		ACH	592
000550		QPLS=RXUL*QU1	ACH	593
000551		QZRO=(1.-D0UL*QL1+RXUL*QU2)	ACH	594
000555		QMIN=1.-D0U*QL0	ACH	595
	C		ACH	596
000560		PUR=(EZAL+D0UL*QL2-RXUL*QU2)	ACH	597
	C		ACH	598
000567	1283	QDEN=1./(QZRO+QMIN*EU(I-1))	ACH	599
	C		ACH	600
000572		EU(I)=-QPLS*QDEN	ACH	601
000574		FU(I)=(PUR-QMIN*EU(I-1))*QDEN	ACH	602
	C		ACH	603
000577	1282	QL0=QUJ	ACH	604
000600		QL1=QU1	ACH	605
000602		QL2=QU2	ACH	606
000603		IF(I.NE.I03.OR.KCXB.NE.1) GO TO 129	ACH	607
	C		ACH	608
000616		D0UL=PHACTR*(1.+XURI)	ACH	609
000621		EZAL=(EZ(I+1,J)+EZ(I,J))*EXQT+2.*SIGR*CJZ(I,J)-D0U*HF(I,J) *+RXL*HF(I-1,J)	ACH	610
000632		RXUL=RXU	ACH	611
	C		ACH	612
000634	129	CONTINUE	ACH	613
	C		ACH	614
	C	IF SCHEME IS EXPLICIT, WE JUST FINISH	ACH	615
	C	THE OUTER LOCATIONS,	ACH	616
	C		ACH	617
	C		ACH	618

001637		IF(KIMP.LE.J) GO TO 148	ACH	619
C			ACH	620
C		THIS IS THE REMAINDER OF THE IMPLICIT BRANCH. WE	ACH	621
C		START WITH OUTER BOUNDARY CONDITIONS AND WORK BACK	ACH	622
C		DOWN THRU I'S WITH RECURSION FORMULAS, ETC.	ACH	623
C			ACH	624
C		OUTER B.C. FOR NOW IS A MESS	ACH	625
C			ACH	626
001641		IF(KCX9.EQ.1) GO TO 1292	ACH	627
001651	1291	DJU=PHACTR*(1.+XURI)	ACH	628
001653		EZAL=(EZ(I+1,J)+EZ(I,J))*EXKOT+2.*SIGR*CJZ(I,J)-DJU*HP(I,J)	ACH	629
		*+RXL*HP(I-1,J)	ACH	630
001664		CURLY=(DJU*OL1-1.)	ACH	631
001666		EZ(IM1,J)=(EZAL+FU(IM2)*CURLY+DJU*OL2)/(1.-EU(IM2)*CURLY-DJU*OL1)	ACH	632
C			ACH	633
001676		GO TO 1293	ACH	634
C			ACH	635
001677	1292	EZ(IM1,J)=0.	ACH	636
C			ACH	637
001703	1293	DO 139 IC=1,IM2	ACH	638
001731		I=IM2-IC+1	ACH	639
001733		IA=I+1	ACH	640
C			ACH	641
001734		EZ(I,J)=EU(I)*EZ(IA,J)+FU(I)	ACH	642
001743		IF(J.GT.1) HP(I,J-1)=HP2B(I)	ACH	643
001744		HP2B(I)=QS3(I)*EZ(I,J)+QS1(I)*EZ(IA,J)+QS2(I)	ACH	644
001752		EX(I,J)=EX2B(I)	ACH	645
001754		EX2B(I)=EXAS(I)+C1S(I)*HP2B(I)	ACH	646
C			ACH	647
001760		IF(J.EQ.JM2.AND.KCZ9.EQ.1) EX2B=0.	ACH	648
001763	139	CONTINUE	ACH	649
C			ACH	650
C		FIX UP LAST HP-VALUE.	ACH	651
C			ACH	652
001767		HP(IM1,J)=0.	ACH	653
C			ACH	654
001773		GO TO 149	ACH	655
C			ACH	656
C		AT THE END OF AN I-ROW, WE STORE	ACH	657
C		THE LAST EZ2R AND APPLY BOUNDARY	ACH	658
C		CONDITIONS TO GET BELOW-GROUND HP(IM1,J)	ACH	659
C			ACH	660
001800	148	EZ(IM1,J) = EZ2R	ACH	661
001802		HP(IM2,J) = HP2R	ACH	662
C			ACH	663
001803		HP(IM1,J)=0.	ACH	664
C			ACH	665
001804	149	CONTINUE	ACH	666
C			ACH	667
C		AFTER THE JM2-TH I-ROW, STORE	ACH	668
C		THE LAST EX2B-VALUES AND APPLY	ACH	669
C		OUTER-ELLIPOID BOUNDARY CONDITIONS	ACH	670
C		TO H(T,JM1)	ACH	671
C			ACH	672
001807		DO 193 I=1,IM2	ACH	673
C			ACH	674
001824		EX(I,JM1) = EX2B(I)	ACH	675
001826		IF(KIMP.GT.J) HP(I,JM2)=HP2B(I)	ACH	676

011030	C	HP(I, JM1) = HP(I, JM3-1)-3.*HP(I, JM3)+3.*HP(I, JM2)	ACH	677
011033	C		ACH	678
011033	199	CONTINUE	ACH	579
	C		ACH	680
011035		RETURN	ACH	581
011036		END	ACH	682
			MRGH	203

SUBPROGRAM LENGTH
311400

FUNCTION ASSIGNMENTS

STATEMENT ASSIGNMENTS

101	-	000057	107	-	000077	108	-	000107	115	-	000134
115	-	000137	117	-	000161	118	-	000170	123	-	000215
124	-	000220	125	-	000252	126	-	000262	127	-	000462
129	-	000635	139	-	000764	148	-	000774	149	-	001005
1281	-	000624	1282	-	000600	1283	-	000566	1291	-	000643
1292	-	000700	1293	-	000704						

BLOCK NAMES AND LENGTHS

PHYS1	-	000045	PHYS2	-	000733	PHYS3	-	023533	DRIVR3	-	016545
DRIVR4	-	000310									

VARIABLE ASSIGNMENTS

AAA	-	000000C02	AXM	-	011430	AXMI	-	011324	AXMLI	-	011330
AXMU	-	011140	AXMUI	-	011326	AXF	-	001120	AXEI	-	011323
AZM	-	002250	AZMJ	-	011312	AZMLJ	-	011316	AZMU	-	010760
AZMUJ	-	011314	AZP	-	001740	AZPJ	-	011311	AC	-	011336
A1	-	011337	BPHI	-	011723C03	BXI	-	011641C03	BZETA	-	011672C03
B0	-	011340	B1	-	011341	CJX	-	000000C04	CJZ	-	004704C04
CL	-	011270	CURLY	-	011375	G1L	-	011342	C1S	-	006170
C1U	-	011343	DTAU	-	011275	DTODX	-	011301	DTODXU	-	007630
DTODZ	-	011303	DTODZU	-	010450	OXI	-	000001C02	DZETA	-	000311C02
DSU	-	011373	DSUL	-	011372	D1L	-	011346	D1S	-	007010
D1U	-	011347	EPHI	-	011610C03	EPS	-	003113C02	EU	-	005350
EX	-	000000C03	EXA	-	011353	EXAS	-	006500	EXI	-	000000C03
EXKDT	-	011365	EXKDTP	-	011306	EX2B	-	002560	EZ	-	004704C03
EZA	-	011354	EZAL	-	011374	EZAR	-	011355	EZBS	-	007320
EZETA	-	004704C03	EZ2B	-	003070	EZ2R	-	011322	FU	-	005660
GDPH	-	011331	GX	-	011332	GXN	-	004530C02	GZ	-	011333
GZN	-	002603C02	GZNJ	-	011317	HP	-	011723C03	HPA	-	011352
HP2B	-	003400	HP2R	-	011321	I	-	011300	IA	-	011377
IG	-	011376	IM1	-	000624C02	IM2	-	000625C02	IM3	-	000626C02
J	-	011302	JM1	-	000631C02	JM2	-	000631C02	JM3	-	000632C02
KCXB	-	011273	KCZB	-	011274	KIMP	-	011272	PHACTR	-	011335
PUR	-	011367	QDEN	-	011356	QL0	-	011366	QL1	-	011364
QL2	-	011370	QMIN	-	011365	QFLS	-	011362	QS0	-	004220
QS1	-	004430	QS2	-	005040	QU0	-	011357	QU1	-	011360
QJ2	-	011361	QZRO	-	011363	RXL	-	011350	RXU	-	011351
RXUL	-	011371	RZL	-	011344	RZU	-	011345	SIG	-	003423C02
SIGMA	-	011641C04	SIGR	-	011334	SIGR0	-	003710	SIGG	-	011277
SPHACT	-	011310	SRA	-	011307	SRXNUM	-	001763C02	SRZNUM	-	002740C02
TAUED1	-	000000C01	TAUED2	-	000001C01	XBJX	-	000000C05	XBSIG	-	000000C05
XI	-	000633C02	XJPHI	-	011610C04	XJXI	-	000000C04	XJZETA	-	004704C04


```

DY=DZ
YMAX=ZMAX
X0=R0
JGND=NY/2 + 1
DO 30 I=1,NX
30 X(I)=R0 + FLOAT(I-1)*DR
DY=2.0*YMAX/FLOAT(NY-1)
K=NY
DO 40 J=1,NY
Y(K)=YMAX-FLOAT(J-1)*DY
40 K=K-1
DO 50 I=1,NX
F(I)=X(I)
50 FP(I)=1.0
DO 60 J=1,NY
G(J)=Y(J)
60 GP(J)=1.0

```

```

C
C   *** DEFINE THE CONSTANTS ***
C

```

```

C=2.998E+8
PI=3.14159265
EPS=8.854E-12
MU=4.0E-7*PI
EMU=1.0/SQRT(EPS*MU)
NXM1=NX-1
NXM2=NX-2
NYM1=NY-1
NYM2=NY-2
NG=NY/2 + 1
EPI=1.0/(2.0*EPS)
CALL SETP
TS=R(1,NYM1)/C + 0.5*DZ/C + DT
IF(T0.LT.TS) T0=TS

```

```

C
C   *** SUMMARY OF RUN DATA PRINTED
C

```

```

CALL DATE(DAY)
CALL TIME(HMS)
CALL RDS(KOMENT, DAY, HMS)

```

```

C
C   *** ADVANCE THE FIELDS IN TIME ***

```

```

DO 100 K=1,NT
T=T0 + FLOAT(K)*DT
TMP=T-0.5*DT
RWF=C*TMP
CALL SIGMA(TMP)
CALL CURENT(TMP)
DO 110 I=1,NX
DO 110 J=1,NY
ER1(I,J)=ER2(I,J)
BP1(I,J)=BP2(I,J)
EZ1(I,J)=EZ2(I,J)
110 CONTINUE

```

C *** STEP THE FIELDS IN RANGE ***

C
C
C
DO 200 I=2,NXM1
IM1=I-1
IP1=I+1
AA2=FMU*(FP(IM1)/DX+0.5/F(I-1))

AA3=-FP(I)*DT/(2.0*DX)
DO 201 JJ=JGND,NY
J=NY-JJ+JGND
JIM=NY-J+1
IF(RWF.GT.R(I,JIM)) GO TO 202
201 CONTINUE
REFLECT=.FALSE.
DO 203 J=JGND,NY
IF(RWF.GT.R(I,J)) GO TO 204
203 CONTINUE
GO TO 511
204 J1DMN=J
J1DMX=NY
GO TO 205
202 J1DMN=J+1
J1DMX=NY-1
J2DMX=J
J2DMN=NY-J+1
REFLECT=.TRUE.
IF((J2DMX-J2DMN).LE.0.0) REFLECT=.FALSE.
205 CONTINUE

C *** ADVANCE THE FIELDS OVER ALTITUDE TO GET IMPLICIT COEFFICIENTS

C
C
C
F(J2DMN-1)=0.
FF(J2DMN-1)=0.
RP2(I,J2DMX+1)=0.
DO 250 J=J1DMN,J1DMX
FRB4=SQRT(ER1(I,J)**2 + EZ1(I,J)**2)
CJR=-SQRT(JR(I,J)**2+J7(I,J)**2)
ARG=+SIG(I,J)*DT/FP5
IF(ARG.EQ.0.0) GO TO 250
FARG=EXP(-ARG)
OFARG=1.0-FARG
IF(ARG.LT.1.0E-5) OFARG=FS(ARG)
ERN=FRB4*FARG-CJR*OFARG/SIG(I,I)
ER2(I,J)=ERN*X(I)/R(I,J)
EZ2(I,J)=-ERN*(HOB-Y(J))/R(I,J)
250 CONTINUE
IF(.NOT.REFLECT) GO TO 200
DO 300 J=J2DMN,J2DMX
JIM=NY-JWF+1
JM1=J-1
JP1=J+1
GAM1=(SIG(I,J)+SIG(I,JM1))*EPI
TH1=DT*GAM1
ET1=EXP(-TH1)
IF(TH1.GT.1.0E-4) GO TO 310

```

OET1=FS(TH1)
GO TO 320
310 OET1=1.0-ET1
320 GAM2=(SIG(IM1,J)+SIG(I,J))*EPI
TH2=GAM2*DT
ET2=EXP(-TH2)
IF(TH2.GT.1.0E-4) GO TO 330
OET2=FS(TH2)
GO TO 340
330 OET2=1.0-ET2
340 GAM3=(SIG(I,J)+SIG(I,JP1))*EPI
TH3=GAM3*DT
ET3=EXP(-TH3)
IF(TH3.GT.1.0E-4) GO TO 350
OET3=FS(TH3)
GO TO 360
350 OET3=1.0-ET3
360 A1(J)=OET1*GP(JM1)*EMU/(2.0*GAM1*DY)
A2(J)=OET2*AA2/GAM2
A3=AA3
A4=GP(J)*DT/(2.0*DY)
A5=1.0-A3*A2(J)
AL1=OET3*GP(J)*EMU/(2.0*GAM3*DY)
C1(J)=FR1(I,JM1)*ET1 + OET1*(-JR(I,JM1)/EPS-
$(GP(JM1)*EMU/(2.0*DY))*(BP1(I,J)-BP1(I,JM1)))/GAM1
C2(J)=-EZ2(IM1,J)+(EZ1(IM1,J)+FZ1(I,J))*ET2+OET2*(-2.0*JZ(IM1,J)
$/EPS-(FP(IM1)*EMU/DX)*(BP1(I,J)-BP1(IM1,J)-BP2(IM1,J))-
$(EMU/(2.0*F(IM1))*(BP2(IM1,J)+BP1(IM1,J)+BP1(I,J)))/GAM2
C3=BP1(I,J)+(DT*FR(I)/(2.0*DX))*(EZ1(IP1,J)-EZ1(I,J)-EZ2(IM1,J))-
$(GP(J)*DT/(2.0*DY))*(ER1(I,J)-FR1(I,JM1))
C4=C3-A3*C2(J)
CL1=ER1(I,J)*ET3+OET3*(-JR(I,J)/EPS-
$(GP(J)*EMU/(2.0*DY))*(BP1(I,JP1)-BP1(I,J)))/GAM3
B1=A4*AL1
R2=A5+A1(J)*A4-AL1*A4
B3=A1(J)*A4
B4=C4+A4*(C1(J)-CL1)
E(J)=-B1/(B2+B3*E(J-1))
FF(J)=(B4-B3*FF(JM1))/(B2+B3*E(JM1))
300 CONTINUE
C
C *** NOW ADVANCE OVER ALTITUDE TO GET THE FIELDS ***
DO 400 JJ=J2DMN,J2DMX
J=J2DMX-JJ+J2DMN
JP1=J+1
BP2(I,J)=E(J)*BP2(I,JP1)-FF(J)
EZ2(I,J)=C2(J)-A2(J)*BP2(I,J)
400 CONTINUE
DO 410 J=J2DMN,J2DMX
JM1=J-1
ER2(I,J)=C1(J)-A1(J)*(BP2(I,J)-BP2(I,JM1))
410 CONTINUE
200 CONTINUE
C
C *** SET THE FIELDS AT THE OUTER BOUNDRY ***

```

C

```
DO 500 J=1,NY  
ER2(NX,J)=(3.0*FR2(NXM1,J)-ER2(NXM2,J))/2.0  
BP2(NX,J)=(3.0*RP2(NXM1,J)-BP2(NXM2,J))/2.0  
EZ2(NX,J)=(3.0*EZ2(NXM1,J)-EZ2(NXM2,J))/2.0
```

500 CONTINUE

C

C

C

```
*** CALL OVTPVT TO DO THE PRINTS AND PLOTS
```

511 CONTINUE

```
CALL OVTPVT(K,T)
```

100 CONTINUE

```
STOP10
```

```
END
```

```
SUBROUTINE CONST(E, RG, RE, EE)
  RG=50.8273+E*(74.5729+E*(-7.0112+E*.2939))
  IF(E.GT.1.6) GO TO 10
  EE=E*(.0631+E*(.8108+E*(-.5918+E*.1609)))
  GO TO 20
10 EE=E*(.3871+E*(.08945+E*(-.01037+E*.0004419)))
20 IF(E.GT.2.1) GO TO 30
  RE=-.003476+E*(-.03067+E*(.8050-E*.13992))
  RETURN
30 RE=-1.0847+E*(1.4679+E*(.04584-E*.001688))
  RETURN
  END
```

```

SUBROUTINE CURENT(TT)
REAL JR,JZ
COMMON ER1(20,20), EZ1(20,20), BP1(20,20)
COMMON ER2(20,20), EZ2(20,20), BP2(20,20)
COMMON JR(20,20), JZ(20,20), SIG(20,20)
COMMON R(20,20), CON(20,20), X(20), Y(20)
COMMON/SGRID/YMAX,DY,NG,NY,J,XO,DX,NX,I,NG
REAL LAM
COMMON/TRNS/QE,LAM,RE,EE
COMMON/WOUT/AL,BE,TP,CY,CX,YLD,EFF,EGB,HOB
REAL JRR
DO 20 I=1,NX
DO 20 J=NG,NY
T=TT-R(I,J)/2.998E+8
JRR=-CON(I,J)*SOURCE(T)*QE*RE
COSINE=X(I)/R(I,J)
SINE=(HOB-Y(J))/R(I,J)
JR(I,J)=JRR*COSINE
JZ(I,J)=-JRR*SINE
20 CONTINUE
RETURN
END

```



```

SUBROUTINE OVTPVT(ITIME,T)
INTEGER PRR,PLR
REAL JR,JZ
COMMON ER1(20,20), EZ1(20,20), RP1(20,20)
COMMON ER2(20,20), EZ2(20,20), BP2(20,20)
COMMON JR(20,20), JZ(20,20), SIG(20,20)
COMMON R(20,20), CON(20,20), X(20), Y(20)
COMMON/PLTS/PLR,NPX,NPY,IPX(10),IPY(10)
COMMON/PRNTS/PRR,NWX,NWY,NOX,NOY,IWX(10),IWY(10),IOX(10),IOY(10)
COMMON/SGRID/YMAX,DY,NY,J,X0,DY,NX,I,NG
DIMENSION XX(8),BUF(511),LAB(6)
EQUIVALENCE(XK,XX(1)),(T1,XX(2)),(XJR,XX(3)),(XSIG,XX(4)),(XER,XX(
$5)),(XJZ,XX(6)),(XEZ,XX(7)),(XRP,XX(8))
DATA LAB/2HJR,2HJZ,3HSIG,2HER,2HEZ,2HBP/
DATA IRUF/0/

```

C
C
C

```

*** WRITE THE OBSERVER OUTPUT TAPE ***

```

```

TI=T
DO 10 II=1,NOX
DO 10 IJ=1,NOY
IK=(II-1)*NOY + IJ
XK=IK
I=IOX(II)
J=IOY(IJ)
XJR=JR(I,J)
XSIG=SIG(I,J)
XER=ER2(I,J)
XJZ=JZ(I,J)
XEZ=EZ2(I,J)
XRP=RP2(I,J)
DO 20 L=1,8
BUF(IBUF+L)=XX(L)
20 CONTINUE
IRUF=IRUF + 8
IF(IRUF.LT.504) GO TO 30
WRITE(1) BUF
IRUF=0
30 CONTINUE
10 CONTINUE

```

C
C
C

```

*** PRINT OUT FIELD VALUES ***

```

```

IF(MOD(ITIME,PRR).NE.0) GO TO 200
DO 100 IJ=1,NWY
J=IWY(IJ)
WRITE(6,120) T,Y(J)
120 FORMAT(// * TIME=*1PF10.3,10X,*Y=*1PF10.3,/4X,*RANGE*,9X,*JR*,11X
$,*JZ*,10X,*SIG*,11X,*ER*,11X,*FZ*,11X,*BP*)
DO 101 II=1,NWX
I=IWX(II)
TR=T-R(I,J)/2.998E+8
WRITE(6,130) X(I),JR(I,J),JZ(I,J),SIG(I,J),ER2(I,J),EZ2(I,J),BP2(I
$,J),TR
101 CONTINUE

```

```
130 FORMAT(1P8E13.4)
100 CONTINUE
200 CONTINUE
```

```
C
C *** PROFILE AND RANGE PLOTS AND PRINTS ***
C
```

```
IF(MOD(ITIME,PLR).NE.0) GO TO 500
*** PROFILE PRINT ***
```

```
C
C DO 610 II=1,NPX
C I=IPX(II)
C WRITE(6,630) X(I)
630 FORMAT(/** PROFILE AT X=* 1PE11.3,/)
C DO 610 J=1,NY
C WRITE(6,615) Y(J),JR(I,J),JZ(I,J),SIG(I,J),ER2(I,J),EZ2(I,J),BP2(I
C $,J)
615 FORMAT(1PE11.3,1P6E20.7)
610 CONTINUE
```

```
C
C *** RANGE PRINT ***
C DO 620 IJ=1,NPY
C J=IPY(IJ)
C WRITE(6,640) Y(J)
640 FORMAT(/** RANGE PRINT AT Y= *.1PE11.3,/)
C DO 620 I=1,NX
C WRITE(6,615) X(I),JR(I,J),JZ(I,J),SIG(I,J),ER2(I,J),EZ2(I,J),BP2(I
C $,J)
620 CONTINUE
```

```
C
C *** PROFILE PLOT ***
C
```

```
DO 701 IJ=1,NPY
J=IPY(IJ)
CALL PROFILE(NX,NY,J,JR,LAB(1))
CALL PROFILE(NX,NY,J,JZ,LAB(2))
CALL PROFILE(NX,NY,J,SIG,LAB(3))
CALL PROFILE(NX,NY,J,ER2,LAB(4))
CALL PROFILE(NX,NY,J,EZ2,LAB(5))
CALL PROFILE(NX,NY,J,BP2,LAB(6))
701 CONTINUE
```

```
C
C *** RANGE PLOT ***
C
```

```
DO 702 II=1,NPX
I=IPX(II)
CALL RANGER(NX,NY,I,JR,X,LAB(1))
CALL RANGER(NX,NY,I,JZ,X,LAB(2))
CALL RANGER(NX,NY,I,SIG,X,LAB(3))
CALL RANGER(NX,NY,I,ER2,X,LAB(4))
CALL RANGER(NX,NY,I,EZ2,X,LAB(5))
CALL RANGER(NX,NY,I,BP2,X,LAB(6))
702 CONTINUE
500 CONTINUE
RETURN
END
```

```
SUBROUTINE PROFILE(NX,NY,J,V,Y,LAB)
DIMENSION V(NX,NY)
COMMON/WSPT/VB(200)
DO 10 I=1,NY
10 VB(I)=V(J,I)
CALL GRAPH(3,NY,0,0,LAB,3H Y ,0,VB,Y,8.,8.,4.,0.)
RETURN
END
```

```
SUBROUTINE RANGER(NX,NY,I,V,X,LAB)
DIMENSION V(NX,NY)
COMMON/WSPT/VB(200)
DO 10 J=1,NX
10 VB(J)=V(J,I)
CALL GRAPH(3,NX,0,0,3H X ,LAB,0,X,VR,8.,8.,0.,0.)
RETURN
END
```

```

SUBROUTINE RDS(KOMENT, DAY, HMS)
REAL JR, JZ
COMMON ER1(20,20), EZ1(20,20), BP1(20,20)
COMMON ER2(20,20), EZ2(20,20), BP2(20,20)
COMMON JR(20,20), JZ(20,20), SIG(20,20)
COMMON R(20,20), CON(20,20), X(20), Y(20)
COMMON/TGRID/T0,DT,NT,K
COMMON/SGRID/YMAX,DY,NY,J,X0,DX,NX,I,NG
REAL LAM
COMMON/TRNS/QE,LAM,RE,EE
COMMON/WOUT/AL,BE,TP,CY,CX,YLD,EFF,EGB,HOB
COMMON/PRNTS/PRR,NWX,NWY,NOX,NOY,IWX(10),IWY(10),IOX(10),IOY(10)
COMMON/PLTS/PLR,NPX,NPY,IPX(10),IPY(10)
DIMENSION KOMENT(8),XX(6)
WRITE(6,10)
10 FORMAT(*1*,19X,*IG2D--A TWO DIMENSIONAL EMP CODE TO CALCULATE THE
$FIELDS ABOVE AN INFINITELY CONDUCTING GROUND*)
WRITE(6,20) DAY,HMS
20 FORMAT(46X,A10,2X,A10)
WRITE(6,30) KOMENT
30 FORMAT(27X,8A10,/)
WRITE(6,40) PRR,PLR
40 FORMAT(30X,*PRINT RATIO*,63X,*PLOT RATIO*/34X,I3,71X,I3//)
L1=NOX*NOY
L2=NWX*NWY
WRITE(6,41) L1,L2,NPX,NPY
41 FORMAT(4X,*NUMBER TAPE OBSERVERS*,14X,*NUMBER PRINT OBSERVERS*,15X
$, *NUMBER OF PROFILES*,14X,*NUMBER OF RANGE PLOTS*/13X,I3,32X,I3,32
$,I3,32X,I3,/)
WRITE(6,42)
42 FORMAT(1X,*NO.*,8X,*X*,12X,*Y*,10X,*NO.*,8X,*X*,12X,*Y*,16X,*NO.*
$,8X,*X*,23X,*NO.*,8X,*Y*)
KK=MAX0(L1,L2,NPX,NPY)
I1=0
I2=0
J1=1
J2=1
DO 43 K=1,KK
I1=I1 + 1
I2=I2 + 1
IF(I1.LE.NOX) GO TO 44
I1=1
J1=J1 + 1
44 IF(I2.LE.NWX) GO TO 45
I2=1
J2=J2 + 1
45 I3=IOX(I1)
I4=IWY(I2)
J3=IOY(J1)
J4=IWY(J2)
IF(K.GT.10) GO TO 777
I5=IPX(K)
J5=IPY(K)
777 CONTINUE
XX(1)=X(I3)

```

```

XX(2)=Y(J3)
XX(3)=X(I4)
XX(4)=Y(J4)
XX(5)=X(I5)
XX(6)=Y(J5)
IF(K.LE.L1) GO TO 46
XX(1)=-0.0
XX(2)=-0.0
46 IF(K.LE.L2) GO TO 47
XX(3)=-0.0
XX(4)=-0.0
47 IF(K.LE.NPX) GO TO 48
XX(5)=-0.0
48 IF(K.LE.NPY) GO TO 49
XX(6)=-0.0
49 WRITE(6,401) K,XX(1),XX(2),K,XX(3),XX(4),K,XX(5),K,XX(6)
401 FORMAT(2(I3,I3,1P2F13.3,4X), 8Y,I3,3X,1PE13.3,15X,I3,3X,E13.3)
43 CONTINUE
WRITE(6,60) T0,DT,NT,X0,DX,NX,YMAX,DY,NY
60 FORMAT(4X,*TSTART*,10X,*DT*,12X,*NT*,16X,*R0*,12X,*DR*,12X,*NR*,
$15X,*ZMAX*,11X,*DZ*,12X,*NZ*/, 2(1PE11.4,4X,1PE11.4,7X,I3,11X),
$1PE11.4,4X,1PE11.4,7X,I3)
WRITE(6,100)
WRITE(6,101) YLD,EFF,AL,BE,TP,CY,EGB,LAM,EE,RE
100 FORMAT(/58X,*SOURCE CALCULATION*/56X,*DIRECT BEAM GAMMAS ONLY*
$,/,6X,*YLD*,10X,*EFF*,10X,*AL*.11X,*BE*.11X,*TP*,12X,*C*.11X,*EGB*
$,10X,*LAM*,10X,*EE*.11X,*RE*)
101 FORMAT(1P10E13.3)
RETURN
END

```

SUBROUTINE SETP

REAL JR,JZ

COMMON ER1(20,20), EZ1(20,20), RP1(20,20)

COMMON ER2(20,20), EZ2(20,20), RP2(20,20)

COMMON JR(20,20), JZ(20,20), SIG(20,20)

COMMON R(20,20), CON(20,20), X(20), Y(20)

COMMON/WOUT/AL,RE,TP,CY,CX,YLD,EFF,EGB,HOB

COMMON/SGRID/YMAX,DY,NY,J,X0,DX,NX,I,NG

REAL LAM

COMMON/TRNS/QE,LAM,RF,EE

DATA PI,QE/3.141592653,1.592E-19/

CY=1.0

CX=CY*EXP(AL*TP)

C
C
C

*** FIND TOTAL AREA ***

DT=TP/50

TOTAL=0.0

T=-0.5*DT

DO 10 I=1,10000

T=T + DT

P=SOURCE(T)

IF(P.LT.TOTAL*.0001) GO TO 20

10 TOTAL=TOTAL + P

STOP 01

20 TOTAL=TOTAL*DT

C
C

CY=2.62E+28*YLD*EFF/(EGB*TOTAL)

CX=CY*EXP(AL*TP)

CALL CONST(EGB,LAM,RE,EE)

DO 30 J=1,NY

YY=(HOB-Y(J))**2

DO 30 I=1,NX

XX=X(I)*X(I)

RR=SQRT(YY+XX)

R(I,J)=RR

30 CON(I,J)=EXP(-RR/LAM)/(4.0*PI*RR*RR*LAM)

RETURN

END

```

SURROUTINE SIGMA(TT)
REAL JR,JZ
COMMON ER1(20,20), EZ1(20,20), RP1(20,20)
COMMON ER2(20,20), EZ2(20,20), RP2(20,20)
COMMON JR(20,20), JZ(20,20), SIG(20,20)
COMMON R(20,20), CON(20,20), X(20), Y(20)
REAL LAM
COMMON/TRNS/QE,LAM,RF,EE
COMMON/SGRID/YMAX,DY,NY,J,X0,Dx,NX,I,NG
NP=NG+1
NM=NG-1
DO 20 I=1,NX
JJ=NG
DO 21 J=NP,NY
JJ=JJ-1
T=TT-R(I,J)/2.998E+8
Q=CON(I,J)*SOURCE(T)*EE*1.0E+6/34.0
SIG(I,J)=Q*0.1*1.0E-8*QE
SIG(I,JJ)=SIG(I,J)
21 CONTINUE
SIG(I,NG)=0.5*(SIG(I,NP)+SIG(I,NM))
20 CONTINUE
RETURN
END

```



```
FUNCTION SOURCE(T)
COMMON/WOUBT/AL,RE,TP,CY,CX,YLD,EFF,EGB,HOB
IF(T.LE.0.0) GO TO 20
IF(T.GT.4.0*TP) GO TO 10
SOURCE=CY*EXP(AL*T)/(1.0+EXP((AL+BE)*(T-TP)))
RETURN
10 SOURCE=CX*EXP(BE*(TP-T))
RETURN
20 SOURCE=0.0
RETURN
END
```

APPENDIX D

D.1

Several implicit finite difference schemes to solve the low altitude environment problem were programmed and checked out. However, none of them performed as well on the test problems as did the explicit algorithms described in Sections 2.1 and 2.2. A brief description of two of the implicit methods is given in the subsections below.

D.2

The scheme discussed here is an alternating direction implicit set of finite difference equations. For the equations implicit in the ξ direction, we combine Maxwell's equations to yield

$$\kappa \frac{\partial E_{\zeta}}{\partial \tau} - Q_{\tau} \frac{\partial H_{\varphi}}{\partial \tau} = -z_0 j_{\zeta} - z_0 \sigma E_{\zeta} + \psi_2 \frac{\partial H_{\varphi}}{\partial v} \quad (D.1)$$

$$\begin{aligned} \kappa Q_{\tau} G_2 \frac{\partial E_{\zeta}}{\partial \tau} + (G_1 - \kappa \kappa_m) \frac{\partial H_{\varphi}}{\partial \tau} &= G_1 z_0 (j_{\xi} + \sigma E_{\xi}) + \kappa G_1 \psi_1 \frac{\partial E_{\xi}}{\partial u} \\ &+ G_1 \psi_1 \frac{\partial H_{\varphi}}{\partial u} - \kappa G_2 \psi_2 \frac{\partial E_{\zeta}}{\partial v} \end{aligned} \quad (D.2)$$

The finite difference form of these equations chosen for the code is

$$\begin{aligned} \frac{\kappa}{\Delta \tau} (E_{\zeta ij}^k - E_{\zeta ij}^{k-1}) - \frac{Q_{\tau}}{\Delta \tau} (H_{\zeta i, j}^k - H_{\zeta i, j}^{k-1}) &= -z_0 j_{\zeta i, j}^{k-1/2} - \frac{z_0}{2} \sigma_{i, j}^{k-1/2} (E_{\zeta ij}^k \\ &+ E_{\zeta i, j}^{k-1}) + \frac{\psi_2}{2\Delta v} \left[Q_{11} (H_{\zeta i, j-1}^k - H_{\zeta i, j+1}^k) + Q_{12} (H_{\zeta i, j-1}^{k-1} - H_{\zeta i, j+1}^{k-1}) \right] \end{aligned} \quad (D.3)$$

and

$$\begin{aligned}
& \frac{\kappa Q_{\tau} G_2}{\Delta \tau} \left(E_{\zeta i, j}^k - E_{\zeta i, j}^{k-1} \right) + \frac{G_1 - \kappa \kappa_m}{\Delta \tau} \left(H_{\zeta i, j}^k - H_{\zeta i, j}^{k-1} \right) = G_1 z_0 \left(j_{\xi i, j}^{k-1/2} \right. \\
& \quad \left. + \sigma_{i, j}^{k-1/2} E_{\xi i, j}^{k-1/2} \right) + \frac{\kappa G_1 \psi_1}{2 \Delta u} \left(E_{\xi i+1, j}^{k-1/2} - E_{\xi i-1, j}^{k-1/2} \right) + \frac{G_1 \psi_1}{2 \Delta u} \left(H_{\xi i+1, j}^{k-1/2} \right. \\
& \quad \left. - H_{\xi i-1, j}^{k-1/2} \right) - \frac{\kappa G_2 \psi_2}{2 \Delta v} \left[Q_{21} \left(E_{\zeta i, j-1}^k - E_{\zeta i, j+1}^k \right) + Q_{22} \left(E_{\zeta i, j-1}^{k-1} - E_{\zeta i, j+1}^{k-1} \right) \right]
\end{aligned} \tag{D.4}$$

Equations (D.3) and (D.4) can be cast in the form

$$-\mathbf{A} \vec{g}_{j+1} + \mathbf{B}_j \vec{g}_j - \mathbf{C}_j \vec{g}_{j-1} = \vec{d}_j \tag{D.5}$$

where

$$\vec{g}_j = \begin{pmatrix} E_{\zeta i, j}^k \\ \\ \\ H_{\zeta i, j}^k \end{pmatrix} \tag{D.6}$$

Equation (D.5) represents a five-diagonal matrix for the solution of the finite difference equations. It is solved in a way that is analogous to the usual three-diagonal case. We seek a solution of the form

$$\vec{g}_j = \mathbf{E}_j \vec{g}_{j+1} + \vec{f}_j \tag{D.7}$$

By substitution into equation (D.5), one finds

$$\mathbf{E}_j = (\mathbf{B}_j - \mathbf{C}_j \mathbf{E}_{j-1})^{-1} \mathbf{A}_j \quad (\text{D.8})$$

$$\vec{\mathbf{f}}_j = (\mathbf{B}_j - \mathbf{C}_j \mathbf{E}_{j-1})^{-1} (\vec{\mathbf{d}}_j + \mathbf{C}_j \vec{\mathbf{f}}_{j-1}) \quad (\text{D.9})$$

The system is solved by first solving the recursion equations (D.8) and (D.9) to obtain the \mathbf{E}_j and $\vec{\mathbf{f}}_j$ terms and then obtaining the fields from equation (D.7). The boundary conditions on \mathbf{E}_j and $\vec{\mathbf{f}}_j$ are

$$\mathbf{E}_1 = 0, \quad \vec{\mathbf{f}}_1 = \vec{\mathbf{g}}_1 \quad (\text{D.10})$$

On alternate passes through the mesh, implicit equations in the ζ direction are used. In this case, Maxwell's equations are combined to yield

$$\kappa \frac{\partial \mathbf{E}_\xi}{\partial \tau} - \frac{\partial \mathbf{H}}{\partial \tau} = -z_o \mathbf{j}_\xi - z_o \sigma \mathbf{E}_\xi - \psi_1 \frac{\partial \mathbf{H}}{\partial u} \quad (\text{D.11})$$

$$\begin{aligned} \kappa G_1 \frac{\partial \mathbf{E}_\xi}{\partial \tau} + (G_2 - \kappa \kappa_m) \frac{\partial \mathbf{H}}{\partial \tau} &= Q_\tau G_2 z_o (\mathbf{j}_\zeta + \sigma \mathbf{E}_\zeta) - Q_\tau G_2 \psi_2 \frac{\partial \mathbf{H}}{\partial v} \\ &+ \kappa G_1 \psi_1 \frac{\partial \mathbf{E}_\xi}{\partial u} - \kappa G_2 \psi_2 \frac{\partial \mathbf{E}_\zeta}{\partial v} \end{aligned} \quad (\text{D.12})$$

The finite difference equations are

$$\frac{\kappa}{\Delta\tau} (E_{\xi i, j}^k - E_{\xi i, j}^{k-1}) - \frac{1}{\Delta\tau} (H_{\xi i, j}^k - H_{\xi i, j}^{k-1}) = -z_o^j{}^{k-1/2} - \frac{z_o}{2} \sigma_{i, j}{}^{k-1/2}$$

$$\left(E_{\xi i, j}^k + E_{\xi i, j}^{k-1} \right) - \frac{\psi_1}{2\Delta u} \left[Q_{11} (H_{\xi i+1, j}^k - H_{\xi i-1, j}^k) + Q_{12} (H_{\xi i+1, j}^k - H_{\xi i-1, j}^{k-1}) \right]$$

(D. 13)

and

$$\frac{\kappa G_1}{\Delta\tau} (E_{\xi i, j}^k - E_{\xi i, j}^{k-1}) + \frac{G_2 - \kappa \chi_m}{\Delta\tau} (H_{\xi i, j}^k - H_{\xi i, j}^{k-1}) = Q_{\tau} z_o G_2 \left[j \zeta_{i, j}^{k-1/2} + \sigma_{i, j}{}^{k-1/2} E_{\zeta i, j}^{k-1/2} \right] - \frac{Q_{\tau}}{2\Delta v} \psi_2 G_2 (H_{\zeta i, j-1}^{k-1/2} - H_{\zeta i, j+1}^{k-1/2}) + \frac{\kappa}{2\Delta u} \psi_1 G_1$$

$$\left[Q_{21} (E_{\xi i+1, j}^k - E_{\xi i-1, j}^k) + Q_{22} (E_{\xi i+1, j}^{k-1} - E_{\xi i-1, j}^{k-1}) \right]$$

$$- \frac{\kappa}{2\Delta v} \psi_2 G_2 (E_{\zeta i, j-1}^{k-1/2} - E_{\zeta i, j+1}^{k-1/2})$$

(D. 14)

By making the substitution, $j \rightarrow i$, equations (D. 5) through (D. 10) are appropriate for obtaining the solution of the finite difference equations (D. 13) and (D. 14) above.

D.3

The finite difference equations discussed in this section employ second order exponential differencing. The implicit equations are tri-diagonal. The reduction from a five-diagonal system is achieved by writing the $\nabla \times \vec{E}$ term in Faraday's Law explicitly. Although the term is explicit, it is centered in time and is of second order accuracy. This is accomplished by using a difference scheme that is multilevel in the time dimension. The finite difference equations are

$$\begin{aligned}
 E_{\zeta i, j}^k &= E_{\zeta i, j}^{k-1} e^{-\bar{x}} + \frac{1}{\sigma_{i, j}^k} \left[1 - \frac{1}{\bar{x}} (1 - e^{-\bar{x}}) \right] \left[-j \zeta_{i, j}^k + \frac{Q_{\tau}}{z_0 \Delta \tau} \left(H_{\phi i, j}^{k+1/2} - H_{\phi i, j}^{k-1/2} \right) \right. \\
 &\quad \left. + \frac{\psi_2}{4 z_0 \Delta v} \left(H_{\phi i, j-1}^{k+1/2} - H_{\phi i, j+1}^{k+1/2} + H_{\phi i, j-1}^{k-1/2} - H_{\phi i, j+1}^{k-1/2} \right) \right] \\
 &\quad + \frac{1}{\sigma_{i, j}^{k-1}} \left[\frac{1}{\bar{x}} (1 - e^{-\bar{x}}) - e^{-\bar{x}} \right] \left[-j \zeta_{i, j}^{k-1} + \frac{Q_{\tau}}{z_0 \Delta \tau} \left(H_{\phi i, j}^{k-1/2} - H_{\phi i, j}^{k-3/2} \right) \right. \\
 &\quad \left. + \frac{\psi_2}{4 z_0 \Delta v} \left(H_{\phi i, j-1}^{k-1/2} - H_{\phi i, j+1}^{k-1/2} + H_{\phi i, j-1}^{k-3/2} - H_{\phi i, j+1}^{k-3/2} \right) \right] \quad (D. 15)
 \end{aligned}$$

$$\begin{aligned}
E_{\xi i, j}^k &= E_{\xi i, j}^{k-1} e^{-\bar{x}} + \frac{1}{\sigma_{i, j}^k} \left[1 - \frac{1}{\bar{x}} (1 - e^{-\bar{x}}) \right] \left[-j_{\xi i, j}^k + \frac{1}{z_0 \Delta \tau} (H_{\phi i, j}^{k+1/2} - H_{\phi i, j}^{k-1/2}) \right. \\
&\quad \left. - \frac{\psi_1^i}{2 z_0 \Delta u} (H_{\phi i, j}^{k+1/2} - H_{\phi i-1, j}^{k+1/2} + H_{\phi i+1, j}^{k-1/2} - H_{\phi i, j}^{k-1/2}) \right] \\
&\quad + \frac{1}{\sigma_{i, j}^{k-1}} \left[\frac{1}{\bar{x}} (1 - e^{-\bar{x}}) - e^{-\bar{x}} \right] \left[-j_{\xi i, j}^{k-1} + \frac{1}{z_0 \Delta \tau} (H_{\phi i, j}^{k-1/2} - H_{\phi i, j}^{k-3/2}) \right. \\
&\quad \left. - \frac{\psi_1^i}{2 z_0 \Delta u} (H_{\phi i, j}^{k-1/2} - H_{\phi i-1, j}^{k-1/2} + H_{\phi i+1, j}^{k-3/2} - H_{\phi i, j}^{k-3/2}) \right] \quad (D. 16)
\end{aligned}$$

and

$$\begin{aligned}
\frac{Q_\tau G_2}{2 \Delta \tau} (E_{\zeta i, j}^k - E_{\zeta i, j}^{k-2}) + \frac{G_1}{2 \Delta \tau} (E_{\xi i, j}^k - E_{\xi i, j}^{k-2}) - \frac{\chi_m}{3 \Delta \tau} (H_{\phi i, j}^{k+1/2} - H_{\phi i, j}^{k-5/2}) \\
= \frac{G_1 \psi_1^i}{2 \Delta u} (E_{\xi i+1, j}^{k-1} - E_{\xi i-1, j}^{k-1}) - \frac{G_2 \psi_2}{2 \Delta v} (E_{\zeta i, j-1}^{k-1} - E_{\zeta i, j+1}^{k-1}) \quad (D. 17)
\end{aligned}$$

Equations (D. 15) through (D. 17) can be combined to yield the following tri-diagonal equation for the magnetic field

$$-A_j H_{\phi i, j+1}^k + B_j H_{\phi i, j}^k - C_j H_{\phi i, j-1}^k = D_j$$

A solution of the form

$$H_{\phi i, j}^k = E_j H_{\phi i, j+1}^k + F_j$$

exists in which

$$E_j = \frac{A_j}{B_j + A_j E_{j-1}}$$

$$F_j = \frac{D_j - A_j F_{j-1}}{B_j + A_j E_{j-1}}$$

The appropriate boundary conditions are

$$E_1 = 0 ,$$

$$F_1 = H_{\phi i, 1}^k$$

REFERENCES

1. Graham, W. R., "The Electromagnetic Fields Produced by a General Current Distribution in a Conductive Environment under Certain Symmetry Conditions," Theoretical Note 21 of AFWL EMP Theoretical Note Series; also published as an AFWL Report WL-TR-64-153, AFWL, Kirtland AFB, N. M., 1965.
2. Graham, W. R., "Close-In EMP II (U)," Rand Report RM-5789-PR, The RAND Corp., Santa Monica, Calif., 1968 (S/RD). (See also: Graham, W. R., and E. R. Parkinson, "ONDINE: A Numerical Solution to Maxwell's Equations in One Dimension," Rand Report R-701-DASA (DASA-2647), The RAND Corp., Santa Monica, Calif., 1971.)
3. Longley, H. J., and C. L. Longmire, "Development of the GLANC EMP Code," LANC-R-7, Los Alamos Nuclear Corporation, Los Alamos, N. M., 1971.
4. Longley, H. J., and C. L. Longmire, "Development and Testing of LEMP1," LASL Report LA-4346, Los Alamos Scientific Laboratory, Los Alamos, N. M., 1970.
5. Dalich, S. J., and K. D. Granzow, "Two Dimensional Ground Burst Electromagnetic Pulse Computational Methods," Science Applications, Inc., Report No. SAI-73-514-AQ, Part 1 of Final Report, prepared under AFWL Contract No. F29601-72-C-0117, February 1974.
6. Knight, R. L., "Numerical Solutions of Maxwell's Equations with Azimuthal Symmetry in Prolate Spheroidal Coordinates," Theoretical Note 62 of AFWL EMP Theoretical Note Series, 1969.
7. Granzow, K. D., and D. D. Babb, "Extrapolating Electromagnetic Fields from Values in a Spherical Region," Note 54, AFWL EMP 2-3, AFWL EMP Theoretical Note Series, June 1965.
8. Radasky, W. A., and R. L. Knight, "HAPS--A Two-Dimensional High Altitude EMP Environment Code," EMP Theoretical Note 125 of EMP Theoretical Note Series, Air Force Weapons Laboratory, Albuquerque, N. M., November 1971.

REFERENCES (Cont'd.)

9. Courant, R., and D. Hilbert, Methods of Mathematical Physics, John Wiley & Sons, Inc., New York, 1962.
10. Courant, R., and K. O. Friedrichs, Supersonic Flow and Shock Waves, Interscience Publishers, Inc., New York, 1948.
11. Fox, L., Numerical Solution of Ordinary and Partial Differential Equations, Addison Wesley, Reading, Mass., 1962.
12. Peebles, G. H., "Numerical Programs for Solving Hyperbolic Systems by the Method of Characteristics: Radio Emission from a Nuclear Explosion: Part I," Note 46, AFWL EMP 2-2, AFWL EMP Theoretical Note Series, March 1966.